Bucknell University
Bucknell Digital Commons

Honors Theses | Student Theses

2016

Design of Steel Structures by Advanced 2nd-Order Elastic Analysis-Background Studies

Erik Johannes Giesen Loo
Bucknell University, ejgl001@bucknell.edu

Follow this and additional works at: https://digitalcommons.bucknell.edu/honors_theses

Recommended Citation
Giesen Loo, Erik Johannes, "Design of Steel Structures by Advanced 2nd-Order Elastic Analysis-Background Studies" (2016). *Honors Theses*. 349.
https://digitalcommons.bucknell.edu/honors_theses/349

This Honors Thesis is brought to you for free and open access by the Student Theses at Bucknell Digital Commons. It has been accepted for inclusion in Honors Theses by an authorized administrator of Bucknell Digital Commons. For more information, please contact dcadmin@bucknell.edu.

DESIGN OF STEEL STRUCTURES BY ADVANCED 2ND-ORDER ELASTIC ANALYSIS – BACKGROUND STUDIES

by

Erik Johannes Giesen Loo

A Thesis

Presented to the Honors Council for Honors

in Civil Engineering at Bucknell University

(Bachelor of Science in Civil and Environmental Engineering)

April 2016

Approved by: _____

Dr. Ronald D. Ziemian, Thesis Advisor
Department of Civil and Environmental Engineering

_____

Dr. Jean Batista Abreu, Thesis Advisor
Department of Civil and Environmental Engineering

_____

Dr. Michael Malusis, Department Chairperson
Department of Civil and Environmental Engineering

ACKNOWLEDGMENTS

First and foremost, I would like to express my most sincere gratitude to Professor Ronald D. Ziemian, for providing me the opportunity to work on this research project and for his support throughout the development of this honors thesis. I have learned much in his courses and in this research. I would also like to express my gratitude to Professor Jean Batista Abreu, who co-advised my honors thesis, for his support and help in the development of the thesis, and Professors Stephen Buonopanne, Kelly Salyards, and Deborah Sills for expanding my knowledge with their expertise, and encouraging me to do research. I would like to thank Professors Jessica Newlin and Douglas Gabauer for building a solid foundation in MATLAB that proved essential, the most representative of examples being the implementation of a binary search engine. My sincere appreciation goes to my friend, Mustafa Abbas, for sharing with me his solid and innovative ideas and knowledge of computer science, which really enhanced the quality of the work presented herein. I am also grateful to my friends, Xiaolong Li, Hein Tun, Aradhana Agarwal and May Thu Nwe Nwe, whose diligent work in the civil engineering field inspired me to do research and write an honors thesis. Finally, I would like to thank the civil engineering faculty and staff, my friends at Bucknell and most importantly, my mum and dad; without whom none of this would have been possible.

TABLE OF CONTENTS

ACKNOWLEDGMENTS iii

TABLE OF CONTENTS iv

LIST OF TABLES vii

LIST OF FIGURES viii

ABSTRACT xii

CHAPTER 1: INTRODUCTION 1

1.1. Thesis Statement 1

1.2. Research Purpose 1

1.3. Thesis Overview 5

CHAPTER 2: BACKGROUND 6

2.1. Stability Design Requirements 6

2.2. Interaction Equation 8

2.3. Axial Strength Calculation 10

2.4. Stability Analysis Methods 13

2.5. Previous Studies 17

2.5.1. Surovek-Maleck and White Studies: 17

2.5.2. Ziemian and McGuire study 19

2.5.3. Martinez-Garcia Study 21

2.5.4. Nwe Nwe Study 22

2.6. Adding Initial Member Imperfections 22

2.7. Modeling Residual Stresses 24

CHAPTER 3: METHODOLOGY 25

3.1. Initial Member Imperfections 27

3.2. Secant τ_b-factor vs. tangent τ_b-factor 31

3.3. Interaction Equation and Applied Load Ratio 32

3.4. Description of frames 34

System 1a – Ziemian and Miller (1997) Unsymmetrical Frame (Major-axis) 35

System 1b – Ziemian and Miller (1997) Unsymmetrical Frame (Minor-axis) 36

System 2 –Maleck (2001) Industrial Frame (Major-axis Bending) 37

System 3 – Grain Storage Bin (Major-axis Bending) 38

System 4 – Vogel (1985) Multi-Story Frame (Major-axis Bending) 39

System 5 – Martinez-García (2002) Gable Frame (Major-axis) 40

System 6 – Martinez-García (2002) Moment Frame (Major-axis) 41

System 7a –Two Bay Moment Frames, Unequal Heights (Major-axis) 42

System 7b –Two Bay Moment Frames, Unequal Heights (Major-axis) 43

System 7c – Two Bay Braced Frame, Unequal Heights (Major-axis) 44

System 7d – Two Bay Braced Frame, Unequal Heights (Minor-axis) 45

System 8 – Vierendeel Truss 46

System 9 – El Zanaty Frame 47

3.5. System 7d Detailed Example 47

3.6. Minor-axis Column Study 52

CHAPTER 4: RESULTS 57

4.1. Effect of Initial Imperfections 58

4.2. Secant vs. tangent τ_b 59

4.3. Column Study Results 60

What if F_y = 36 ksi instead of 50 ksi? 63

CHAPTER 5: CONCLUSIONS 64

5.1. Summary of Results 64

5.2. Recommendations for further research 66

Appendix A. Plastic-hinge vs. Distributed Plasticity 68

Appendix B. Binary Search Engine 69

Appendix C. Benchmark Frame Results 70

C.1. System 1a – Ziemian and Miller (1997) Unsymmetrical Frame (Major-axis) .. 71

C.2. System 1b – Ziemian (1990) Unsymmetrical Frame (Minor-axis) 73

C.3. System 2 Maleck (2001) Industrial Frame (Majox Axis) 75

C.4. System 3 Grain Storage Bin (major-axis) 77

C.5. System 4 Vogel (1985) Multi-Story Frame (major-axis) 78

C.6. System 5 Martinez-García (2002) Gable Frame (major-axis) 80

C.7. System 6 Martinez-García (2002) Moment-Frame (major-axis) 82

C.8. System 7a – Two Bay Moment Frames with Unequal Heights 84

C.9. System 7b – Two Bay Moment Frames, Unequal Heights 86

C.10. System 7c – Two Bay Braced Frame with Unequal Heights 88

C.11. System 8 – Vierendeel Truss 90

C.12. System 9 – El Zanaty Frame 92

Appendix D. Column Study Results 94

References 97

LIST OF TABLES

Table 1. Brief explanation of stability design requirements 6

Table 2. Comparison of design methods. Modified from (AISC, 2010, p.273) 16

Table 3. H1-1 and λ values for frame 7d 50

Table 4. Summary of design by DM and Design by advanced elastic analysis results (secant τ_b) 57

Table 5. Effect of neglecting initial imperfections (tangent τ_b) 58

Table 6.% difference between using secant and tangent τ_b factor in design by DM and DEA 59

Table 7. Maximum conservative and unconservative % radial error 62

Table A 1. Plastic-hinge vs. distributed plasticity. Adapted from Surovek (2012, pg. 14) 68

Table C 1. System 1a H1-1 and λ values 71

Table C 2. System 1b H1-1 and λ values 73

Table C 3. System 2 H1-1 and λ values 75

Table C 4. System 3 H1-1 and λ values 77

Table C 5. System 4 H1-1 and λ values 79

Table C 6. System 5 H1-1 and λ values 80

Table C 7. System 6 H1-1 and λ values 83

Table C 8. System 7a H1-1 and λ values 84

Table C 9. System 7b H1-1 and λ values 86

Table C 10. System 7c H1-1 and λ values 88

Table C 11. System 8 H1-1 and λ values 90

Table C 12. System 9 H1-1 and λ values 92

Table D 1. Conservative and Unconservative Errors in Minor-axis Column Study 96

LIST OF FIGURES

Figure 1. (a) Column-curve with residual stresses, (b) AISC column-curve with residual stresses and initial member imperfections. Adapted from (Segui, 2013) 10

Figure 2. Stress pattern. From Galambos and Ketter (1959) and Surovek (2012) 24

Figure 3. Flow diagram for adding out-of-straightness imperfections 30

Figure 4. Interaction Equation at λ = 1.0 and λ at Interaction Equation = 1.0 33

Figure 5. Ziemian and Miller Frame (Major-axis). Modified from Nwe Nwe (2014) 35

Figure 6. Ziemian and Miller Frame (Minor-axis). Modified from Nwe Nwe (2014) 36

Figure 7. Maleck 11-Bay Industrial Frame, Originally from Surovek (2012, p.33) 37

Figure 8. Maleck 3-Bay Industrial Frame, Modified from Surovek (2012) 37

Figure 9. (a) Grain Storage Bin. (b) Analysis Representation. Modified from Nwe Nwe (2014) 38

Figure 10. Vogel (1985) Frame (Major-axis) Modified from Nwe Nwe (2014) 39

Figure 11. Martinez-García Gable Frame. Modified from Nwe Nwe (2014) 40

Figure 12. Martinez-García Moment Frame. Modified from Nwe Nwe (2014) 41

Figure 13. System 7a. Modified from Martinez-García (2002) 42

Figure 14. System 7b. Modified from Martinez-García (2002) 43

Figure 15. System 7c. Modified from Martinez-García (2002) 44

Figure 16. System 7d (Minor-axis) Modified from Martinez-García (2002) 45

Figure 17. Vierendeel Truss. Modified from Martinez-García (2002) 46

Figure 18. El-Zanaty Frame, modified from Ziemian (2002) 47

Figure 19. Frame 7d with factored loads 48

Figure 20. (a) Lateral displacement of both frame 7d bays. (b) Lateral displacement of the right bay 51

Figure 21. Kanchanalai Frame and column study, modified from Ziemian (2002) 52

Figure 22. Column Study Main Routine 53

Figure 23. Sub-routine for determining pure axial load capacity of columns 54

Figure 24. Sub-routine for finding combined axial load and horizontal load of columns 55

Figure 25. Computing radial error (a) Using P/P_y as the ordinate (b) Using P/P_{FE++} as the ordinate 56

Figure 26. W8X58 P/Py vs. M1/Mp for L/r = 40, Fy = 50 ksi 60

Figure 27. W8X58 P/Py vs. M1/Mp for L/r = 60, Fy = 50 ksi 61

Figure 28. W8X58 P/Py vs. M1/Mp for L/r = 80, Fy = 50 ksi 61

Figure 29. W8X58 P/Py vs. M1/Mp for L/r = 100, Fy = 50 ksi 62

Figure 30. W8X31, weak 60 compared to SP_W60_G0 from Maleck (2003) 63

Figure B 1. Binary Search Engine Flowchart ……...69

Figure C 1. System 1a Factored Loads 71

Figure C 2. System 1a Lateral Displacement Plots 72

Figure C 3. System1b Factored Loads 73

Figure C 4. System 1b Lateral Displacement Plots 74

Figure C 5. System 2 Factored Loads 75

Figure C 6. System 2 Lateral Displacement Plots 76

Figure C 7. System 3 Factored Loads and lateral displacement plot 77

Figure C 8 System 4 Factored Loads 78

Figure C 9. System 4 Lateral Displacement Plot 78

Figure C 10. System 5 Factored Loads 80

Figure C 11. System 5 Lateral Displacement Plots 81

Figure C 12. System 6 Factored Loads 82

Figure C 13. System 6 Lateral Displacement Plots 82

Figure C 14. System 7a Factored Loads 84

Figure C 15. System 7a Lateral Displacement Plots 85

Figure C 16. System 7b Factored Loads 86

Figure C 17. System 7b Lateral Displacement Plots 87

Figure C 18. System 7c Factored Loads 88

Figure C 19. System 7c Lateral Displacement Plots 89

Figure C 20. System 8 Factored Loads 90

Figure C 21. System 8 Lateral Displacement Plots 91

Figure C 22. System 9 Factored Loads 92

Figure C 23. System 9 Lateral Displacement Plots 93

Figure D 1. W8X58, weak axis bending, L/r = 40, Fy = 50 ksi 94

Figure D 2. W8X58, weak axis bending, L/r = 60, Fy = 50 ksi 94

Figure D 3. W8X58, weak axis bending, L/r = 80, Fy = 50 ksi 95

Figure D 4. W8X58, weak axis bending, L/r = 100, Fy = 50 ksi 95

ABSTRACT

Design by advanced second-order elastic analysis (DEA) is based on the premise that reliance on approximate methods to account for parameters in design can be reduced by directly modeling them in the analysis. Current analysis methods often rely on equations based on effective buckling lengths to determine the axial capacity of beam-columns; however, complex systems may not possess clearly defined effective-lengths or the axial force may vary significantly within such lengths. By employing a rigorous second-order (geometric nonlinear) analysis that explicitly models system and member initial geometric imperfections and reduces member stiffness to account for partial yielding within the analysis, it has been established that a simplified form of the axial capacity can be employed in the design process. Instead of using buckling-length-based column strength equations that consider member out-of-straightness imperfections and the effect of residual stresses on partial yielding, the engineer is granted the ability to use the axial cross-sectional strength. Twelve benchmark frames were analyzed using design by advanced second-order elastic analysis and the results were compared to current analysis methods in the 2010 American Institute of Steel Construction's *Specification for Structural Steel Buildings.* The research described herein and studies performed by other form the basis for the revised Appendix on Design by advanced elastic analysis appearing in the forthcoming 2016 American Institute of Steel Construction's *Specification for Structural Steel Buildings.* This method effectively removes the need to consider member length when calculating the axial strength of beam-columns.

CHAPTER 1: INTRODUCTION

1.1. Thesis Statement

By directly modeling system and member initial geometric imperfections within the structural analysis, adequate designs can be obtained that are comparable to those obtained using current methods appearing in the 2010 American Institute of Steel Construction's Specification for Structural Steel Buildings.

1.2. Research Purpose

Structural steel members tend to be slender by virtue of their relatively high stiffness and strength to weight ratios, thereby emphasizing the importance of designing for stability. The factors affecting stability that need to be considered include: (1) flexural, shear and axial member deformations; (2) second-order effects; (3) system and member initial geometric imperfections; (4) stiffness reduction due to inelasticity accentuated by residual stresses; and (5) including uncertainty in strength and stiffness terms. Off of these, this thesis shall focus on member and system deflections and their resulting second-order effects. Both effects are increased due to initial geometric imperfections such as system imperfections due to erection tolerances, also called out-of-plumbness, and member imperfections, or out-of-straightness, which occur during the manufacturing process. It is noted that out-of-plumbness is the relative displacement of the top and bottom of a frame whereas out-of-straightness is the deflection of a member between end connections, usually in the form of single curvature bending (Ziemian, 2010, p.27, 41). An additional factor that

can reduce the rigidity of the system and impact stability is the presence of residual stresses, which is caused by the differential cooling of hot-rolled steel at the end of the rolling process (Ziemian, 2010, p.29).

The presence of deflections that produce additional moment requires the use of second-order analysis, i.e. an analysis that formulates equilibrium on the deformed shape. In fact, modern stability design provisions are based on the premise that internal forces are calculated using this type of analysis (AISC, 2010, p.275). Second-order analysis can account for deflections, the resulting second-order effects and, if explicitly modeled, the impact of initial geometric imperfections. Although yielding and residual stresses can be explicitly modeled through material-inelastic analysis procedures, they are currently computationally prohibitive for designing large structural systems. Consequently, AISC's current analysis method employs a reduced material stiffness coupled with a yield surface criterion in lieu of directly modeling partial and full-yielding, which may be accentuated by the presence of residual stresses. Using a yield surface criterion is called a concentrated plasticity or plastic-hinge analysis, whereas direct modeling of yielding and residual stresses along the length and cross-section is referred to as distributed plasticity analysis (See Appendix A for further explanation). If the plastic-hinge analysis does not allow force redistribution beyond the first plastic-hinge, it may be called a material linear and reduced elastic analysis. The focus of this research is to verify that by explicitly modeling initial geometric imperfections and using a reduced material stiffness, a proposed plastic-hinge second-order material-linear analysis can accurately estimate the results from a rigorous second-order inelastic analysis.

CHAPTER 1: INTRODUCTION

Traditional U.S. design approaches do not directly account for the aforementioned factors that influence stability. Instead, they use effective-length K-factors and a column strength curve, which is defined in Section 2.3, that reduces member strength with increased slenderness (Ziemian, 2010, p.48). This is coupled with a carefully calibrated beam-column interaction equation to account for the destabilizing effects of out-of-plumbness, residual stresses and partial yielding on the system (Surovek-Maleck and White, 2004a, p.1186). To ensure stability, the American Institute of Steel Construction (AISC)'s *Specification for Structural Steel Buildings* (2010), henceforth called the 2010 Specification, stipulates the use of a member-by-member design check, which is presented in Section 2.2, that compares internal second-order forces and moments to member axial and bending strengths. If all member checks conform to the requirements of the design equation, then the system is assumed stable (Maleck and White, 2004a, p.1187).

In 2005, AISC introduced the design by direct analysis method, often abbreviated as design by DM, which simplifies the design process by no longer requiring the calculation of an effective-length K-factor. Instead, this method requires modeling out-of-plumbness, either by offsetting the coordinates of the nodes of the top of each story with respect to the bottom of the story or using notional loads to achieve the same effect, and reducing the flexural stiffness, EI, of members by 0.8 and a τ_b factor to account for the effect of member initial imperfections, partial yielding, residual stresses and uncertainty in stiffness on the system behavior. In comparison to the effective-length method, design by DM provides a more transparent design methodology by granting the engineer the ability to use the unbraced length of the members as the effective-length thereby removing the reliance on

effective-length *K*-factors, which can involve cumbersome and error prone calculations (Ziemian, 2010, p.48). However, a column strength curve defined in terms of the unbraced member length is still employed to account for member out-of-straightness and cross-section partial yielding caused by residual stresses.

The method explored herein, design by advanced second-order elastic analysis; or simply, design by advanced elastic analysis, which will be incorporated in AISC's 2016 Specification (AISC, 2015, App.1), grants the engineer the ability to avoid reliance on the column-curve and instead use the cross-section axial strength as the member's compression strength. The requirements of this method include accounting for partial yielding and residual stresses, albeit with a reduction factor, and explicitly modeling out-of-straightness.

In proving this method, design by advanced elastic analysis achieves three main goals, which were originally suggested by Surovek-Maleck and While (2004a, 1186): (1) the development of a more streamlined design procedure, (2) more transparent design calculations that use estimates of the actual internal forces and resistances, and (3) a more natural extension from simple elastic analysis to higher-tiered methods. This method not only provides an alternative analysis method, but the opportunity to design more complex structures, and to perform a relatively simple verification of the results of design by advanced second-order inelastic analysis, or simply, design by advanced inelastic analysis, present in both the 2010 and 2016 Specification, which in turn can be used to address extraordinary issues with greater confidence.

The overarching goal of the research was to review the AISC's 2016 Specification proposed revision to Appendix 1, Section 1.2 Design by advanced elastic analysis. This is done by comparing the results from twelve frames analyzed with the proposed method against the results obtained using design by DM, and design by advanced inelastic analysis. MASTAN2, developed by Ziemian (2015), is used to perform the analyses required for design by advanced elastic analysis and design by DM, and FE++2015, developed by Alemdar (2001) is used to perform design by advanced inelastic analysis.

1.3. Thesis Overview

The chapters in this thesis are outlined here.

Chapter 1 presents the thesis statement and describes the purpose of the research by introducing the concept of stability design and the overarching goals of the method.

Chapter 2 provides the background information. It presents the stability design requirements, the necessary design equations, and previous research done.

Chapter 3 presents the frame study methodology, the twelve frames investigated, and the methodology of the minor-axis beam-column study.

Chapter 4 presents the results for both the frames and the minor-axis column study.

Chapter 5 provides a summary of this research and highlights the overall conclusions from the research followed with recommendation for further research.

CHAPTER 2: BACKGROUND

2.1. Stability Design Requirements

The AISC 2016 specification establishes five stability design requirements in Chapter C, which are provided in Table 1. The subsection of Chapter C or the commentary is also given. Also included in the table (in italics) is how these requirements were satisfied in this research.

Table 1. Brief explanation of AISC stability design requirements

Requirement	Explanation	Reference
(1) Flexural, shear, and axial member deformations	Stability analysis must consider all pertinent deformations: axial, bending, shear, torsion and connection deformations. *Shear deformations were neglected in this research because they were considered to have a negligible impact on the frames investigated.*	C.2.1
(2) Second-order effects (P-Δ and P-δ)	It is imperative to formulate equilibrium on the deformed shape by means of a rigorous second-order elastic analysis (Ziemian, 2010, p. 698). *While analysis software such as MASTAN2 (Ziemian and McGuire, 2015) is good at capturing P-Δ effects, it is often necessary to subdivide elements to better capture P-δ effects.*	C.2.1

(3) System and member initial geometric imperfections	Initial geometric imperfections need to be conservatively assumed and should equal the maximum tolerances permitted in the *AISC Code of Standard Practice for Steel Buildings and Bridges* (AISC, 2000), unless otherwise noted: out-of-plumpness equal to 1/500 of the story height and out-of-straightness of 1/1000 of the member length.	C.2.2.
(4) Stiffness reduction due to inelasticity accentuated by residual stresses	A factor of 0.8 must be applied to *all* stiffnesses that contribute to the stability of the structure. In slender columns, 0.8 is equivalent to the resistance factor Φ (= 0.9) times the out-of-straightness 0.877 reduction factor. In short columns, 0.8 accounts for inelastic softening. The τ_b factor, which will be described in Section 2.3 and 3.2, is applied to *all* stiffnesses (and not only *EI* as required by AISC 2010).	C.2.3.
(5) Including uncertainty in strength and stiffness.	The aforementioned 0.8 factor applied to the elastic modulus also accounts for the uncertainty in stiffness. The strength terms use resistance factors as specified in Chapter D, E and F.	Comm. C.2.3
*Note: member twist will also need to be considered per the 2016 Specification (AISC, 2015)		

Factors affecting stability that are not included in this study are local buckling, bracing elements, connection or loading eccentricities, and construction sequencing stresses (Ziemian, 2010, p.29, 714).

2.2. Interaction Equation

AISC has established the following interaction equation (Equation 1) to verify that all members in a structural system have adequate axial and bending capacity to resist the internal second-order forces and moments (AISC, 2010, p.73; Ziemian, 2010, p. 385):

If $\frac{P_u}{\Phi_c P_n} \geq 0.2$

$$\frac{P_u}{\Phi_c P_n} + \frac{8}{9}\left(\frac{M_{ux}}{\Phi_b M_{nx}} + \frac{M_{uy}}{\Phi_b M_{ny}}\right) \leq 1.0, \tag{1a}$$

else

$$\frac{P_u}{2\Phi_c P_n} + \left(\frac{M_{ux}}{\Phi_b M_{nx}} + \frac{M_{uy}}{\Phi_b M_{ny}}\right) \leq 1.0, \tag{1b}$$

where

$P_u \equiv$ ultimate axial load resisted by the member (internal force)

$P_n \equiv$ nominal axial strength of the member

$M_{ux} \equiv$ second-order major-axis moment resisted by the member (internal force)

$M_{nx} \equiv$ nominal major-axis bending strength of the member

$M_{uy} \equiv$ second-order minor-axis moment resisted by the member (internal force)

$M_{ny} \equiv$ nominal minor-axis bending strength of the member

$\Phi_c \equiv$ axial strength resistance (safety) factor

$\Phi_b \equiv$ bending strength resistance (safety) factor

Equation 1, which was established by calibration to the results of several advanced second-order inelastic analyses of stability critical frames (Kanchanalai, 1977), ensures that no structural member fails. If this is the case, then the system is said to be stable (Suvorek-Maleck and White, 2004a, p.1187). Equation 1 resembles the yield-surface criterion for the cross-section of a beam-column subject to axial force and major-axis and minor-axis bending. However, it not only accounts for full-yielding of the cross-section (formation of a plastic-hinge), but also for member length failure modes, such as buckling. Although the yield surface for beam-columns subject to minor-axis bending is more convex than its major-axis counterpart, these members tend to fail significantly inside this surface due to the fact that yielding progresses from the flange tips inward, thereby reducing the flexural rigidity significantly faster than in beam-columns subject to major-axis bending (Maleck and White, 2004a, p.1191). To account for this possibility, AISC uses the same form of the major-axis interaction equation for minor-axis, and for the case of beam-columns subject to both major and minor-axis bending linearly interpolates between both curves. Regardless of the use of a smaller interaction surface, minor-axis results are of particular interest because the current stiffness reduction factor does not appear to fully capture this type of progressive yielding.

With the possibility of both system and member instabilities accounted for by the analysis, design by advanced elastic analysis will no longer require the consideration of member length in calculating axial capacity. Thus, the interaction equation will act as a yield surface criterion. That is, design by advanced elastic analysis is essentially a first-hinge limit-state design procedure (Ziemian, 2010, p.726).

2.3. Axial Strength Calculation

Current design methods often rely on length-based column-curve equations that consider the limit states of full-yielding of the cross-section, elastic and inelastic member buckling, as described in Chapter E of the 2010 Specification, when determining the axial load capacity of columns (AISC, 2011, p.31-43). Assuming that columns are modeled as originally straight members in the analysis, these equations reduce strength to account for partial yielding that originates from the axial load acting on the residual stresses, and the gradual instability caused by axial force acting on a member with out-of-straightness imperfection. The graphs in Figure 1 illustrate these concepts.

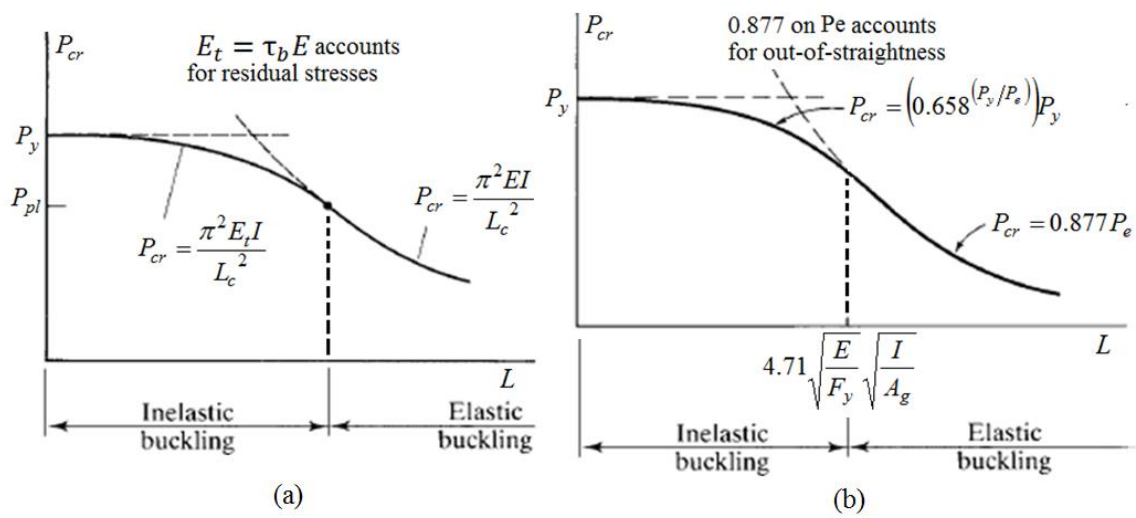

Figure 1. (a) Column-curve with residual stresses, (b) AISC column-curve with residual stresses and initial member imperfections. Adapted from (Segui, 2013)

The column-curve in Figure 1(a) shows the reduction in the buckling load arising from the presence of residual stresses, and is obtained by applying a τ_b factor (which will

be described in Section 2.7) to the elastic modulus within the Euler buckling equation. The curve in Figure 1(b), used in AISC Specification, not only accounts for residual stresses, but also employs a 0.877 factor on the Euler buckling load to account for the gradual instability due to the out-of-straightness imperfection. The inelastic buckling equation in Figure 1(b) differs from the one in Figure 1(a) because it was fitted to experimental data to account for the amalgam of residual stresses and minor levels of out-of-straightness in short columns. As seen in Figure 1, inelasticity and residual stresses predominantly affect short columns, in which large applied loads combined with residual stresses exceed the yield stress in portions of the cross-section thereby causing partial yielding and a loss in member stiffness. Similarly, out-of-straightness is most prominent in slender columns, where second-order effects manifest themselves as part of a positive feedback loop between lateral deflections and internal moments.

The current design by DM procedure uses the equations in Figure 1(b) to calculate the axial capacity. These equations are a function of the unbraced length. Neglecting any strength gain due to strain-hardening, full-yielding of the cross-section, P_y, represents the axial load upper limit:

$$P_y = F_y A_g \,, \tag{2}$$

where

$F_y \equiv$ yield stress

$A_g \equiv$ gross area of the cross-section.

The theoretical elastic buckling limit state is found by computing the Euler buckling strength, P_e, which assumes a perfectly straight, perfectly elastic, prismatic, pinned-supported column (Ziemian, 2010, p.23):

$$P_e = \frac{\pi^2 EI}{L_c^{\ 2}}, \tag{3}$$

where

$E \equiv$ Young's modulus, or elastic modulus *(29 000 ksi or 300 GPa for steel)*

$I \equiv$ cross-sectional moment of inertia.

The range of limit states from full-yielding to elastic buckling are coupled to formulate the AISC's column member-length nominal axial strength, P_n, as follows (AISC, 2010, p.33):

For $\frac{P_y}{P_e} \leq 2.25$,

$$P_n = \left(0.658^{\left(P_y/P_e\right)}\right)P_y \tag{4a}$$

For $\frac{P_y}{P_e} > 2.25$,

$$P_n = 0.877 P_e \tag{4b}$$

Unfortunately the equations can be difficult to apply for complex structural systems in which the member effective-lengths are not clearly defined e.g., arches, and thus, still pose a challenge to engineers. Because design by advanced elastic analysis does not consider member length to calculate the axial capacity of beam-columns, the design of such systems can be greatly facilitated. This combined analysis and design method is based on the principle that directly modeling those parameters that are known to affect member strength within a rigorous second-order elastic analysis removes the need to use

approximate methods to account for them (Maleck, 2003, p.2). For example, modeling out-of-straightness reduces the maximum load that can be applied by virtue of increased internal moments. In the case of residual stresses, applying a stiffness reduction τ_b–factor to the elastic modulus in the analysis assures inelastic buckling occurs prior to full-yielding. Modeling out-of-straightness and the effect of residual stresses, the need to employ Equation 4 is eliminated, thereby simplifying the axial strength calculation to one of computing the cross-sectional capacity, which can be accomplished by using Equation 2. In essence, design by advanced elastic analysis relies on more accurate estimates of the actual internal forces and moments to assess system strength by using a cross-section interaction equation (yield surface) check. In doing so, this analysis not only provides a better estimate of the internal forces, but also an enhanced representation of system behavior.

2.4. Stability Analysis Methods

By 2016, there will be four AISC stability analysis methods: ELM, design by DM, design by advanced elastic analysis and design by advanced inelastic analysis. ELM has been in the specification since 1961 and it was relocated from the main body of the Specification to Appendix 7 in 2010. In ELM, many factors affecting stability are not directly modeled and instead, effective-length *K*-factors are used to account for out-of-plumbness and spread of plasticity stiffness reductions (AISC, 2010, p.509). One method for calculating *K*-factors involves the use of sidesway-uninhibited frame alignment charts

based on the relative rigidity of a column with respect to the girders it frames onto, according to:

$$G = \frac{\Sigma(E_c I_c / L_c)}{\Sigma(E_g I_g / L_g)}$$

where $c \equiv$ subscript relating to columns, and $g \equiv$ subscript relating to girders. Unfortunately, *K*-values rely on many simplifying assumptions which are often violated, such as purely elastic behavior, only prismatic members, all rigid connections, reverse curvature bending of the columns, all columns buckling simultaneously, and no significant axial force in the beams (AISC, 2010, p.511). On a more positive note, ELM relies on the column-curve shown in Section 2.3 to account for out-of-straightness and yielding due to residual stresses, and this does not require modeling system imperfections and employing a stiffness reduction factor.

In 2005, design by DM was introduced in Appendix 1, and in 2010, it was included in Chapter C of the Specification as the preferred method of design by AISC. Design by DM simplifies the analysis by modeling out-of-plumbness explicitly or using notional loads, and reducing all stiffnesses by 0.8 to account for spread of plasticity, as well as a τ_b-factor to account for loss of stiffness due to residual stresses. In doing so, it removes the need to consider *K*-factors greater than unity (i.e., K = 1.0 in all cases). As with ELM, design by DM relies on the column-curve to account for out-of-straightness and partial yielding of the cross-section accentuated by residual stresses.

Design by advanced elastic analysis takes the next step towards a more transparent analysis method by requiring explicit modeling of out-of-straightness in addition to explicit modeling of out-of-plumbness and using stiffness reductions factors of 0.8 and τ_b. Thus the need to use the column-curve has been removed. In other words, the engineer may simply employ the axial cross-sectional strength when using Equation 1.

All three methods rely on the interaction equation to ensure system stability. In ELM and design by DM, the equation is calibrated to account for member-length failures, whereas in design by advanced elastic analysis, it acts solely as a cross-section yield surface criterion (See Section 2.2).

In contrast, design by advanced inelastic analysis requires explicit modeling of spread-of-plasticity and residual stresses within the analysis. In doing so, it removes the need to employ the interaction equation to assess stability and can thereby produce more efficient designs because load redistribution after the first plastic-hinge formation is permitted. Reductions previously applied to account for spread-of-plasticity (0.877 and τ_b) are no longer required. Instead, uncertainty factors of 0.9 are applied to the material elastic modulus and yield stress. The reader is referred to Appendix A for more information on this method.

The aforementioned design methods are compared with regards to the stability design requirements in Table 2:

Table 2. Comparison of design methods. Modified from (AISC, 2010, p.273)

<table>
<tr><th colspan="2">Chapter C stability design requirements</th><th>Effective-length Method (ELM)</th><th>Design by direct analysis method (DM)</th><th>Design by advanced elastic analysis</th><th>Design by advanced inelastic analysis*</th></tr>
<tr><td colspan="2">1 Consider all deformations</td><td colspan="4">All methods consider flexural, shear, axial and connection deformations</td></tr>
<tr><td colspan="2">2 Consider second-order effects (P-Δ and P-δ effects)</td><td colspan="2">Second-order analysis or
B1 and B2 factors</td><td colspan="2">Rigorous second-order analysis, including twist</td></tr>
<tr><td rowspan="3">3 Consider geometric imperfections (out-of-plumbness and out-of-straightness)</td><td>Effects of out-of-plumbness on structure response</td><td>If $B2 > 1.5$, use notional loads.</td><td>Direct Modeling, <u>or</u> notional loads.</td><td colspan="2" rowspan="2">System out-of-plumbness directly modeled.

Member out-of-straightness directly modeled.

Notional loads <u>not</u> permitted.</td></tr>
<tr><td>Effect of out-of-straightness on structure response</td><td rowspan="3">Full, nominal stiffness EI.

Member out-of-straightness and reduced stiffness due to inelasticity are considered by using KL from a sidesway (K>1) buckling analysis

Reduced member strength by virtue of KL > L</td><td>0.877 factor on E
(Φ x 0.877 = 0.8)</td></tr>
<tr><td>Effect of out-of-straightness on member strength</td><td>Member strength formulas, with KL= L</td><td colspan="2">Member cross-sectional strengths*</td></tr>
<tr><td rowspan="2">4 Stiffness reduction due to inelasticity and residual stresses</td><td>Effect on structure response</td><td colspan="2">τ_b factor on flexural stiffness
$EI_e = 0.8\tau_b EI$**</td><td colspan="2" rowspan="2">$EI_e = 0.9EI$
Residual stresses directly modeled</td></tr>
<tr><td>Effect on member strength</td><td>Member strength formulas, with KL = L</td><td>Member cross-sectional strengths</td></tr>
<tr><td rowspan="2">5 Uncertainty in stiffness and strength</td><td>Effect on structure response</td><td colspan="2">Φ factor on E
(Φ x 0.877 = 0.8)</td><td colspan="2" rowspan="2">Φ-factor on E and F_y incorporated into the analysis.</td></tr>
<tr><td>Effect on member strength</td><td colspan="2">Φ-factors in strength formulas</td></tr>
<tr><td colspan="6">*Design by advanced inelastic analysis extends design by advanced elastic analysis by explicitly modeling residual stresses and yielding, and allowing force redistribution. The analysis permits going beyond the formation of the first plastic-hinge.
**Reduction shall also be applied to the torsional stiffnesses GJ and EC_w in design by advanced elastic analysis.</td></tr>
</table>

As shown in the table, with less reliance on member strength equations, it becomes apparent that the more advanced methodologies are more readily suited for complex

geometries. As for conventional frames, the use of design by DM is still recommended because of its simplicity and accuracy.

2.5. Previous Studies

2.5.1. Surovek-Maleck and White Studies:

Design by DM is based on the modified elastic analysis-design method, ME, proposed by Maleck (2001). ME uses a reduction factor of 0.8 on the major-axis flexural stiffness and 0.7 on the minor-axis, whereas design by DM uses 0.8 on both. These reductions are coupled with the τ_b-factor in both methods. Similar to design by DM, direct modeling of out-of-plumbness grants the engineer the opportunity to use the unbraced length as L_c when calculating the axial capacity.

Maleck (2001) performed a comprehensive parametric study with nominal stiffness and strength terms (i.e. Φ was not applied) on four portal frame configurations and two braced-beam columns to assess the accuracy of ME with respect to design by advanced inelastic analysis, ELM and a notional load approach. The parameters included the slenderness ratio, column orientation and column end restraint. Maleck showed that including system out-of-plumbness imperfections and reducing the member's stiffness significantly improved the prediction of second-order moments in beam-columns and lead to unconservative error of less than 6% in the stability crucially frames analyzed. (Maleck, 2001, p.238).

To ensure that these results could be used in design, Surovek-Makeck and White (2003, 2004a, 2004b) analyzed a subset of 10 major-axis configuration and 7 minor-axis configuration frames using factored strength and stiffness terms to verify their claim that factoring both strength and stiffness terms provide the same results as applying a 0.9 factor to the abscissa and ordinate of a graph with the results of a study with nominal strength and stiffness terms (as in Maleck, 2001). This, indeed, proved to be true.

To quantify the error, they plotted the applied force vs. moment, normalized against the cross-section full-yield limit state (i.e., plots of P/P_y vs M/M_p), and then computed the percent radial error of ME and NL with respect to design by advanced inelastic analysis. The errors found for ME were -6% to +16% for frames under major-axis bending, and -6% to 20% for minor-axis bending. NL has -8% to 21% error for major-axis, and -13% to 20% for minor-axis; ELM showed -9% to 21% error for major-axis and -17% to 20% for minor-axis. The greatest unconservatism was observed at a dimensional slenderness of 1.3. Overall, ME and NL performed better than ELM, providing less error and capturing the structural behavior more consistently and accurately.

The high level of unconservatism observed in stability-critical frames with beam-columns under minor-axis sparked the minor-axis column study detailed in Section 3.5 to assess the performance of the design by advanced elastic analysis method with respect to the design by advanced inelastic analysis method. The columns studied in this section have a pinned base, rotation-restrained top configuration that emulates the symmetrical pinned base frames studied by Maleck (2001).

To reduce the unconservatism, Maleck and White (2004b, p. 1200) suggest using an appropiate equivalent uniform rigidity, EI_e, that accounts for moment gradient in beam-columns to produce a more accurate representation of material non-linear behaviour. Ziemian (2002) has proposed the modified tangent modulus, explained hereinafter, as a way of calculating EI_e. Alternatively, Nwe Nwe (2014) suggests factoring EI_y by 0.7 instead of 0.8, as in the original ME study by Maleck (2001).

2.5.2. Ziemian and McGuire study

As explained in Sections 2.3 and 2.7, the τ_b-factor was developed to account for partial yielding of the cross-section of a concentrically loaded column due to the combined effect of residual stresses and applied axial force. Technically, this reduction factor is only appropriate for beam-columns under pure axial force, but it has been shown to provide acceptable results for frames with beam-columns under major-axis bending (Ziemian and McGuire, 2002, p.1302). Nevertheless, partial yielding greatly impacts beam-columns subject to minor-axis flexure as explained in Section 2.2: '*...yielding progresses from the flange tips inward, reducing the flexural rigidity significantly faster than in beam-columns subject to major-axis bending (Maleck and White, 2004a, p.1191).'* This effect cannot be properly captured by the τ_b-factor because its equation is not a function of bending moment. One solution involves explicit modeling of member-length partial yielding, i.e. the distributed plasticity approach described in Appendix A. However, this would be computationally prohibitive and an EI_e approach is preferred.

Ziemian and McGuire (2002) have proposed to modify the τ_b-factor to obtain a more accurate EI_e. This EI_e accounts for varying partial yielding along the member length and cross-section. Combining EI_e and a yield surface criterion serves as the basis for a second-order plastic-hinge analysis that accurately models system behavior, including response well beyond the formation of the first plastic-hinge. By performing various distributed analysis using the Galambos and Ketter (1959) stress pattern, Ziemian and McGuire (2002, p.1302) developed the following τ factor, which considers the combined effects of axial force and minor-axis bending on beam-columns with residual stresses

$$\tau = \min\begin{pmatrix} 1.0 \\ (1+2p)((1-(p+\alpha m_y)) \end{pmatrix}, \tag{5}$$

where

$$p = \max(P/P_y, (0.5-\alpha m_y)/2$$

$$m_y = M_y / M_{py}$$

$\alpha = 0$ for major-axis bending and $\alpha = 0.65$ for minor-axis bending.

The benchmark frames presented in Section 3.4 were analyzed using EI_e (with E and F_y factored by 0.9) and load-displacement plots of these results were plotted to provide further evidence corroborating the predictive accuracy of EI_e, especially when compared to design by advanced inelastic analysis. The built-in MASTAN2 yield surface criterion was used for the EI_e analyses:

$$p^2 + m_z^2 + m_y^4 + 3.5p^2 m_z^2 + 3p^6 m_y^2 + 4.5 m_z^4 m_y^2 = 1$$

where $p = P/P_y$; $m_z = M_z/M_{pz}$; and $m_y = M_y/M_{py}$ (Ziemian, 2002, p.1301). This equation is often considered a more accurate representation of the yield surface than Equation 1.

2.5.3. Martinez-Garcia Study

Martinez-Garcia (2002) performed a comprehensive benchmark study of 12 frames using an effective-length method and design by DM for the AISC 2005 Specification. The effective-length method involves the use of notional loads equivalent to 2% of the gravity load, *K*-factors and the use of in-plane and out-of-plane interaction equations to account for stability. The *K*-factors used in this approach are based on elastic critical load analyses, which can be considered at a story level, i.e., simultaneous buckling of a story, or the entire structure, i.e., all beams/columns buckle simultaneously (Martinez-Garcia, 2002, p.36-37).

Design by DM, which has been described in Section 2.4, relies on second-order elastic analysis and notional loads (or direct modeling of story out-of-plumb initial imperfections) to increase the internal moments and compensate for the increase in axial capacity of columns by assuming L_c equal to the unbraced length (K=1). It uses the same in-plane interaction equation as the effective-length method to account for both in-plane and out-of-plane instabilities (Martinez-Garcia, 2002, p.38-39). The results were thoroughly compared to the results of advanced inelastic analysis using the finite element analysis software NIFA, developed at the School of Civil Engineering at the University of Sydney. This research showed that design by DM provides robust results for frames with beam-columns subject to major-axis bending.

2.5.4. Nwe Nwe Study

Nwe Nwe (2014) performed frame and column studies to verify what she termed the modified design by direct analysis method, MDM. This method consists of using the cross-sectional axial strength (Equation 3) instead of the column-curve (Equation 4) within the interaction equation (Equation 1). Nevertheless, it did not stipulate explicit modeling of member initial imperfections within the analysis. Nwe Nwe (2014) analyzed the twelve frames from the study by Martinez-Garcia (2002). Her study shows that using the cross-sectional axial strength instead of the member-length strength provides acceptable results for frames with beam-columns subject to major-axis bending, especially when compared to design by DM and design by advanced inelastic analysis. Nwe Nwe did note unconservative error greater than 5% for frames with beam-columns subject to minor-axis bending. From her research, she suggests factoring the minor-axis flexural stiffness by 0.7 instead of 0.8; that is, use $0.8EI_{major}$ and $0.7EI_{minor}$ in the analysis.

2.6. Adding Initial Member Imperfections

Initial geometric imperfections are often distinguished as system and member imperfections (Ziemian, 2010, p.716). System imperfections consist of story out-of-plumbness, which is the relative displacement of the top and bottom of the members in a story. A worst case-scenario of such out-of-plumbness can usually be chosen out of the four possible directions of lean in a three-dimensional building frame. Member out-of-straightness, or the initial deflection between member ends, is much more difficult to define.

Even though single curvature or double curvature bending imperfections are normally assumed, their real configuration may be very complicated (Ziemian, 2010, p. 41).

In the work presented later in this thesis, the geometric imperfections follow the recommendations by requirement (3) in Section 2.1: out-of-plumpness equal to 1/500 of the story height, and out-of-straightness of 1/1000 of the member length. Instead of using bow imperfections, member imperfections are employed by using scaled deflections from first-order elastic analyses. The rationale for using first-order deflections instead of buckling solutions stems from the fact that instability occurs gradually, as in a first-order analysis, and not necessarily due to bifurcation or sudden buckling. This is a simpler approach than the one proposed by Alvarenga, A. and Silveria R. (2009), who suggest using the rescaled collapse configuration following an inelastic second-order analysis.

Alternatively, Agüero et al. (2015a, 2015b) propose using a single imperfection instead of separate system and member imperfections. Their proposed imperfection, akin to the buckling mode, aims at capturing not only bending but also torsional effects due to axial force and applied moments. Similarly, Shayan et al. (2014) propose the use of a rational method backed by a probabilistic study. In their proposed method, initial imperfections are modeled as a linear combination of the first three eigenmodes for unbraced frames, and the first six for braced frames with modeling errors of up to 8 and 2.5% respectively.

2.7. Modeling Residual Stresses

Residual stresses need to be considered in the analyses, either directly or by using approximate representation. FE++2015 models residual stresses directly in the analysis using the Lehigh stress pattern (Galambos and Ketter, 1959, p.30) shown in Figure 3.

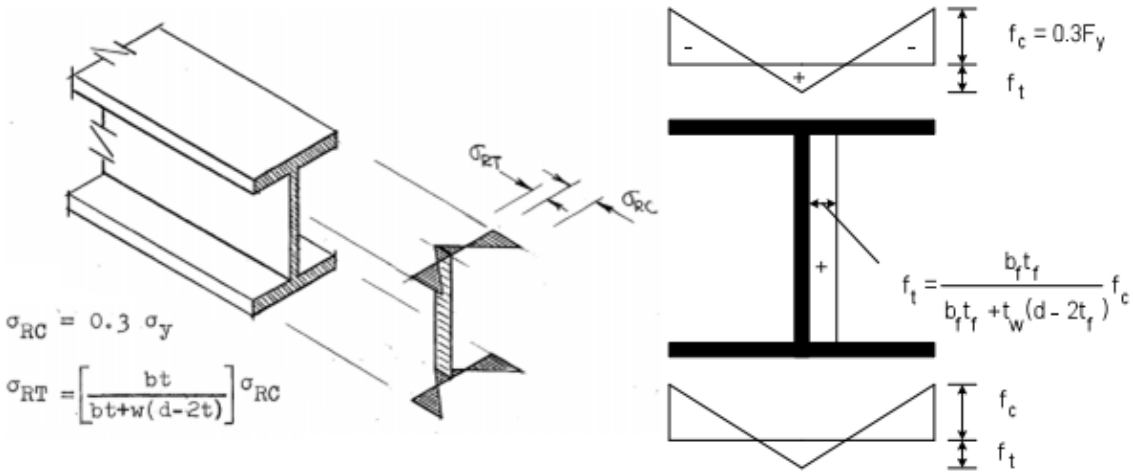

Figure 2. Stress pattern. From Galambos and Ketter (1959) and Surovek (2012)

As an alternative, AISC's 2010 Specification requires the use of Equation 6 to compute a reduction τ_b-factor which is to be applied to the flexural stiffnesses of all the members that contribute to the stability of the structure. In the 2016 Specification, this requirement may be extended to all stiffnesses including axial and flexural, which facilitates the analysis because the stiffness reduction τ_b-factor may simply be applied to the elastic modulus, *E*, which is represented in all stiffnesses values.

$$\tau_b = 4(P_r / P_y)[1-(P_r / P_y)] \quad \text{when} \quad P_r / P_y > 0.5\,, \tag{6a}$$

$$\tau_b = 1 \quad \text{when} \quad P_r / P_y \le 0.5\,, \tag{6b}$$

where P_r is the required axial compressive strength, i.e. second-order internal axial force.

CHAPTER 3: METHODOLOGY

The systems investigated in this research are based on two-dimensional benchmark frames published by ASCE (Surovek, 2012), frames by Martinez-García and Ziemian (2006), and the El-Zanaty frame, as referenced in Ziemian and McGuire (2002). The details of these frames are presented in Section 3.4. It should be noted that certain limitations modeling members with pin connections in FE++2015 (Bulemt Alemdar, 2015), elicited minor changes in frame 7b, 7c and 7d, as presented in Section 3.4.

Each frame has two variations, one with member initial imperfections explicitly modeled and another without such imperfections included. This allowed for comparing the results of design by advanced elastic analysis, which requires modeling system and member imperfections, with design by DM, which only stipulates modeling system story out-of-plumbness. The general procedure for all the frames is summarized as follows:

1) Initial member imperfections were represented in the frames per Section 3.1.
2) Design by advanced inelastic analysis (using FE++2015) was completed on the frame configuration of step 1.
3) The loads were rescaled such that the frames fail at an applied load ratio of unity, λ=1.0, using design by advanced inelastic analysis (later referred to as FE++2015, or simply FE++).
4) The rescaled loading from step 3 was applied to both sets of frames, including those with and without member initial imperfections.

5) Secant stiffness reduction τ_b-factors were determined for both sets of frames at λ = 1.0, per Section 3.2.
6) Second-order elastic analyses (using MASTAN2) were completed on both sets of frames.
7) The AISC interaction equation (Equation 1) was evaluated for all members at λ=1.0 for design by DM and design by advanced elastic analysis, per Section 3.3.
8) The lowest applied load ratio λ at which any member has an interaction equation value of unity is determined. This value is also referred to as the ultimate applied load ratio, ultimate λ (See Section 3.3).
9) Load vs. lateral displacement curves showing results from FE++2015, design by DM, design by advanced elastic analysis, and the modified tangent τ-factor (Etm method) proposed by Ziemian (2002) are plotted to evaluate these methods in predicting system behavior.

The applied load ratios that each method predicts were then compared to the load ratios at failure from design by advanced inelastic analysis (step 3 in above procedure) using the values obtained in step 8. Ideally, this value should be as close to 1.0. Values greater than 1.0 indicate unconservative error, while lower values may be attributed to a member strength limit state that is assumed to compromise the overall stability of the system. Section 3.5 uses frame 7d as a detailed example to illustrate this procedure.

As part of a sensitivity analysis, the effect of not including initial out-of-straightness imperfections in design by advanced elastic analysis was also quantified. The difference between using the secant τ_b-factor from Section 3.2 and the same τ_b-factor applied tangentially in the analysis were also studied. The percent differences in the ultimate load λ-ratios demonstrate whether or not modeling initial imperfections and using the stipulated secant τ_b-factor have a substantial impact in accuracy.

Section 3.6 further describes a minor-axis column study, which was completed to evaluate the unconservatism in beam-columns under minor-axis bending using design by advanced elastic analysis. Because both MASTAN2 and FE++ can be run within the MATLAB platform, MATLAB code was written to perform all of the aforementioned steps, except for steps 3 and 4. While the code is not included within the body of this thesis, the flowcharts presented in this chapter are accurate representations of the code employed.

3.1. Initial Member Imperfections

This section describes how the initial member imperfections were modeled in this study. Each structural member, represented by a series of finite elements between member ends, was modeled using 8 line elements in the MASTAN2 analysis software, and thus their member out-of-straightness is well defined by the end coordinates of these elements. (In addition to modeling initial out-of-straightness, it assists in more accurately capturing P-δ effects). MATLAB code was written to include initial out-of-straightness

imperfections in the MASTAN2 models. Although the flow chart and equations that follow illustrate how the member initial imperfections were added, a brief overview is provided below.

Three coordinate systems are employed:

i. Definition of the global space, with X-, Y-, and Z-axes spanned by the $\{\hat{\imath}\}$, $\{\hat{\jmath}\}$ and $\{\hat{k}\}$ basis;

ii. definition of the local space of each member in its undeflected shape, with x'-,y'-, and z'- axes spanned by the $\{\hat{\imath}'\}, \{\hat{\jmath}'\}$ and $\{\hat{k}'\}$ basis; and

iii. definition the local space of each member in its deflected shape with x''-, y''-, and z''- axes spanned by $\{\hat{\imath}''\}$, $\{\hat{\jmath}''\}$, and $\{\hat{k}''\}$ basis.

It should be noted that vectors in the global space have no subscript or the subscript 'o' to indicate their base location has been shifted to the origin. Vectors in either local coordinate space have the subscript 'local.'

After completing a first-order elastic analysis, each deflected member's coordinates were retrieved, rescaled to have a maximum amplitude of $L/1000$ and rotated to align with the corresponding member's undeflected orientation. After retrieving each of the deflected members' coordinates, these were displaced such that the begin node at the start of the member is at the origin to facilitate subsequent transformations. Rescaling the deflected member requires working in its local space, which can be expressed with the Γ_1 global-to-local transformation matrix:

$$\Gamma_1 = \begin{bmatrix} l_x & m_x & n_x \\ l_y & m_y & n_y \\ l_z & m_z & n_z \end{bmatrix},$$

where

$\{\hat{i}''\} = \lfloor l_x \;\; m_x \;\; n_x \rfloor^T \equiv$ unit vector along deflected shape local *x*-axis in global space,

$\{\hat{j}''\} = \lfloor l_y \;\; m_y \;\; n_y \rfloor^T \equiv$ unit vector along deflected shape local *y*-axis in global space,

$\{\hat{k}''\} = \lfloor l_z \;\; m_z \;\; n_z \rfloor^T \equiv$ unit vector along deflected shape local *z*-axis in global space.

Once rescaled, the coordinates were shifted back to the global space. This was done by pre-multiplying them by the inverse of Γ_1, which equals its transpose, $\Gamma_1^T = \Gamma_1^{-1}$. Then, the rescaled deflected shape was rotated from its position along the deflected member local x''-axis to the undeflected member local x'-axis using the rotation matrix Γ_2:

$$\Gamma_2 = \begin{bmatrix} \cos(\theta) + u_x^2\big(1-\cos(\theta)\big) & u_x u_y\big(1-\cos(\theta)\big) - u_z\sin(\theta) & u_x u_z\big(1-\cos(\theta)\big) + u_y\sin(\theta) \\ u_y u_x\big(1-\cos(\theta)\big) + u_z\sin(\theta) & \cos(\theta) + u_y^2\big(1-\cos(\theta)\big) & u_y u_z\big(1-\cos(\theta)\big) - u_x\sin(\theta) \\ u_z u_x\big(1-\cos(\theta)\big) - u_y\sin(\theta) & u_z u_y\big(1-\cos(\theta)\big) + u_x\sin(\theta) & \cos(\theta) + u_z^2\big(1-\cos(\theta)\big) \end{bmatrix},$$

where

$u = \lfloor u_x \; u_y \; u_z \rfloor^T = \left\{\hat{i}''\right\} \times \{\hat{i}'\} \equiv$ axis of rotation from $\{\hat{i}''\}$ to $\{\hat{i}'\}$.

$\theta = \arccos(\{\hat{i}''\}^T \{\hat{i}'\}) \equiv$ angle of rotation from $\{\hat{i}''\}$ to $\{\hat{i}'\}$.

This rotation accounts for the relative displacement of the element end nodes. Lastly, the deflected shape is shifted such that the start node of the member is returned to its original undisplaced location.

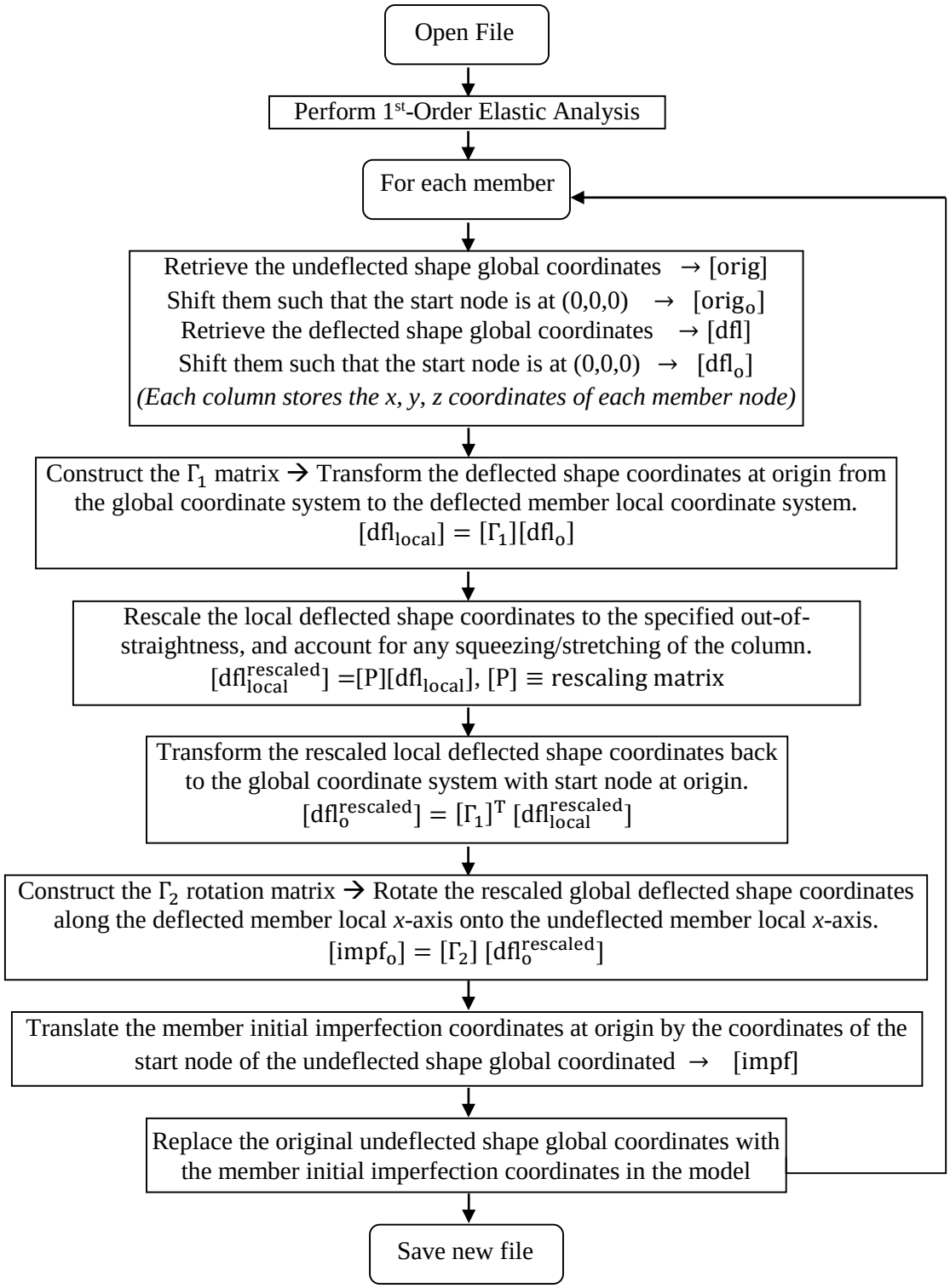

Figure 3. Flow diagram for adding out-of-straightness imperfections

3.2. Secant τ_b-factor vs. tangent τ_b-factor

Residual stresses were included in the analyses using the stiffness reduction τ_b-factor represented in Section 2.7. Equation 6 was used to compute τ_b at an applied load ratio of $\lambda = 1.0$. In other words, τ_b was not updated in the step-wise analysis as more axial load is applied onto the structure. Instead, it was based on the internal axial force distribution at the given applied load. In general, this is defined as a secant factor. This approach presents some complications:

i. Finding τ_b requires an iterative process because the internal forces cannot be obtained without running an analysis that uses the τ_b factor. Luckily, the axial force distribution can be well approximated from a first-order equilibrium analyses as the deformed and undeformed geometries are quite similar.

ii. Secondly, the secant τ_b-factor is constantly varying at each load ratio. That is, if one is interested in determining the internal forces and moments in a member at an applied load ratio λ different from the ultimate applied load λ-ratio, an iterative procedure would be required to determine the τ_b-factor for that given load ratio.

The alternative to the secant τ_b-factor, which was also employed in this study, would be to use a tangent-modulus τ_b-factor, which would simply be to update at each load increment in the analysis (Ziemian, 2010, p.705). This straightforward procedure requires no iterations and provides the τ_b-factor at any given load step. In this study, all frames were analyzed using both secant and tangent τ_b-factors and the percent difference of the results

is calculated. Note that only secant τ_b is computed in a separate algorithm. MASTAN2 by Ziemian and McGuire (2015) modifies each element stiffness matrix by using its built-in tangent τ_b calculator.

A similar stiffness reduction factor approach is the modified tangent factor, which was proposed by Ziemian and McGuire (2002), and is explained in Section 2.5.2. The load-displacement plots that will be presented in Chapter 4 also include the behavior predicted by the use of the modified tangent factor.

3.3. Interaction Equation and Applied Load Ratio

Figure 4 shows the steps used to find the AISC Interaction equation value (Equation 1) per design by DM and design by advanced elastic analysis. This equation is referred to as H1-1 in AISC's 2010 Specification, and was named accordingly in the flow charts and tables that follow. The axial and moment capacities of each member are computed per Section 2.3 and used in conjunction with the internal forces at an applied load ratio of λ = 1.0.

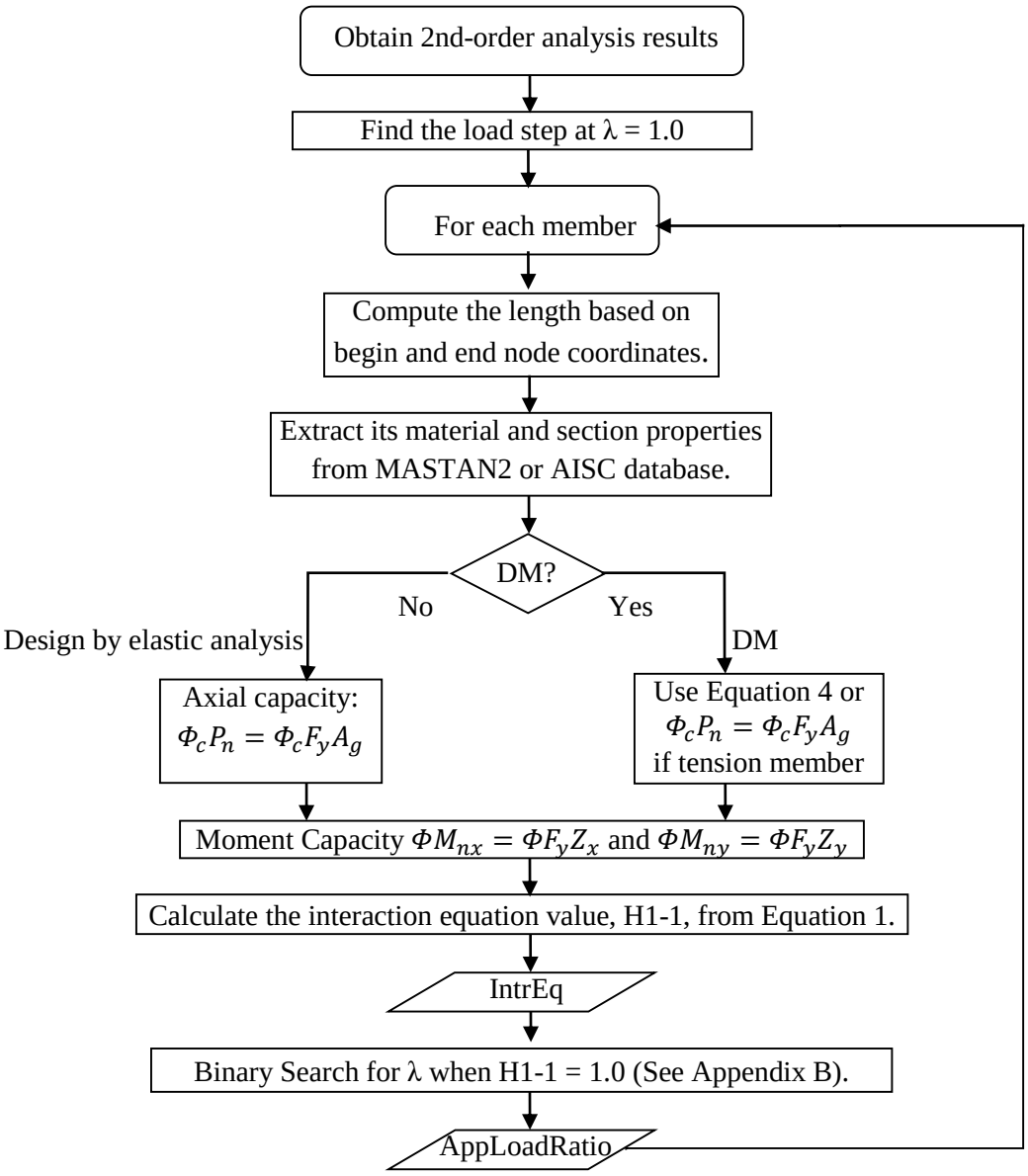

Figure 4. Interaction Equation at λ = 1.0 and λ at Interaction Equation = 1.0

Similarly, to find the applied load ratio λ at which each member has an interaction equation value of unity, a binary search algorithm (Appendix B) was written and performed. The lowest λ at which any member violates the interaction equation is also referred to as the ultimate λ-ratio, because this is the applied load ratio at which the controlling member

has an interaction equation value that exceeds unity. The ultimate λ-ratio was used to compare capacities ratios predicted by design by DM and design by advanced elastic analysis against design by advanced inelastic analysis.

Obtaining applied load ratios λ-values at which each member has an interaction equation value of unity is straightforward when an analysis with tangent τ_b has been performed. However, as stated in Section 3.2, the use of secant τ_b factor renders finding the correct λ value an iterative process that requires at least one analysis per member. Thus, to simplify the process, only the lowest applied load ratio λ was recorded.

3.4. Description of frames

This section provides descriptions of the 12 benchmark frames that were investigated in this research and obtained from studies by (i) Ziemian and Martinez-Garcia (2006) on the feasibility and reliability of design by DM; and (ii) the El-Zanaty frame as studied by Ziemian and McGuire (2002). The figures in this section show the controlling load combination and out-of-plumbness direction for each frame. The loads shown are often provided to several significant figures because they represent the rescaled loads such that the frames fail at an applied load ratio λ of 1.0 according to a rigorous second-order inelastic analysis (FE++2015). All gravity and lateral loads are applied proportionally.

System 1a – Ziemian and Miller (1997) Unsymmetrical Frame (Major-axis)

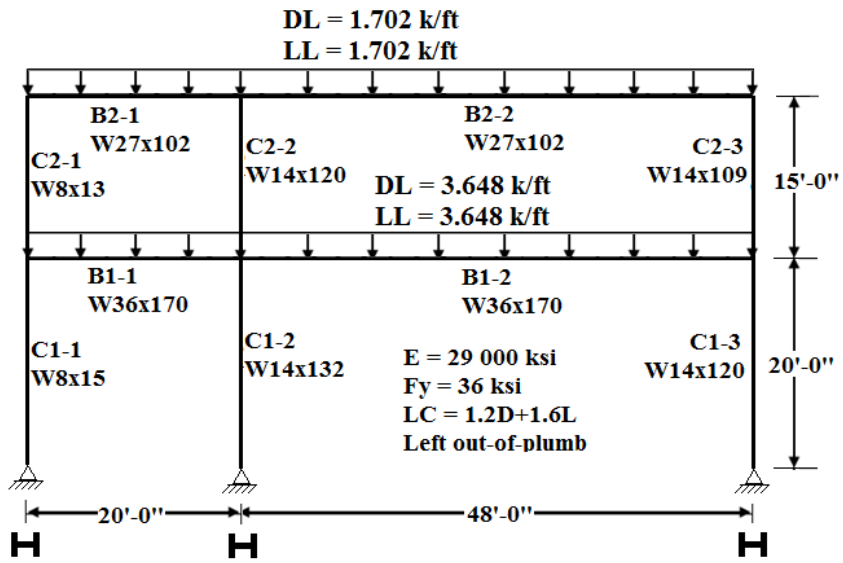

Figure 5. Ziemian and Miller Frame (Major-axis). Modified from Nwe Nwe (2014)

This frame, originally studied by Iffland and Birnstiel (1982) and Ziemian and Miller (1997), represents a two-story industrial frame with a high gravity-to-lateral load ratio typical of low-rise industrial buildings. In the Martinez-García study (2002, p.88), it was established that the load combination shown was the controlling load combination, when combined with a system initial out-of-plumbness to the left. The large gravity load is intended to produce significant second-order effects in the presence of small lateral initial imperfections (Nwe Nwe, 2014, p.26). Furthermore, the left-most columns were designed smaller than the other ones for efficiency reasons and as a result are reduced to leaning columns obtaining their stability from the remaining portion of the frame. As a result, the second-order effects from the high gravity load acting upon them are significantly accentuated (Nwe Nwe, 2014, p.26). All columns are oriented for major-axis bending and the frame is assumed to be fully braced out-of-plane.

System 1b – Ziemian and Miller (1997) Unsymmetrical Frame (Minor-axis)

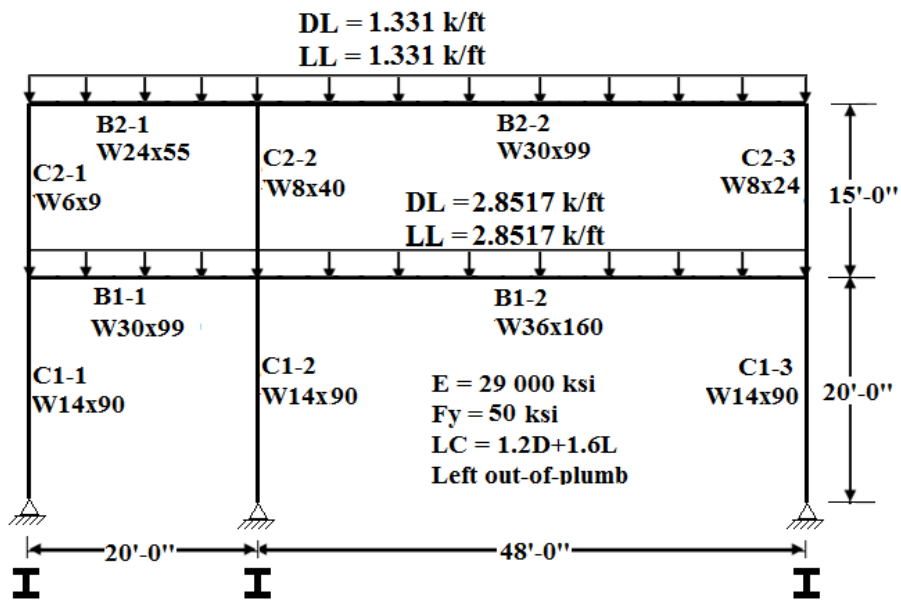

Figure 6. Ziemian and Miller Frame (Minor-axis). Modified from Nwe Nwe (2014)

This frame has the same geometry and dimensions as the previous system, except that the columns are oriented for minor-axis bending. This frame serves as an example to verify the adequacy of design by advanced elastic analysis for investigating frames with members subject to minor-axis bending.

System 2 –Maleck (2001) Industrial Frame (Major-axis Bending)

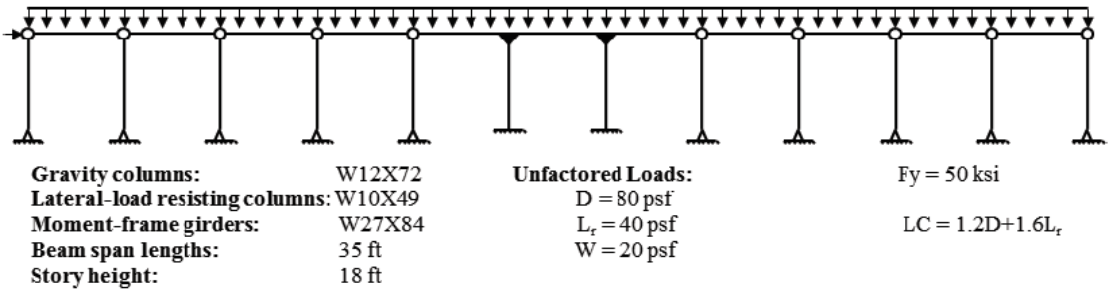

Figure 7. Maleck 11-Bay Industrial Frame, Originally from Surovek (2012, p.33)

The system shown in Figure 7, initially developed by Maleck (2001), is a single-story industrial building with only a few columns providing lateral support for many bays (Surovek, 2012, p. 32). Such buildings usually have a high gravity to wind load ratio causing the behavior to be dominated by the P-Δ effect from the gravity load acting on the out-of-plumbness and subsequent deflections (Surovek, 2012, p.32). Martinez-García and Ziemian (2006) simplified the frame to an equivalent three-bay system with two exterior leaning columns that represent the combined applied load and axial stiffness of the former leaning columns. The equivalent frame can be seen in Figure 8.

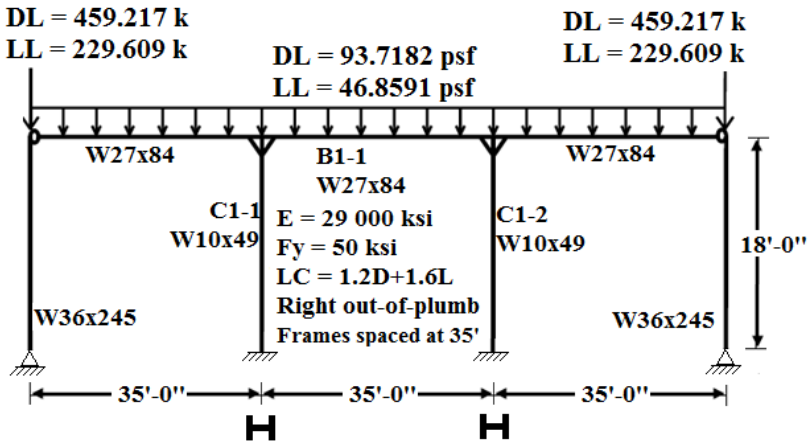

Figure 8. Maleck 3-Bay Industrial Frame, Modified from Surovek (2012)

System 3 – Grain Storage Bin (Major-axis Bending)

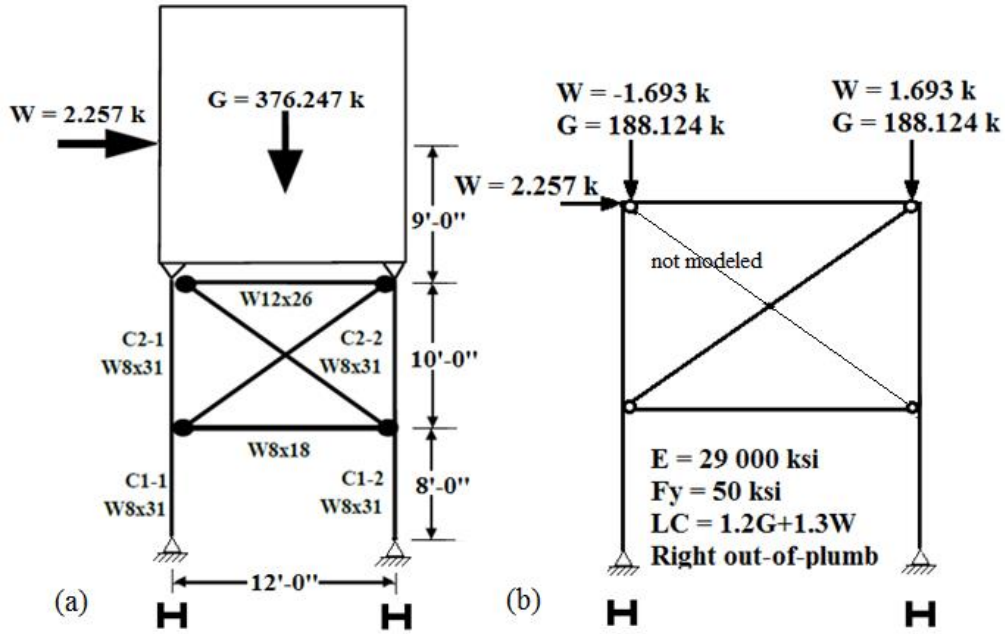

Figure 9. (a) Grain Storage Bin. (b) Analysis Representation. Modified from Nwe Nwe (2014)

Figure 9 shows a structural system that was studied by Martinez-García (2002) and Nwe Nwe (2014). The system represents an elevated structure in which the relatively high location of the gravity load causes significant destabilizing effects (Nwe Nwe, 2014, p. 29). The comparatively large gravity-to-wind load ratio produces significant second-order effects in the presence of a small lateral imperfection or wind loading. The bracing is provided by W4x13 section members, with only the tension member modeled in the analysis. The wind and gravity loads are converted into equivalent single loads as shown in Figure 9(b) (Nwe Nwe, 2014, p.30). All sections are oriented for bending about their major-axis, and the structure is assumed fully braced out of plane.

System 4 – Vogel (1985) Multi-Story Frame (Major-axis Bending)

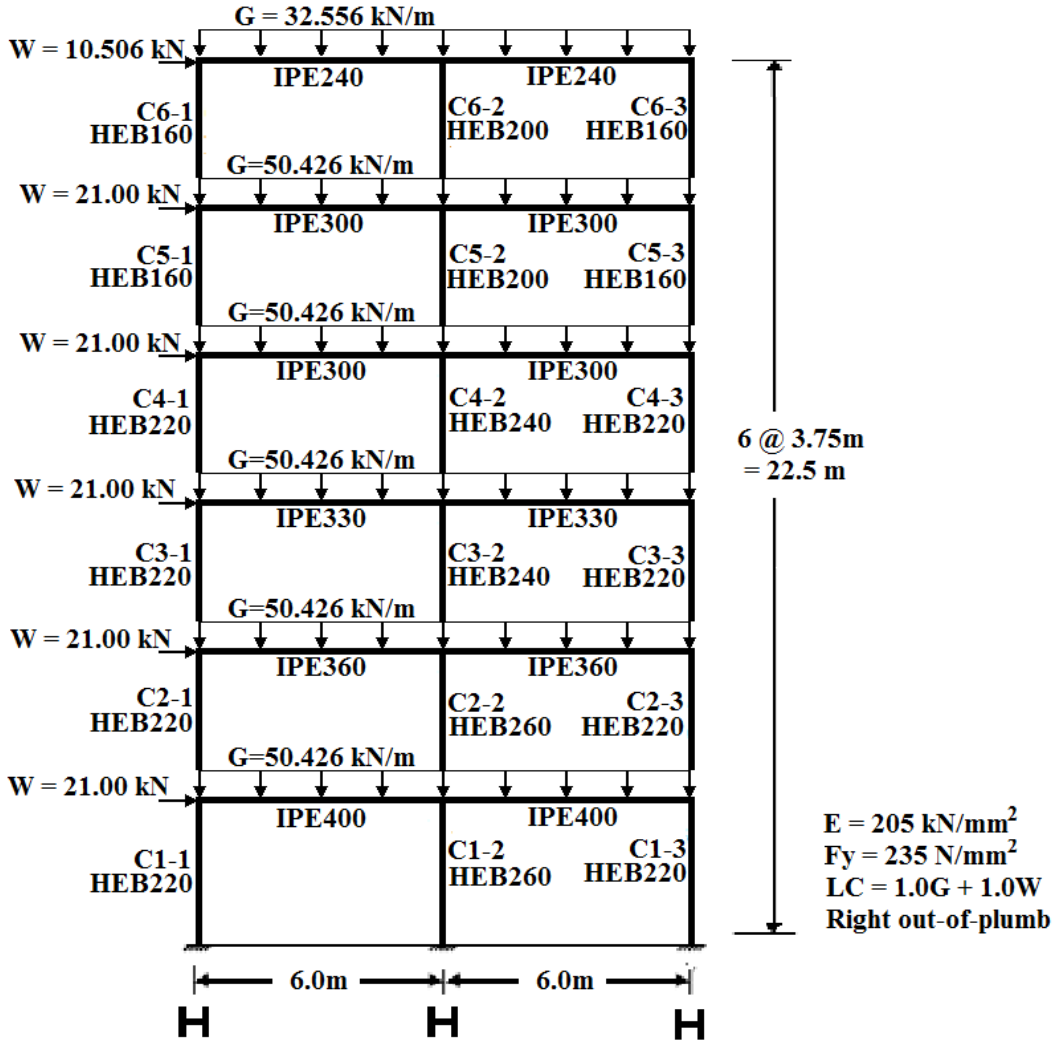

Figure 10. Vogel (1985) Frame (Major-axis) Modified from Nwe Nwe (2014)

The frame shown in Figure 10, originally proposed by Vogel (1984), represents a multi-story building. The frame was studied by Ziemian (1990), Maleck (2001), and Martinez-Garcia and Ziemian (2002, 2006), among others. Vogel (1984) provided factored loads, and thus a load combination of 1.0G + 1.0W is used (Nwe Nwe, 2014, p. 32). The frame columns are European HEB sections (H-shaped) and the beams are IPE sections (I-

shaped). All connections and foundations are assumed rigid. All members are oriented for major-axis bending with the frame fully braced out of plane.

System 5 – Martinez-García (2002) Gable Frame (Major-axis)

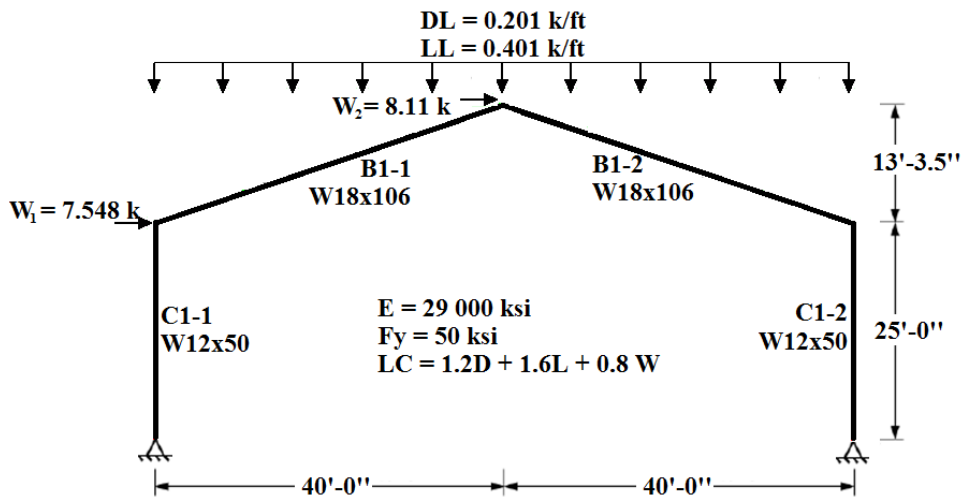

Figure 11. Martinez-García Gable Frame. Modified from Nwe Nwe (2014)

System 5, from Martinez-García (2002), shows a typical industrial gable frame. The frame is statically indeterminate to the second degree and thus becomes a kinematic mechanism after formation of the second plastic-hinge (Nwe Nwe, 2014, p.33). At about 65% of the applied load ratio at failure, formation of the first plastic-hinge causes a substantial reduction in the system lateral stiffness (Surovek, 2012, p. 34). All sections are oriented for major-axis bending, and the structure is assumed fully braced out of plane.

System 6 – Martinez-García (2002) Moment Frame (Major-axis)

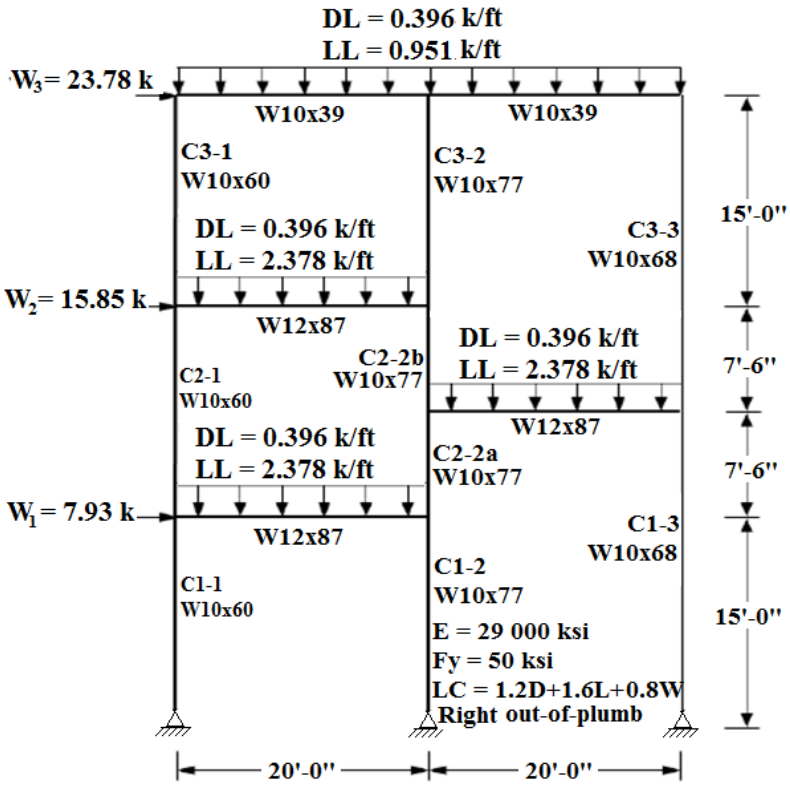

Figure 12. Martinez-García Moment Frame. Modified from Nwe Nwe (2014)

The frame in Figure 12 is an irregular two-bay frame that highlights the difficulty using story-based design methods such as the effective-length method (Surovek, 2012, p. 40; Nwe New, 2014, p. 35). For this frame, only load combination LC1 (1.2D+1.6L+0.8W) which includes both wind load and out-of-plumbness acting to the right, was considered (Nwe Nwe, 2014, p.35). The assumption that this loading condition has the lowest ultimate load can be rationalized by the presence of more slender columns on the right portion of the frame, which become leaning columns upon application of gravity load, whereas the left columns possess greater restraint. All sections are oriented for major-axis bending, and the structure is assumed fully braced out of plane.

System 7a –Two Bay Moment Frames, Unequal Heights (Major-axis)

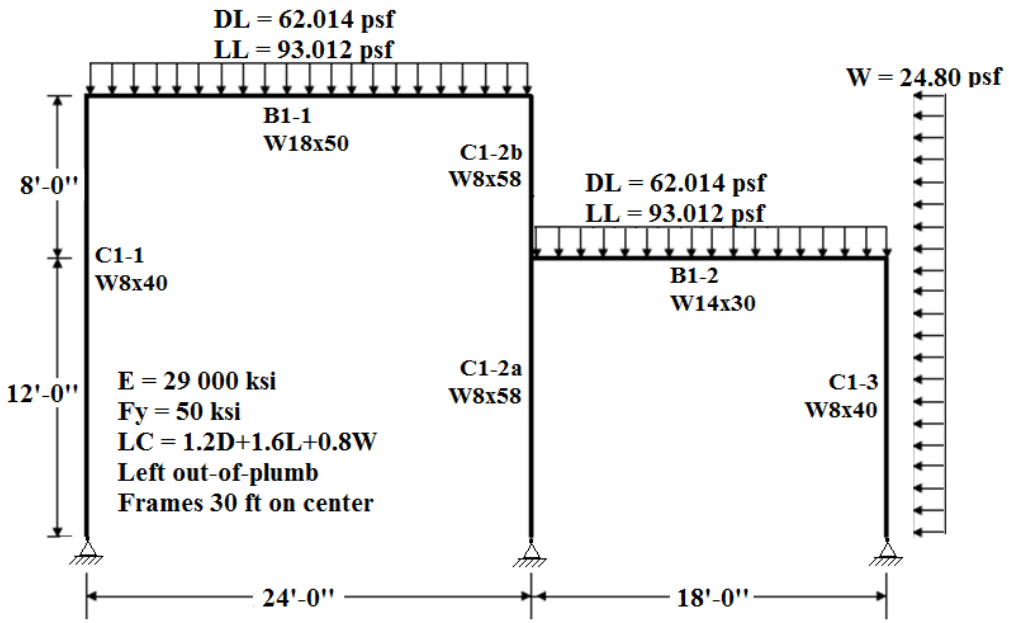

Figure 13. System 7a. Modified from Martinez-García (2002)

This frame was originally presented by Martinez-García (2002) as one with a simple irregular geometry. Systems 7b, 7c and 7d have variations in connection restraint and the presence of lateral bracing. This system has pinned supports at the base, but the connections are otherwise rigid.

System 7b –Two Bay Moment Frames, Unequal Heights (Major-axis)

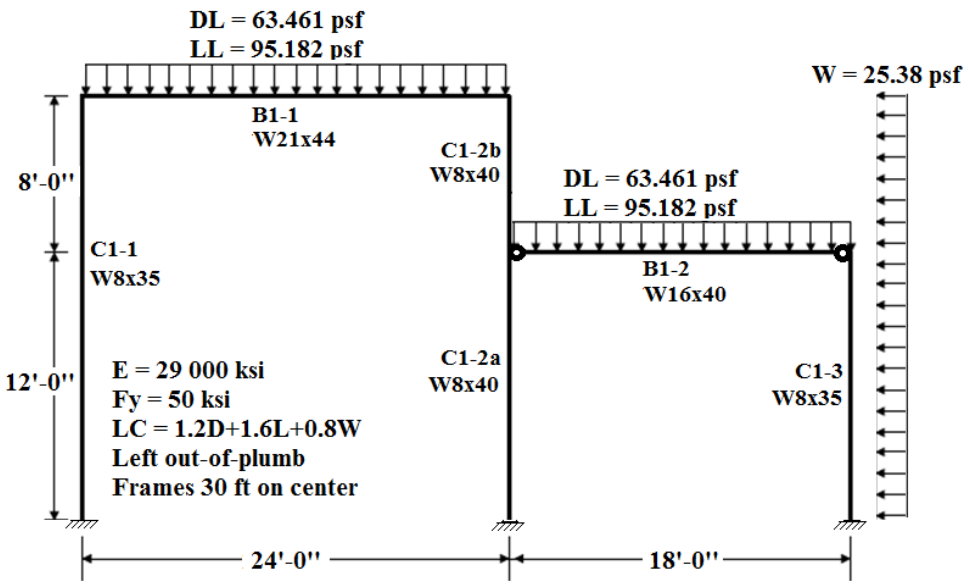

Figure 14. System 7b. Modified from Martinez-García (2002)

System 7b is a variation of system 7a. As originally presented by Martinez-García (2002), it possessed a distributed load atop member B1-2. However; limitations in the FE++2015 analysis software required that the distributed load be represented as two separate concentrated loads at each end of the beam. System 7b is a major-axis bending system that is fully braced out-of-plane. Although this system has fixed base supports, member B1-2 has pinned connections at both of its ends.

System 7c – Two Bay Braced Frame, Unequal Heights (Major-axis)

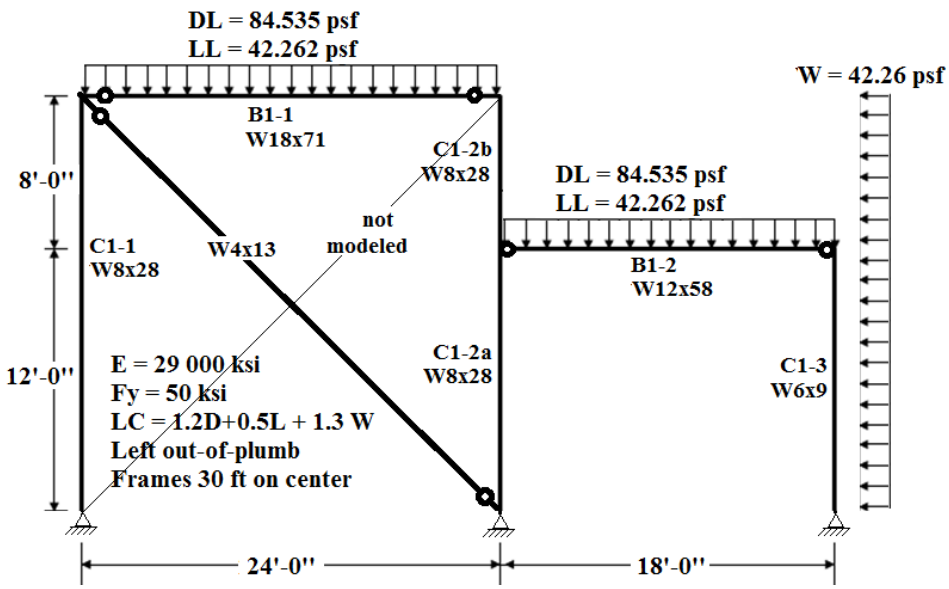

Figure 15. System 7c. Modified from Martinez-García (2002)

System 7c was also originally proposed by Martinez-García (2002) and possessed a distributed load along beams B1-1 and B1-2. As with system 7b, however, these loads had to be represented as concentrated loads at the member ends. It is noted that the leaning column on the right, C1-3, together with pinned member B1-2, form a kinematic mechanism that does not provide any lateral bracing to column C1-2. As such, the unbraced length of C1-2 is not from connection to connection, but rather taken as its entire length.

System 7d – Two Bay Braced Frame, Unequal Heights (Minor-axis)

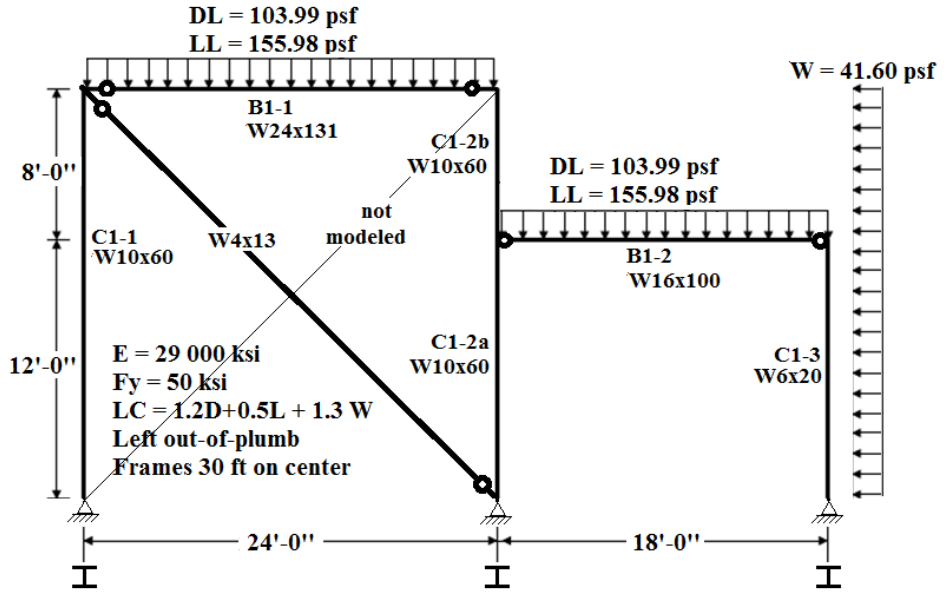

Figure 16. System 7d (Minor-axis) Modified from Martinez-García (2002)

System 7d has the same geometry as the previous three frames. However, the beams' sections are smaller in order to be compatible with the columns which are oriented for minor-axis bending (Nwe Nwe, 2014, p. 40). Similarly, the gravity loads are smaller to account for the fact that smaller sections are used. This system is thoroughly analyzed in Section 3.5 as the example illustrating the design by advanced elastic analysis methodology. As with system 7c, the right leaning column, C3-1, together with member B1-2 form a kinematic mechanism that does not provide lateral bracing to column C1-2, and thus, the unbraced length of C1-2 is taken as its entire length.

System 8 – Vierendeel Truss

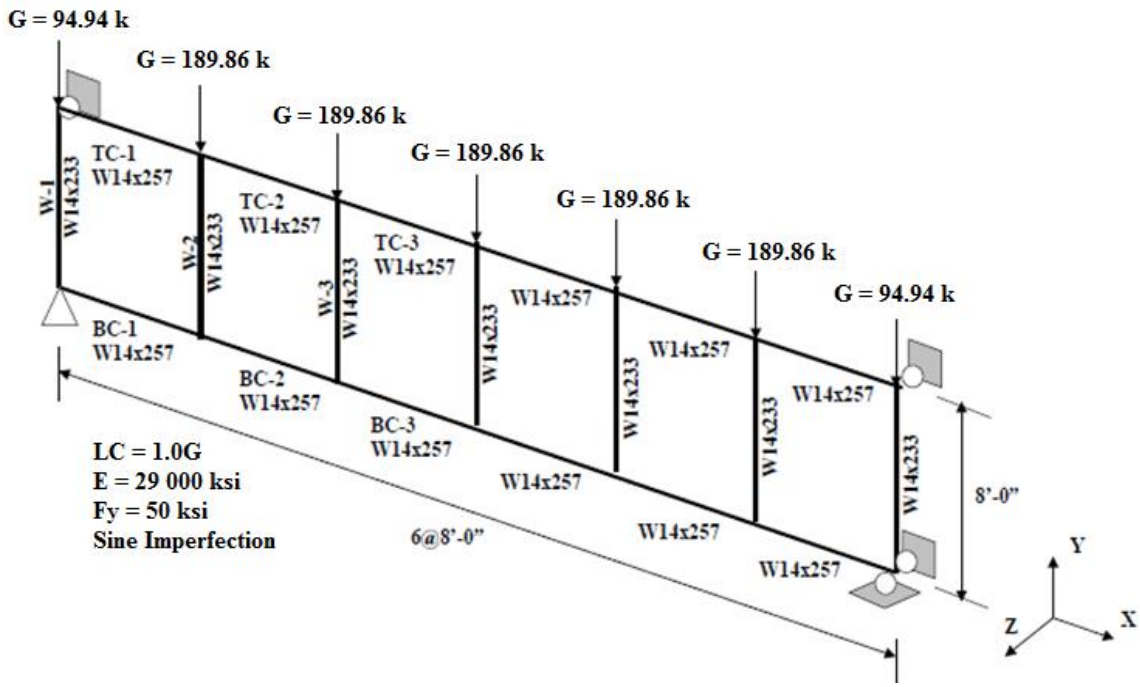

Figure 17. Vierendeel Truss. Modified from Martinez-García (2002)

System 8 was developed by Martinez-García (2002) as a three-dimensional system for his studies of the design by DM. Vierendeel trusses, such as the one shown in Figure 17, are commonly used to support pedestrian walkways. In the study by Nwe Nwe (2014) the sections and loading of the original design were modified to ensure that plastic yielding controls the frame's moment strength. Furthermore, and due to a limitation in FE++2015, torsional warping resistance is not included in this study. Although all sections are oriented for major-axis bending, there are minor-axis bending moments as a result of the three-dimensional half-sine imperfection along the length of the frame (z-axis). The system is not braced out-of-plane. Because of the system symmetry, only results for the members in the left portion of the truss are provided.

System 9 – El Zanaty Frame

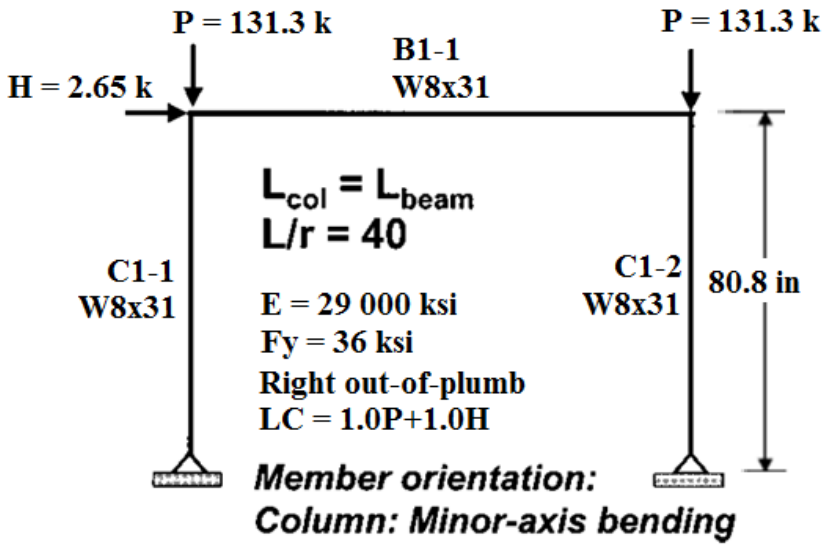

Figure 18. El-Zanaty Frame, modified from Ziemian (2002)

The El Zanaty frame, extracted from the study by Ziemian and McGuire (2002), is a stability critical frame. The beam is oriented for major-axis bending and both columns are oriented for minor-axis bending. Although this frame is very similar to the Kanchanalai frame (1977), it differs in that there are minor levels of overturning moment and the relatively flexible beam provides limited lateral stability.

3.5. System 7d Detailed Example

System7d was chosen as the example to illustrate the general procedure outlines in the beginning of Chapter 3. Following step 1, a first-order elastic analysis was performed and initial member imperfections were incorporated into the model. This frame was subsequently analyzed with FE++2015 using the factored loads shown in Figure 16, which yielded an applied load ratio λ at failure. The loads were then multiplied by the λ-value at

failure, such that performing another FE++ analysis would yield a system strength limit stat at an applied load ratio of $\lambda = 1.0$. The rescaled loads, shown in Figure 19, were then applied to the models of the frame with and without initial member out-of-straightness. The ultimate load ratios, λ values, obtained after analyzing the frame using the modified tangent modulus, Etm, design by advanced elastic analysis, DEA, and design by DM are provided in this figure.

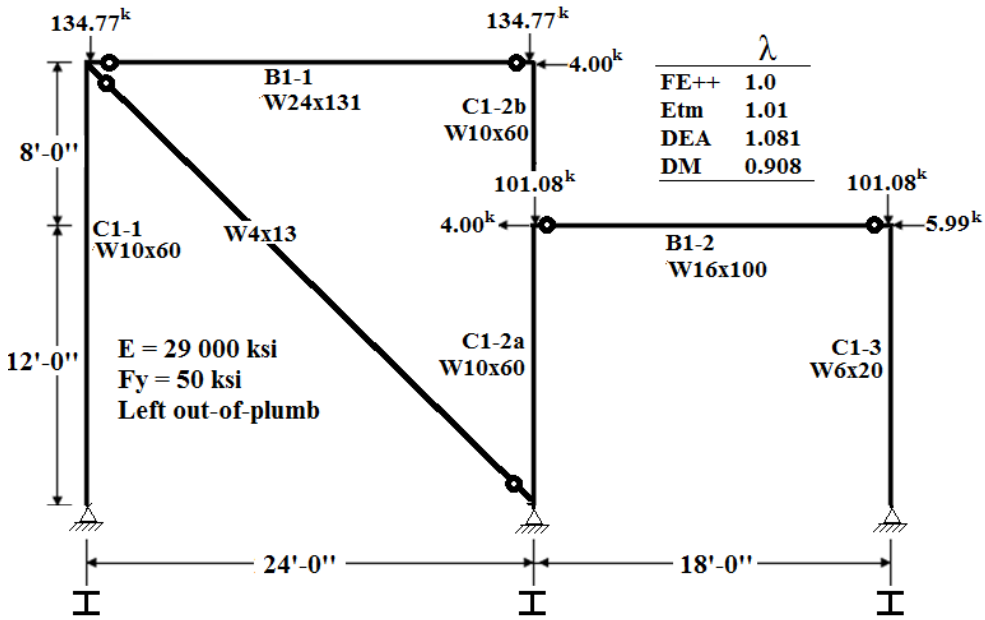

Figure 19. Frame 7d with factored loads

Before performing the second-order analysis needed for the design by advanced elastic analysis and design by DM methods, the secant τ_b factors were obtained from first-order analyses on both frames with and without initial out-of-straightness. It was found that no member had P/P_y greater than 0.5, and thus τ_b is equal to 1.0 for all members. This implies there is no difference in employing a secant τ_b or tangent τ_b in subsequent second-order analyses.

Assessment of the design by advanced elastic analysis method is the more straightforward method and explored first. A second-order analysis is performed on the frame with member out-of-straightness, and then the load step at which the applied load ratio of λ=1.0 is secured. In this case, the load step at which λ = 1.0 was found to be the 100th step, but this may not always the case given the nature of the solver. At this load step, the second-order internal forces and moments of each member were retrieved and used in conjunction with the member axial and moment capacities (i.e., $P_n = F_yA_g$ for the axial capacity, $M_{nx} = Z_xF_y$ and $M_{ny} = Z_yF_y$.) in the interaction equation, Equation 1, for a unity check.

Similarly, for design by DM, a second-order analysis was run on the frame without member out-of-straightness. The next steps were the same as for design by advanced elastic analysis except that the axial capacity is computed using Equation 4. Although these capacities are usually computed assuming the unbraced length of each member is equal to the distance between its end connections, beam B1-2 does not provide any restraint to column C1-2, and thus, the right bay of the frame is simply leaning on this column. As a result, the unbraced length should be taken as the entire length of member C1-2 (20’-0”).

These steps are summarized in the flow chart presented in Section 3.3. Table 3 shows the results for both design by DM and design by advanced elastic analysis procedures. As part of the sensitivity study previously described at the beginning of Chapter 3, design by advanced elastic analysis was also completed for the case of members without initial imperfections.

Table 3. H1-1 and λ values for frame 7d

	Interaction Equation H1-1 at λ = 1.00								
	Direct Analysis Method			**Elastic Analysis without out-of-straightness**			**Elastic Analysis with out-of-straightness**		
Member	$P_u/\Phi P_n$	$M_u/\Phi M_n$	H1-1	$P_u/\Phi P_n$	$M_u/\Phi M_n$	H1-1	$P_u/\Phi P_n$	$M_u/\Phi M_n$	H1-1
C1-1	0.347	--	0.347	0.183	--	0.092	0.184	--	0.092
C1-2a	0.563	0.648	1.140	0.298	0.648	0.874	0.298	0.661	0.885
C1-2b	0.322	0.648	0.898	0.170	0.648	0.733	0.170	0.661	0.746
C1-3	0.748	--	0.748	0.381	--	0.381	0.381	--	0.381
B1-1	0.008	--	0.004	0.007	--	0.004	0.007	--	0.004
B1-2	0.006	--	0.003	0.006	--	0.003	0.006	--	0.003
BRACE	0.096	--	0.048	0.096	--	0.048	0.096	--	0.048

	λ when Interaction Equation H1-1 = 1.00								
	Direct Analysis Method			**Elastic Analysis without out-of-straightness**			**Elastic Analysis with out-of-straightness**		
Member	$P_u/\Phi P_n$	$M_u/\Phi M_n$	λ	$P_u/\Phi P_n$	$M_u/\Phi M_n$	λ	$P_u/\Phi P_n$	$M_u/\Phi M_n$	λ
C1-1	--	--	1.460	--	--	1.460	--	--	1.460
C1-2a	0.508	0.544	0.908	0.322	0.747	1.090	0.324	0.775	1.081
C1-2b	0.347	0.743	1.072	0.202	0.900	1.185	0.200	0.906	1.173
C1-3	0.998	--	1.336	--	--	1.460	--	--	1.460
B1-1	--	--	1.460	--	--	1.460	--	--	1.460
B1-2	--	--	1.460	--	--	1.460	--	--	1.460
BRACE	--	--	1.460	--	--	1.460	--	--	1.460

It is noted that some cells are empty. This is because some members are axial force members and column studies presented in this research cover such cases. The cells with applied load ratios of λ = 1.46 are for members that did not fail before the entire frame collapsed, and thus the $P_u/\Phi P_n$ and $M_u/\Phi M_n$ at which the member reached H1-1 cannot be computed.

Finally, Figure 20 shows the load ratio vs. lateral displacement graphs that show the response of the system as predicted by design by advanced inelastic analysis (FE++), design by advanced elastic analysis, design by DM and the modified tangent modulus. A schematic of the deflected shape is included to help elucidate the plot information.

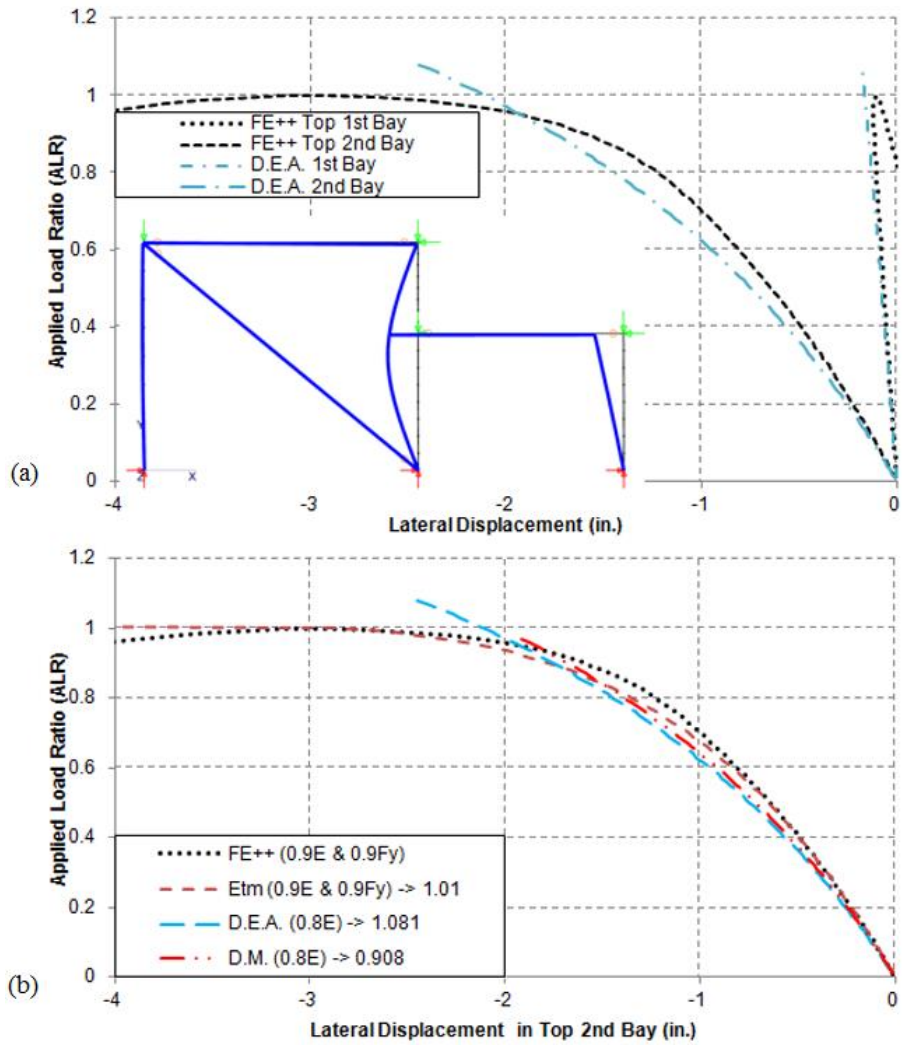

Figure 20. (a) Lateral displacement of both frame 7d bays. (b) Lateral displacement of the right bay

The deflection of the top of each bay was monitored at its top right corner. The deflections of both bays are shown in the Figure 20 (a) to better understand the frame behavior, whereas Figure 20 (b) shows only the top of the 2nd bay for comparative purposes. Similar tables and plots for all other frames are provided in Appendix C. The reader is encouraged to review them to get a full understanding of the behavior of each frame studied and observe the first plastic-hinge locations.

3.6. Minor-axis Column Study

Previous studies (Maleck and White, 2003; Nwe Nwe, 2014) showed that design by DM and a variation of design by DM, MDM, consistently overestimate the strength of beam-columns subject to axial load and minor-axis bending. This is attributed to the progressive yielding from the flange tips inward, which reduces the flexural rigidity of the member at a rate much faster than major-axis bending (Maleck and White, 2004a, p.1191). This effect is not properly captured either by the current τ_b factor, or AISC's minor-axis interaction equation. As a result Nwe New (2014) suggested factoring the minor-axis flexural rigidity by 0.7 instead of 0.8 to account for this. Maleck and White (2004b, p.1203) observed the greatest error at a slenderness of L/r = 98.3 for A992 steel. In the present study eleven typical AISC wide-flange columns with similar depth and width were investigated by varying the slenderness, L/r, between 40, 60, 80, and 100. This was done to quantify the error in design by advanced elastic analysis, using stiffness reduction values of 0.7 and 0.8, through comparisons with results of design by advanced inelastic analysis based on FE++2015. Figure 21 shows the column under investigation, which emulates the Kanchanalai frame studied by Ziemian and McGuire (2002) with a pinned bottom base and top fully restrained against rotation.

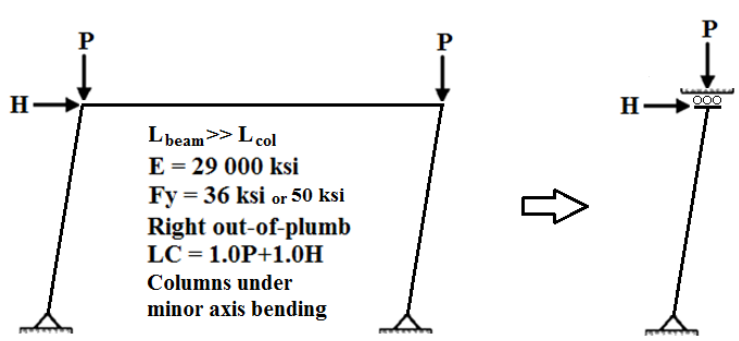

Figure 21. Kanchanalai Frame and column study, modified from Ziemian (2002)

Plots of applied force vs. moment normalized against the cross-section full-yield limit state; i.e. P/P_y vs. M_1/M_p, were created. The first-order moment, M_1, equals H times the column length. Figure 22 provides a flowchart of the MATLAB routine written for finding the axial force and horizontal load combinations at failure. Figure 23 shows the routine for pure axial force case and Figure 24 provides the routine for combined axial and horizontal load.

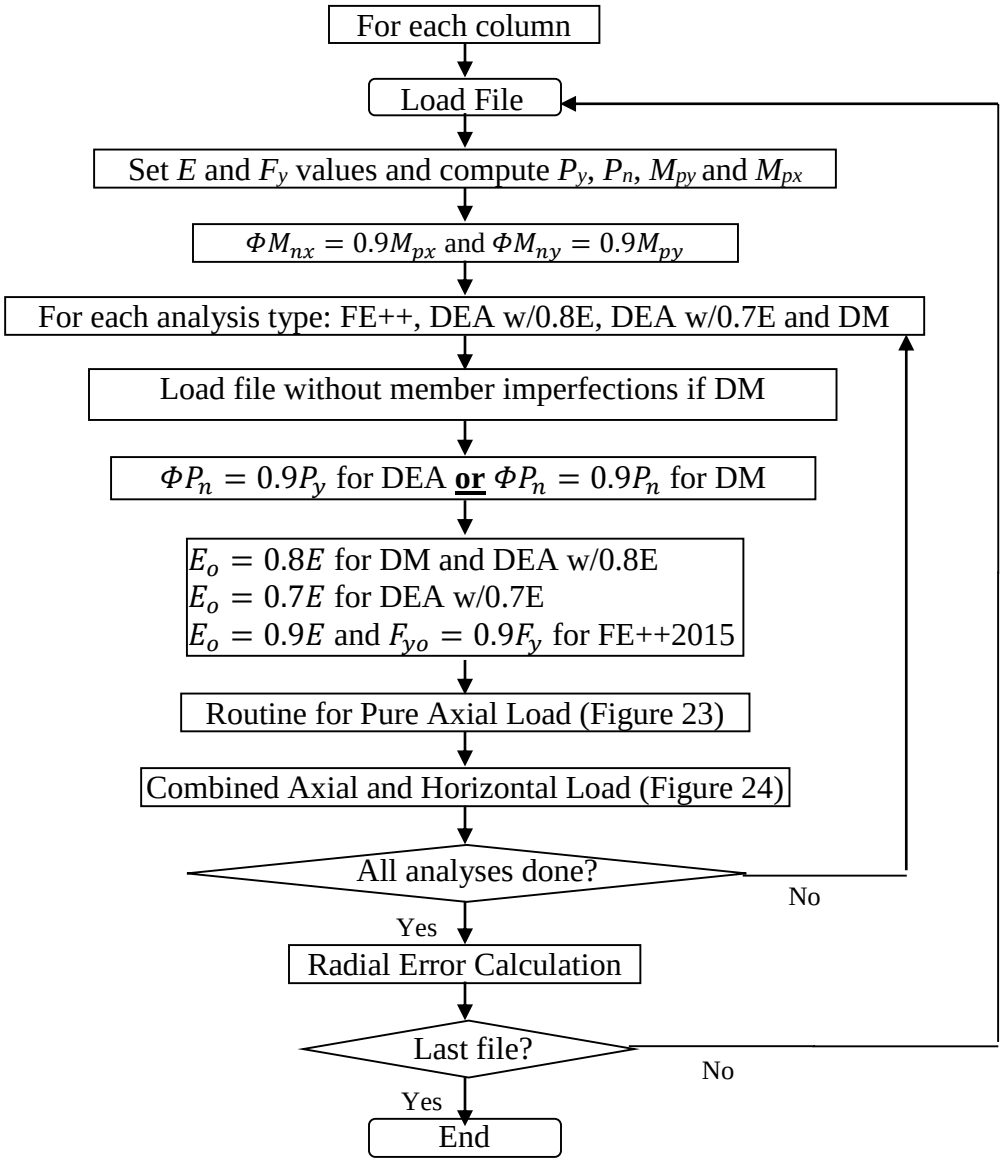

Figure 22. Column Study Main Routine

Design by advanced elastic analysis and design by advanced inelastic analysis were completed on columns that included member initial imperfections, and design by DM studies were completed on ones without. Figure 23 provides a flowchart of the sub-routine employed for finding the axial capacity of each column under pure axial load, and similarly, Figure 24 is for the case of axial and moment capacity under combined axial and horizontal load. In general, the left side of these flow charts represents the procedure for design by DM and design by advanced elastic analysis, and the right side represents FE++2015.

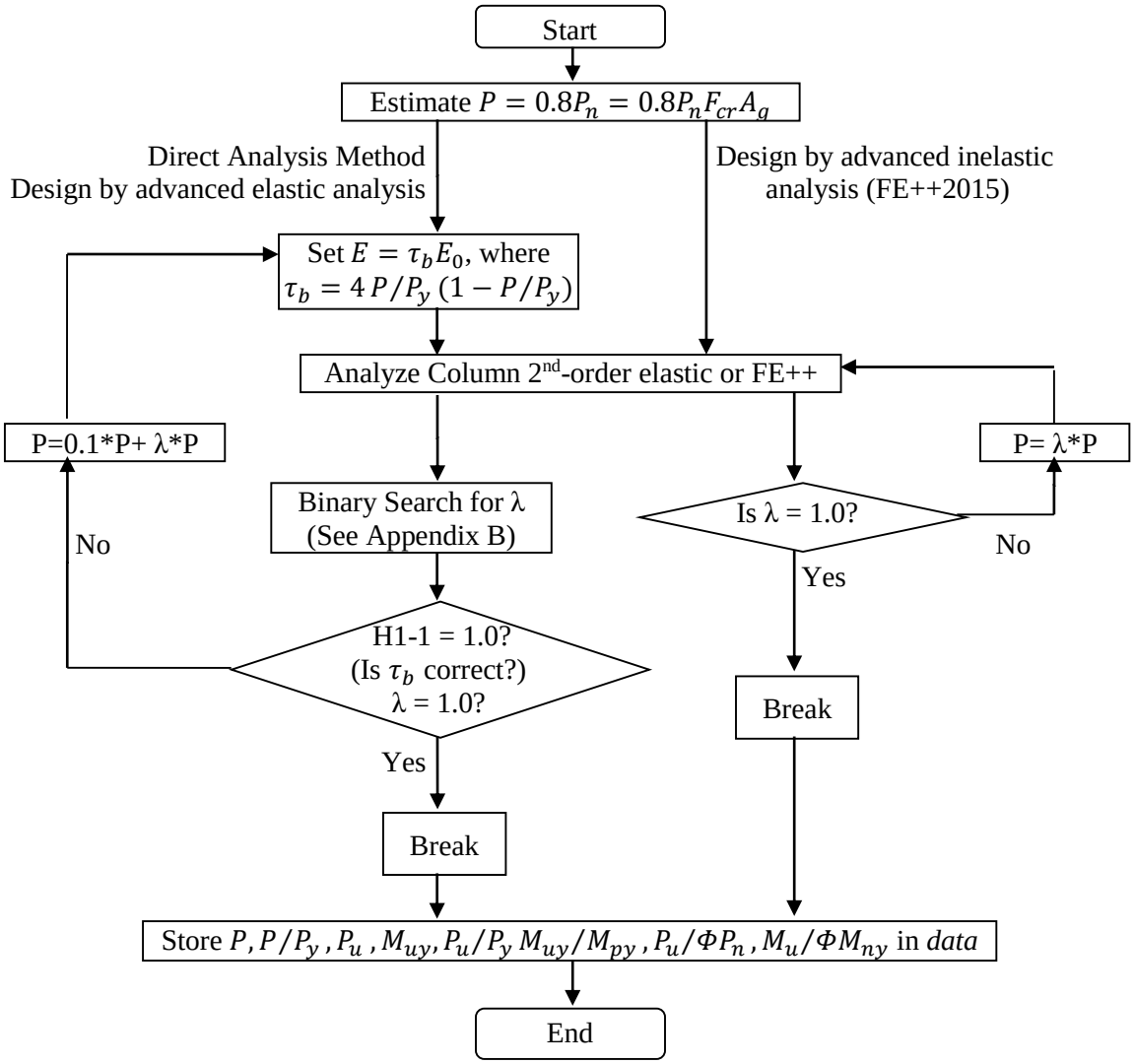

Figure 23. Sub-routine for determining pure axial load capacity of columns

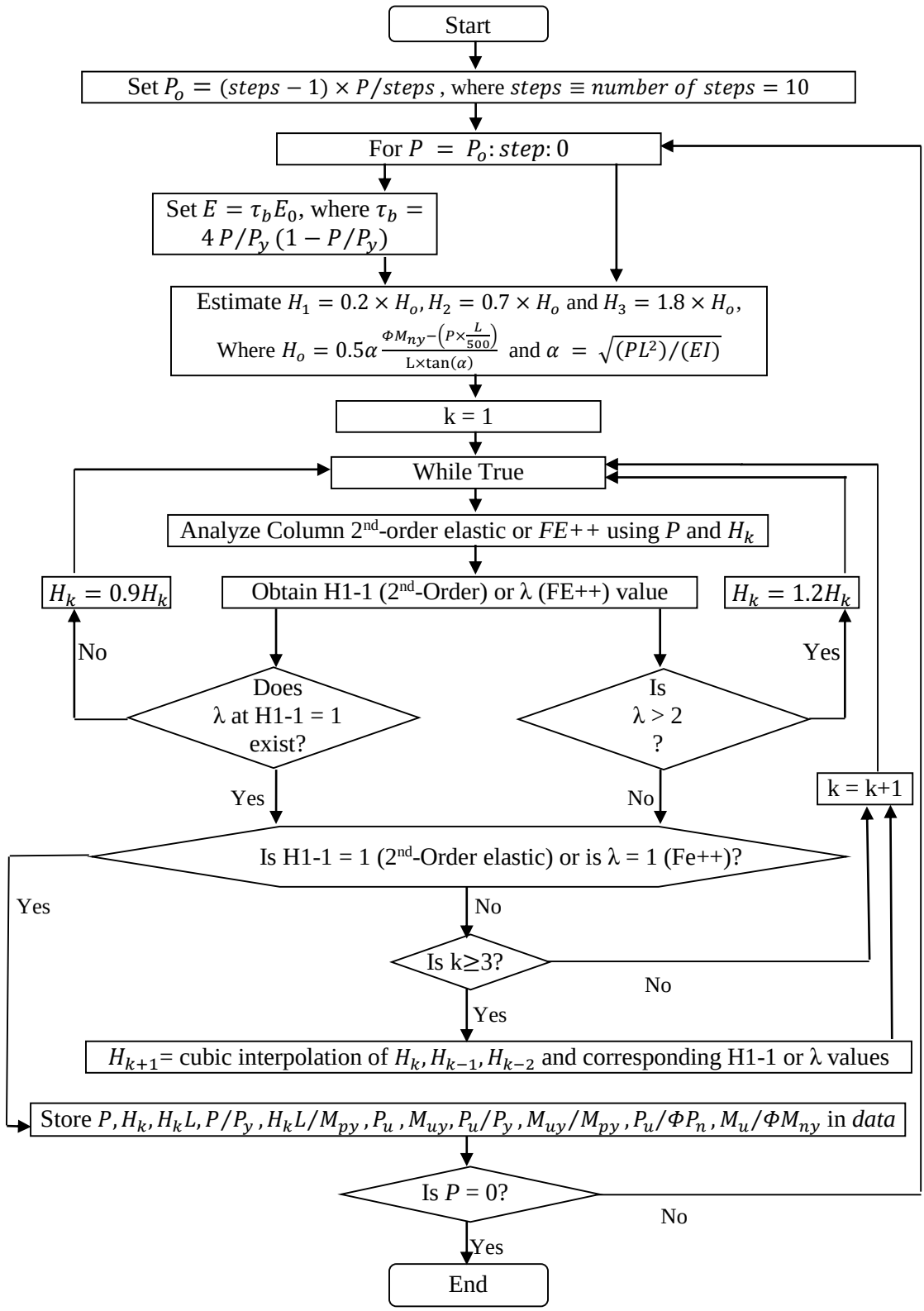

Figure 24. Sub-routine for finding combined axial load and horizontal load of columns

After preparing P/P_y vs. M_1/M_p plots, the radial errors were computed according to Equation 7:

$$\varepsilon = \frac{r_{FE++} - r}{r_{FE++}} \times 100\% \tag{7}$$

Unfortunately, this provided inaccurate results for columns with slenderness L/r ratios of 60, 80 and 100 because their maximum strengths are P/P_y values for FE++ of 0.29, 0.18 and 0.12 respectively. Figure 25 shows that for L/r = 100, most data points investigated are for small P/P_y values which was further complicated the use of cubic splines to interpolate between points.

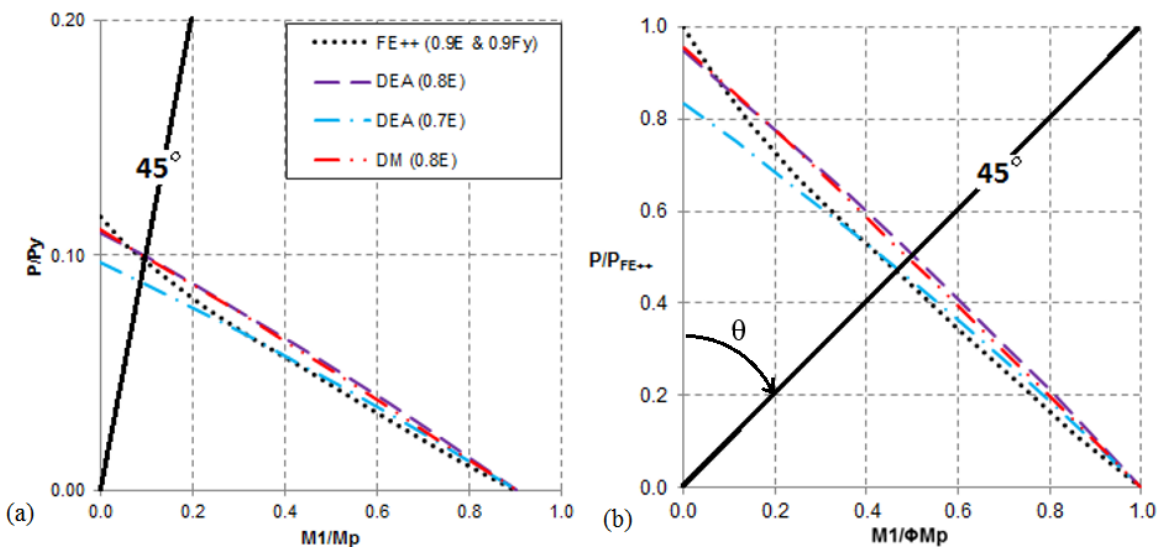

Figure 25. Computing radial error (a) Using P/P_y as the ordinate (b) Using P/P_{FE++} as the ordinate

This difficulty was overcome by first normalizing the plots into P/P_{FE++} vs. $M_1/\Phi M_p$ plots, where P_{FE++} is the maximum axial load predicted by FE++ when no moment is applied. The plots could then be expressed as radial distance vs. angle θ going clockwise from P/P_{FE++} to $M_1/\Phi M_p$ and then applying equation 7 with parabolic interpolation.

CHAPTER 4: RESULTS

The results from design by DM and design by advanced elastic analysis, DEA, are presented in Table 4 in the form of interaction equation H1-1 values (Equation 1), and applied load ratios λ, for the controlling beam and column in each system. Each column provides the largest interaction equation H1-1 value at λ=1.0. The presence of H1-1 values exceeding 1.0 indicate that the given member may fail before the entire load is placed on the system and thereby represents a conservative result. Similarly, the applied load ratio λ at which the first column and beam of a system achieves an interaction equation value of unity is shown. The overall lowest λ among beams and columns dictates how much load the system can resist and thus it is called the ultimate λ. In frame 8, the truss chords were taken as beams, and the web members as columns.

Table 4. Summary of design by DM and Design by advanced elastic analysis results (secant τ_b)

System		1a	1b	2	3	4	5	6	7a	7b	7c	7d	8	9
Maximum H1-1 value at λ = 1.0														
Col.	D.M.	1.20	1.22	1.19	0.98	1.22	1.60	1.10	0.75	1.04	1.05	1.14	0.85	0.93
	D.E.A	1.20	0.99	1.12	0.98	1.16	1.59	1.09	0.67	0.97	0.99	0.88	0.84	0.90
Beam	D.M.	1.31	1.01	0.91	--	--	0.50	0.95	1.21	1.14	--	--	1.87	0.22
	D.E.A.	1.31	1.01	0.92	--	--	0.50	0.95	1.22	1.14	--	--	1.23	0.23
Minimum λ when H1-1 = 1.0														
Col.	D.M.	0.84	0.83	0.95	1.01	0.83	0.65	0.92	1.32	0.96	0.95	0.91	1.14	1.06
	D.E.A	0.84	1.01	0.97	1.01	0.86	0.65	0.93	1.42	1.03	1.01	1.08	1.15	1.08
Beam	D.M.	0.76	0.99	1.05	--	--	1.82	1.05	0.84	0.88	--	--	0.80	1.40
	D.E.A.	0.76	0.99	1.04	--	--	1.83	1.04	0.84	0.88		--	0.97	1.38
Ult. λ	D.M.	0.76	0.83	0.95	1.01	0.83	0.65	0.92	0.84	0.88	0.95	0.91	0.80	1.06
	D.E.A.	0.76	0.99	0.97	1.01	0.86	0.65	0.93	0.84	0.88	1.01	1.08	0.97	1.08
Green cells indicate conservative results and orange cells, unconservative error with respect to FE++2015														

The last two rows of Table 4 show the ultimate applied load ratio λ of each system investigated. These values can be directly compared to the FE++2015 results, all of which fail at an ultimate λ of 1.0. The results were obtained using secant τ_b.

4.1. Effect of Initial Imperfections

Table 5 summarizes the percent differences when not including initial member imperfections in the design by advanced elastic analysis method. Similar to Table 4, each column shows the largest H1-1 and ultimate applied load λ-ratio among the beams and columns of each system. Negative percent differences indicate an increase in unconservative error with respect to the frames with member imperfections. Although lack of out-of-straightness generally results in lower internal moments, force redistribution sometimes leads to positive percentages, e.g., frames 4, 7a and 7b.

Table 5. Effect of neglecting initial imperfections (tangent τ_b)

System		1a	1b	2	3	4	5	6	7a	7b	7c	7d	8	9
Maximum H1-1 value at λ = 1.0														
Column	With imperf.	1.20	0.99	1.12	0.98	1.19	1.59	1.09	0.67	0.97	0.99	0.88	0.84	0.90
	No imperf.	1.20	0.96	1.12	0.95	1.19	1.59	1.09	0.68	0.97	0.99	0.87	0.84	0.89
	% Diff.	-0.3	-2.4	-0.3	-3.3	0.7	0.0	-0.1	1.2	0.5	-0.1	-1.2	-0.1	-1.5
Beam	With imperf.	1.31	1.01	0.92	--	--	0.50	0.95	1.22	1.14	--	--	1.23	0.23
	No imperf.	1.30	1.01	0.91	--	--	0.50	0.95	1.21	1.14	--	--	1.23	0.22
	% Diff.	-0.3	0.0	-0.4	--	--	0.0	-0.1	-0.2	-0.2	--	--	0.0	-1.5
Minimum λ when H1-1 = 1.0														
Column	With imperf.	0.84	1.01	0.97	1.01	0.85	0.65	0.93	1.42	1.03	1.01	1.08	1.15	1.08
	No imperf.	0.84	1.02	0.97	1.03	0.84	0.65	0.93	1.42	1.03	1.01	1.09	1.15	1.09
	% Diff.	-0.3	-1.1	0.0	-1.8	0.6	0.0	0.0	-0.2	0.5	-0.1	-0.9	0.0	-1.1
Beam	With imperf.	0.76	0.99	1.04	--	--	1.83	1.04	0.84	0.88	--	--	0.97	1.38
	No imperf.	0.76	0.99	1.05	--	--	1.83	1.05	0.84	0.88	--	--	0.97	1.40
	% Diff.	-0.3	0.0	-0.2	--	--	0.0	-0.1	-0.1	-0.2	--	--	0.0	-1.4

These results were not expected. Apparently not including initial imperfections has little to no impact on the strength of the frames investigated. Although the largest difference is 2.4% in frame 1b, this did not affect the frame's ultimate applied load λ-ratio. The largest differences in λ were observed in frames 3 and 9 with 1.8 and 1.1% respectively. Note that these results were obtained using a tangent τ_b factor. As indicated in the next section, the differences between using the tangent τ_b instead of the secant τ_b are even smaller than those of neglecting initial imperfections.

4.2. Secant vs. tangent τ_b

The percent differences obtained by using the tangent τ_b-factor in design by DM and design by advanced elastic analysis were quantified with respect to the stipulated secant τ_b-factor. Although frames 1a, 1b, 2, 3, 4, 7a and 7b all possess at least one member where its axial load force exceeds $0.5P_y$, the τ_b-factor only caused significant difference in the performance of frames 1a, 2, 3, 4, 7a, and 7b. Table 6 shows the percent differences observed in these frames between employing a secant τ_b-factor vs. tangent τ_b-factor for both design by DM and design by advanced elastic analysis. The differences are calculated based on the maximum interaction equation H1-1 values and ultimate applied load λ-ratios. As explained in Section 3.2, finding λ for every single member is an iterative and time consuming procedure; and thus, only the ultimate applied load λ-ratio, regardless of member type (beam or column), is compared.

Table 6. % difference between using secant and tangent τ_b factor in design by DM and DEA

			design by direct analysis method, DM						design by advanced elastic analysis,DEA					
System			**1a**	**2**	**3**	**4**	**7a**	**7b**	**1a**	**2**	**3**	**4**	**7a**	**7b**
Maximum H1-1	**Column**	Tangent	1.20	1.19	0.98	1.23	0.75	1.04	1.20	1.12	0.98	1.19	0.67	0.97
		Secant	1.20	1.19	0.98	1.22	0.75	1.04	1.20	1.12	0.98	1.16	0.67	0.97
		% Diff.	-0.03	0.00	0.01	-1.36	0.00	0.00	-0.04	0.02	0.01	-1.81	0.00	0.00
	Beam	Tangent	1.30	0.91	--	--	1.21	1.14	1.31	0.92	--	--	1.22	1.14
		Secant	1.31	0.91	--	--	1.21	1.14	1.31	0.92	--	--	1.22	1.14
		% Diff.	0.11	0.00	--	--	-0.03	-0.08	0.10	0.00	--	--	0.00	0.00
Ultimate λ-ratio		Tangent	0.76	0.95	1.01	0.82	0.84	0.88	0.76	0.97	1.01	0.85	0.84	0.88
		Secant	0.76	0.95	1.01	0.83	0.84	0.88	0.76	0.97	1.01	0.86	0.84	0.88
		% Diff.	0.00	0.00	0.00	1.44	0.03	0.07	0.00	-0.01	0.00	1.86	0.00	0.00

The largest difference was observed in frame 4 with 1.44% for design by DM and 1.86% for DEA. Differences in all other values are negligible. This also demonstrates that

for many frames, the axial load on any member rarely exceeds 50% of its axial yield strength.

4.3. Column Study Results

The P/P_y vs. M_1/M_p curves obtained for given values of L/r were found to be almost identical regardless of the section investigated. The curves in this section are for an A992-steel W8X58-column. Appendix D provides plots of P/P_{FE++} vs $M_1/\Phi M_p$ and plots showing the variation in percent radial error as a function of the angle θ going from the P/P_{FE++} axis towards the M_1/M_p axis for the same W8X58-column. Figure 26 shows the graph for a slenderness ratio L/r of 40.

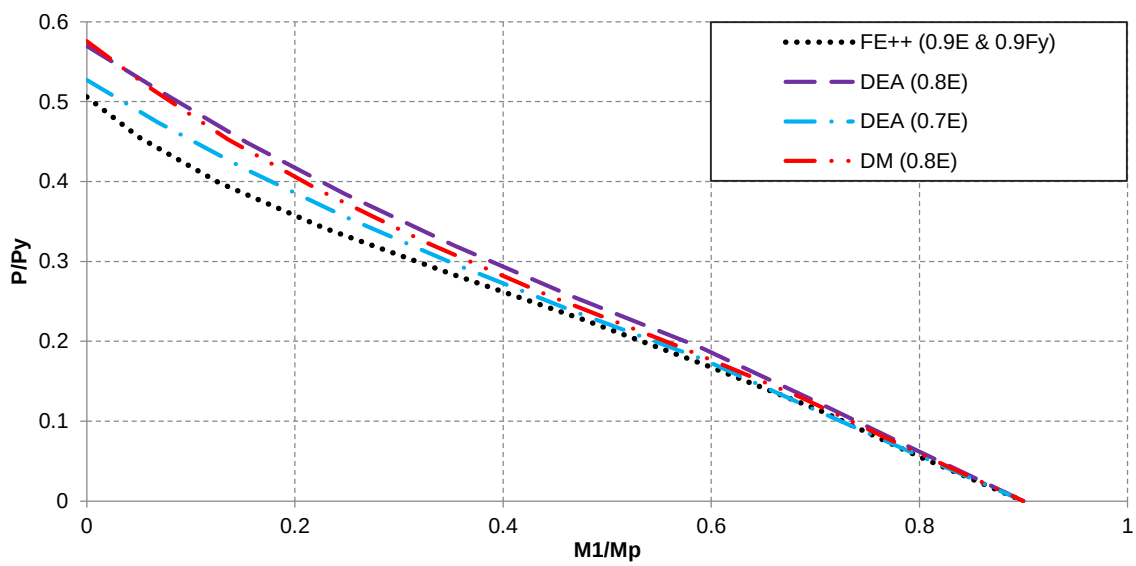

Figure 26. W8X58 P/Py vs. M1/Mp for L/r = 40, Fy = 50 ksi

From Figure 26 one can appreciate that for a slenderness ratio of 40, all methods provide unconservative results with respect to the FE++2015 results for the case of pure axial load. Although the unconservative error increases slightly when minor-axis moment of up to 20% is applied, it gets progressively lower as the applied minor-axis moment

approaches the minor-axis plastic moment capacity. The unconservative error peaks at 15 % for this slenderness ratio.

Similarly, Figure 27 through 29 provides plots of P/P_y vs. M_1/M_p for slenderness ratios L/r of 60, 80 and 100, respectively.

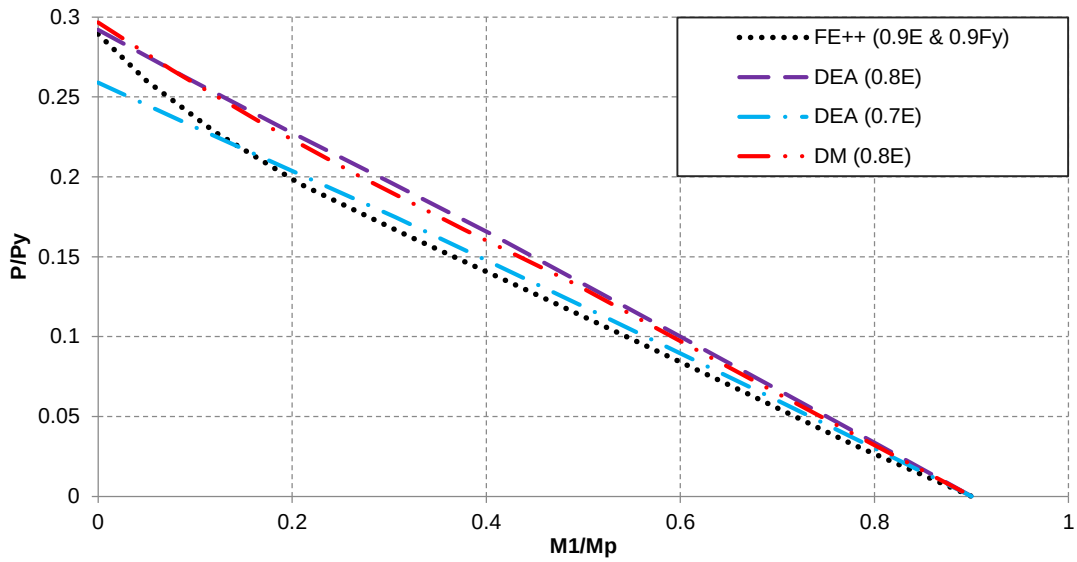

Figure 27. W8X58 P/Py vs. M1/Mp for L/r = 60, Fy = 50 ksi

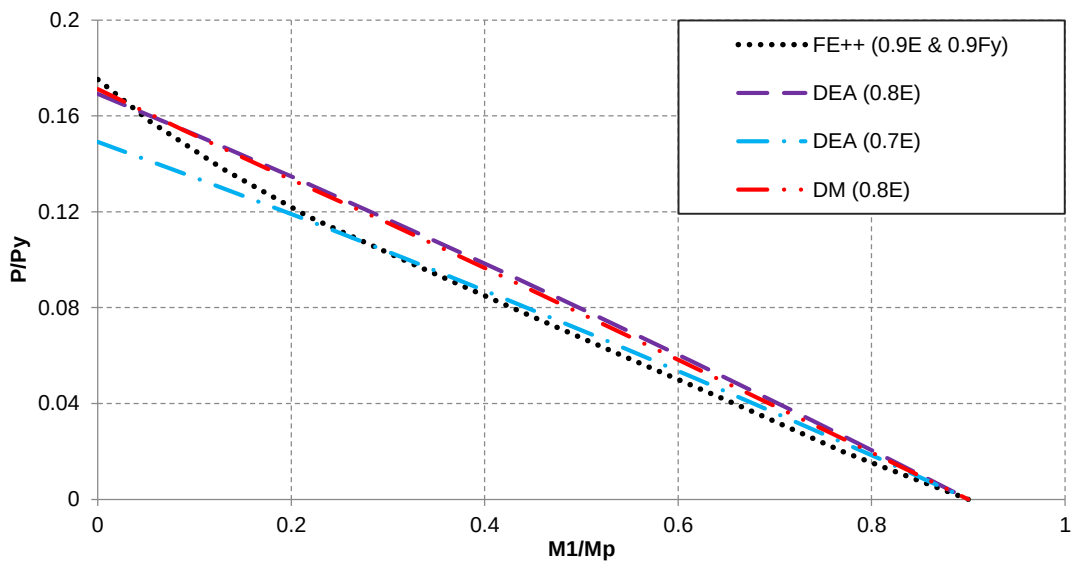

Figure 28. W8X58 P/Py vs. M1/Mp for L/r = 80, Fy = 50 ksi

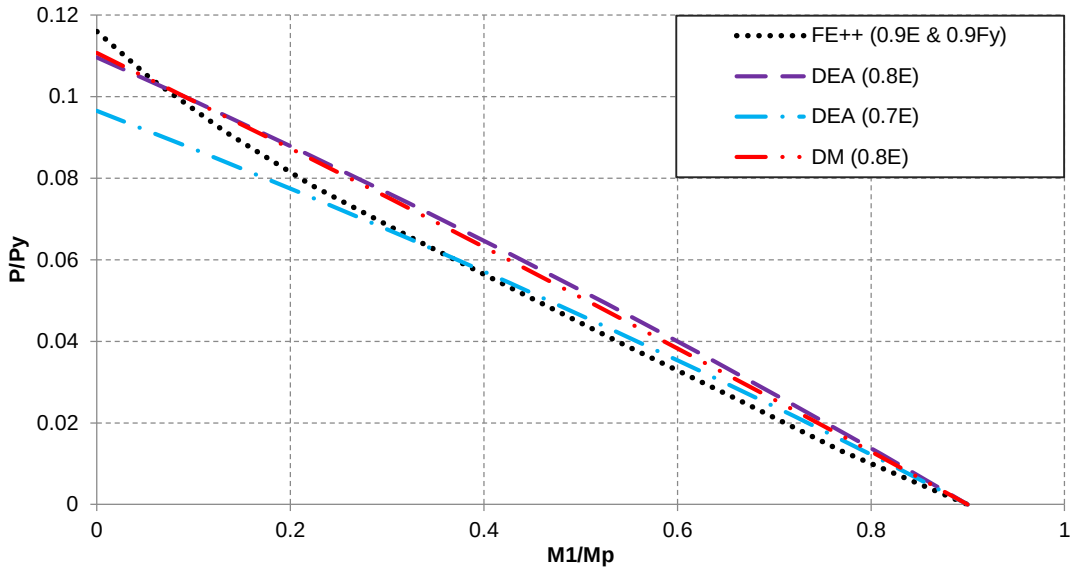

Figure 29. W8X58 P/Py vs. M1/Mp for L/r = 100, Fy = 50 ksi

Although all methods provide conservative estimates of the strength for the case of pure axial capacity when the slenderness ratio is greater than 60, there is still unconservative error when there is combined axial load and minor-axis moment. Appendix D presents plots showing the percent radial error as a function of the angle θ going from the P/P_{FE++} axis towards the M_1/M_p axis and a table with the maximum conservative and unconservative percent radial errors for each beam-column studied. Table 7 provides the average and standard deviation for these errors.

Table 7. Maximum conservative and unconservative% radial error

Slenderness Ratio L/r	Max. Conservative% Error [Mean (st.dev.)]						Max. Unconservative% Error [Mean (st.dev.)]					
	DEAw/0.8E		DEA w/0.7E		DM w/0.8E		DEA w/0.8E		DEA w/0.7E		DM w/0.8E	
40	0.00	(0.00)	0.34	(0.16)	0.00	(0.00)	15.07	(0.32)	7.25	(0.40)	14.74	(0.86)
60	0.00	(0.00)	10.39	(0.41)	0.00	(0.00)	11.49	(0.40)	3.20	(0.29)	9.68	(0.74)
80	3.27	(0.42)	14.74	(0.38)	2.12	(0.45)	8.81	(0.41)	2.70	(0.46)	8.00	(0.59)
100	5.40	(0.35)	16.74	(0.32)	4.44	(0.37)	7.98	(0.41)	3.10	(0.45)	6.56	(0.42)

What if F_y = 36 ksi instead of 50 ksi?

The column study in the previous section investigated steel members with yield strength of F_y = 50 ksi. In previous research, such as the parametric study by Maleck (2003), additional work focused on a yield strength of F_y = 36 ksi. To verify the current research, the results of the analysis of a W8X31 column with *L/r* of 60 were compared to the study of a symmetrical frame with pinned base, L/r of 60, and G = 0 in Maleck (2003). Figure 27 shows that the results of the current study align well with Maleck's study (2003).

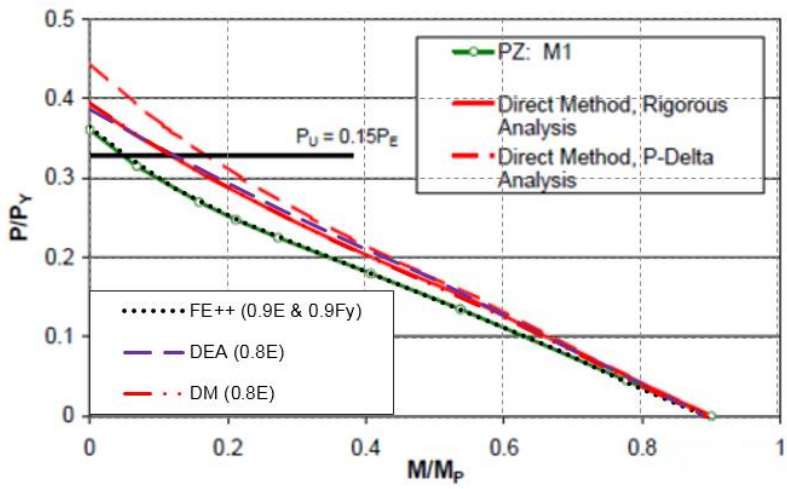

Figure 30. W8X31, weak 60 compared to SP_W60_G0 from Maleck (2003)

In particular, the design by DM method when using a rigorous analysis (by virtue of subdividing the column into 8 pieces to capture P-δ effects) is indiscernible between studies. Similarly, design by advanced elastic analysis showed results very close to design by DM. FE++ results were also in direct agreement with distributed plasticity or plastic zone (PZ) analysis results by Maleck (2003). Moreover, the maximum unconservative error of 11 percent in the current study is consistent with results obtained by Maleck (2003).

CHAPTER 5: CONCLUSIONS

5.1. Summary of Results

The results presented in this thesis support the hypothesis statement that directly modeling both system and member initial geometric imperfections within the structural analysis will provide adequate designs that are comparable to AISC's design by the direct analysis method and AISC's design by advanced inelastic analysis. The accuracy of this approach, termed design by design by advanced elastic analysis, is quantified in terms of the applied load ratio at failure predicted by AISC's design by advanced inelastic analysis.

Frames with members subject to major-axis bending presented little-to-no unconservative error, with frames 3 and 7b having 1 to 3% unconservative error with respect to design by advanced inelastic analysis. In contrast, only frame 3 was unconservative per design by DM. Among the systems with members subject to minor-axis bending, frames 7d and 9 showed 8 to 9% unconservative error when compared to AISC's design by advanced inelastic analysis. Frame 9 also displayed 6% unconservative error when employing design by DM. For frames 7c, 7d and 8, the unbraced lengths could not be simply taken as the distance between member connections, rather the effective compression length was chosen by inspection between two connections that provide adequate lateral bracing. If the distance between connections had been used, AISC's design by DM results would also have been unconservative for these frames.

CHAPTER 5: CONCLUSIONS

As part of a sensitivity completed on the research performed, it was found that not adding the required initial member imperfections, prescribed as L/1000, had no significant impact on the findings. The percent change was less than 1% for all frames, except frame 8 which had a 1.2% difference. Furthermore, when comparing the use of the stiffness reduction tangent τ_b-factor against the stiffness reduction secant τ_b-factor, it was found that the axial load exceeded 50% of the yield stress in only very few frames, including frames 1a, 1b, 3, 4, 7a and 7b. Of these frames, only a few members had stiffness reduction τ_b-factors slightly lower than 1.0. These results demonstrate that for the wide range of frames studied in this research, the τ_b-factor may be taken as 1.0 in almost all members, and as a result there is little difference between using a secant τ_b-factor or tangent τ_b-factor.

Although the column study showed a maximum unconservative error of up to 15% for design by advanced elastic analysis, only 1% greater than the maximum unconservative error for AISC's conventional design by direct analysis method. Factoring stiffness by 0.7 in design by advanced elastic analysis reduced the unconservatism to 7.4%, albeit adding conservative error of up to 17%. This study demonstrated that, in general, design by DM and design by advanced elastic analysis show good agreement with design by advanced inelastic analysis (using FE++2015) in cases of nearly pure axial load and an unconservative error of up to 15% when applied bending moments are introduced. Conversely, by gaining conservative error of 16% in cases of almost pure axial load, design by advanced elastic analysis with stiffness factored by 0.7 became quite accurate for cases with bending with values exceeding M/M_p = 0.2. It is important to remember that even though the column study showed high unconservative error, the impact of a single member

failing is typically reduced as frame redundancy increases. This is exemplified by the frame study where the frames with members oriented for minor-axis bending, including those studied by El-Zanaty, and 7d showed only an 8% unconservative error.

5.2. Recommendations for further research

All of the frames studied in this research, except for frame 8, are fully braced out-of-plane. Moreover, all the sections used are compact wide-flange sections. Thus, it is recommended that further research be performed that investigates the validity of design by advanced elastic analysis on more three-dimensional systems that include members subject to axial load and combined major and minor-axis bending. It is also recommended that further research be used to verify the adequacy of this method for non-compact and slender sections, as well as members that might be vulnerable to lateral torsional buckling. In this regard, it is particularly important that more research be completed that studies the effects of initial member twist imperfections, which may cause a significant reduction in moment capacity.

As for the initial imperfections, further research into alternative methods of applying initial imperfections, as was done by Agüero et al. (2015a, 2015b) and Shayan et al. (2014), is recommended for future inclusion in the AISC specification. In applying methods of design that rely heavily on modeling system and member initial imperfections, the profession will need guidance on defining the magnitude and mode of such imperfections.

CHAPTER 5: CONCLUSIONS

Although a more rigorous study of the stiffness reduction tangent τ_b-factor would help corroborate that its use does, in fact, cause little difference in the analysis with respect to the use of the current secant τ_b-factor, the author believes that focusing on improving a modified tangent τ-factor, which includes both major and minor axis bending terms, would be more beneficial to all design methods. A more accurate factor that accounts for these moments might eliminate the need to reduce stiffness by a factor of 0.8 to account for inelastic softening, and thereby greatly increase the predictive capabilities of the method.

Given that the column curve interaction equation used by AISC to assess beam-columns are the same for a given dimensionless slenderness ratio, $\lambda = L/r\sqrt{F_y/E}$, (or in other words, they depend only on L/r and F_y), more research could be useful in helping to establish definite curves for a wide range of slenderness sections, and then help calibrate a new stiffness reduction τ-factor that accounts for the differences in destabilizing effects due to major-axis and minor-axis bending moments. Of course, more column studies should be performed to account for different end-restraints, section slenderness, members subject to out-of-plane failure modes such as lateral torsional buckling, and members subject to both major and minor-axis bending. With this in mind, the logical next step would be to investigate the feasibility of adding twist imperfections such that moment capacity can be taken as the plastic moment throughout and thereby rely on the analysis to account for the possibility of elastic and inelastic lateral torsional buckling.

Appendix A. Plastic-hinge vs. Distributed Plasticity

The AISC 2016 Specification provides two design by advanced analysis methods, including design by advanced elastic analysis and design by advanced inelastic analysis. The main difference between them lies in the way yielding is modeled. Design by advanced elastic analysis is essentially a first plastic-hinge analysis, whereas design by advanced inelastic analysis uses a distributed plasticity model. In the latter, not only are members subdivided into elements, but each element's cross-section is also discretized into fibers (Surovek, 2012, pg. 13). At each load step, yielding is tracked explicitly along the length and cross-section of members. A plastic-hinge model, on the other hand, uses a yield surface criterion to determine whether the cross-section has *fully* yielded. While there are more mathematically accurate depictions of the yield surface (as described in the study by Ziemian and McGuire reference in Section 2.5.2), the equation presented in Section 2.2 is preferred.

Table A 1. Plastic-hinge vs. distributed plasticity. Adapted from Surovek (2012, pg. 14)

	Plastic-hinge Analysis (Concentrated Plasticity)	**Distributed Plasticity Analysis (Plastic Zone Analysis)**
	Design by advanced elastic analysis*	**Design by advanced inelastic analysis**
Modeling	Plastic-hinges at element ends, otherwise elastic everywhere else.	Fiber discretization at cross-sections and along member length.
Source of Inelasticity	Tracked only at element ends.	Tracked explicitly at the cross-section and along the length.
Spread of Inelasticity	Elastic-perfectly plastic-hinge at element ends.	Gradual development of inelasticity and along length and cross-section.
Material Nonlinear Behavior	τ_b factor accounts for reduced E due to axial force only.	Elastic-plastic model with or without strain hardening defined for each fiber.
Residual Stresses	Indirectly modeled through the use of τ_b	Stress pattern defined uniquely at each fiber.
Geometric Imperfections	Out-of-plumbness and out-of-straightness explicitly modeled in the analysis	
*System assumed stable only until the formation of the first plastic-hinge.		

Appendix B. Binary Search Engine

In general, the binary search routine is used to expedite the search of an indexed value. In this research, a routine was written to find the applied load ratio λ at which the interaction equation H1-1 for a given member reached a value of 1.0. The routine splits the data, i.e., the λ-values, into two halves and determines which half contains the value being seeked. It checks for these domains by computing the interaction equation values at each guess, the first one being the middle of the data set. If the guess is indeed the value being seeked, it stops looking. Otherwise, it determines which half of the data to examine next based on the interaction equation H1-1 value obtained. Iteration proceeds until a λ-value resulting in an interaction equation value of unity is found. The data often does not contain the exact value, in which case, the routine uses linear interpolation.

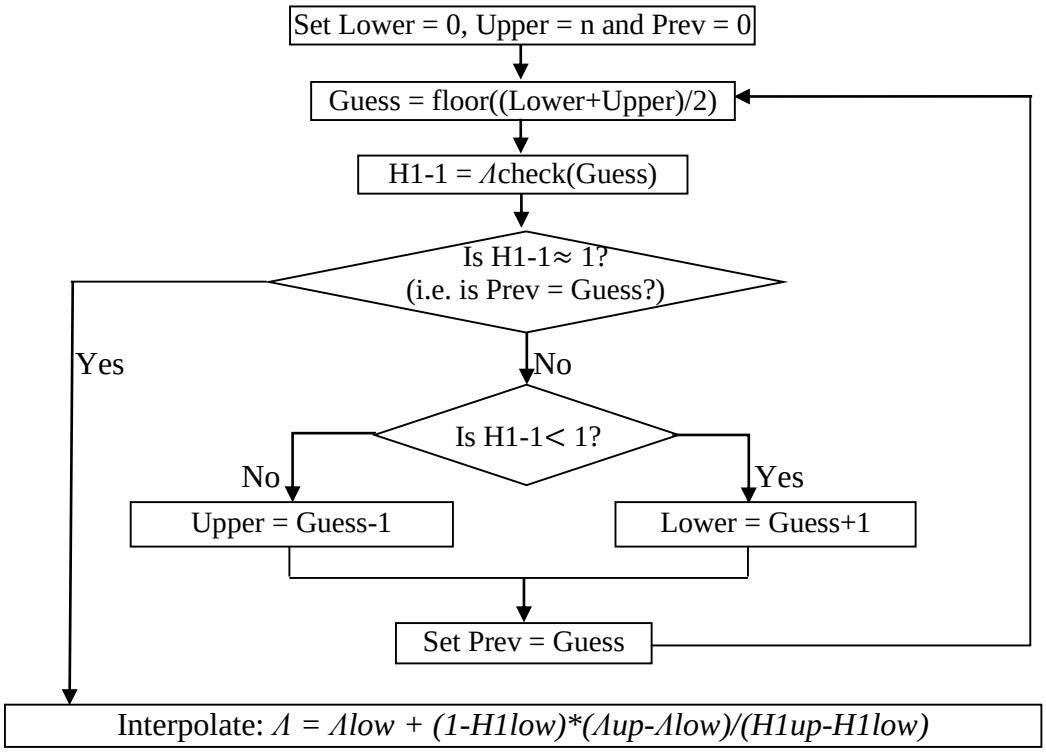

Figure B 2. Binary Search Engine Flowchart

APPENDICES

Appendix C. Benchmark Frame Results

This appendix provides the tables for all members within the frames studied in which the interaction equation H1-1 values are provided at an applied load ratio λ equal to 1.0 and the applied load ratio λ-values at which the interaction equation equals 1.0 for each member of interest. Cells with yellow shading show the conservative controlling values, whereas cells with orange shading show controlling values which are unconservative when compared to AISC's design by advanced inelastic analysis. Similarly, cells with purple shading represent members in which the percent difference is greater than 10% between such methods.

This appendix also provides load vs. displacement plots for each system. Specifically, these graphs plot the applied load ratio, λ, vs. the displacement of the roof or top story of each system. For example, for systems 1a and 1b, the displacement of the top right hand corner is monitored. These graphs also provide plots of results predicted by FE++2015, design by advanced elastic analysis and design by the direct analysis method.

Some of these displacement plots have data from previous research by Martinez-Garcia (2002) superimposed on them in an effort to clearly compare the FE++ results with the NIFA results. In some multistory systems, only FE++ and design by advanced elastic analysis are shown on the plots to better illustrate the displacement. Displacements at each story level is referred to as Δ1, Δ2, etc. In system 6 for example, Δ1, Δ2 and Δ3 indicate the stories on the left side of the frame. To help elucidate the plot information, and to save space, schematics of the deformed frames are shown within these graphs.

C.1. System 1a – Ziemian and Miller (1997) Unsymmetrical Frame (Major-axis)

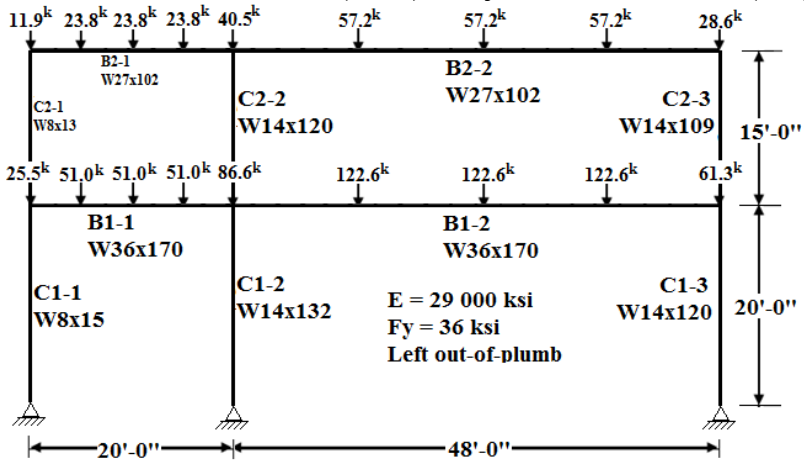

Figure C 1. System 1a Factored Loads

Table C 1. System 1a H1-1 and λ values

1	H1-1 at Applied Load Ratio = 1.00								
	Direct Analysis Method			Elastic Analysis without member imperfections			Elastic Analysis with member imperfections		
Member	$P_u/\Phi P_n$	$M_u/\Phi M_n$	H1-1	$P_u/\Phi P_n$	$M_u/\Phi M_n$	H1-1	$P_u/\Phi P_n$	$M_u/\Phi M_n$	H1-1
C1-1	0.847	0.102	0.938	0.640	0.102	0.731	0.639	0.126	0.750
C1-2	0.510	0.507	0.960	0.472	0.507	0.922	0.473	0.498	0.915
C1-3	0.315	0.356	0.631	0.291	0.356	0.607	0.291	0.336	0.589
C2-1	0.309	0.286	0.563	0.262	0.286	0.516	0.261	0.277	0.507
C2-2	0.168	1.035	1.119	0.161	1.035	1.115	0.161	1.038	1.119
C2-3	0.109	1.143	1.198	0.105	1.143	1.195	0.105	1.147	1.199
B1-1	0.001	1.303	1.304	0.001	1.303	1.304	0.000	1.307	1.308
B1-2	0.041	0.982	1.003	0.041	0.982	1.003	0.042	0.981	1.002
B2-1	0.003	1.203	1.205	0.002	1.203	1.205	0.003	1.204	1.206
B2-2	0.091	1.052	1.098	0.078	1.052	1.092	0.078	1.055	1.094

1	Applied Load Ratio when H1-1 = 1.00								
	Direct Analysis Method			Elastic Analysis without member imperfections			Elastic Analysis with member imperfections		
Member	$P_u/\Phi P_n$	$M_u/\Phi M_n$	Λ	$P_u/\Phi P_n$	$M_u/\Phi M_n$	Λ	$P_u/\Phi P_n$	$M_u/\Phi M_n$	Λ
C1-1	0.905	0.113	1.062	0.851	0.171	1.324	0.823	0.204	1.283
C1-2	0.526	0.525	1.038	0.507	0.551	1.077	0.513	0.549	1.084
C1-3	0.537	0.579	1.802	0.497	0.535	1.807	0.495	0.490	1.800
C2-1			1.860			1.860			1.860
C2-2	0.150	0.926	0.894	0.143	0.923	0.897	0.144	0.929	0.895
C2-3	0.091	0.952	0.836	0.087	0.950	0.838	0.088	0.956	0.835
B1-1	0.001	1.001	0.765	0.001	1.001	0.765	0.000	1.007	0.762
B1-2	0.041	0.974	0.998	0.041	0.974	0.998	0.041	0.973	0.998
B2-1	0.002	1.010	0.830	0.002	1.010	0.830	0.002	0.988	0.830
B2-2	0.083	0.965	0.912	0.072	0.960	0.917	0.072	0.964	0.915

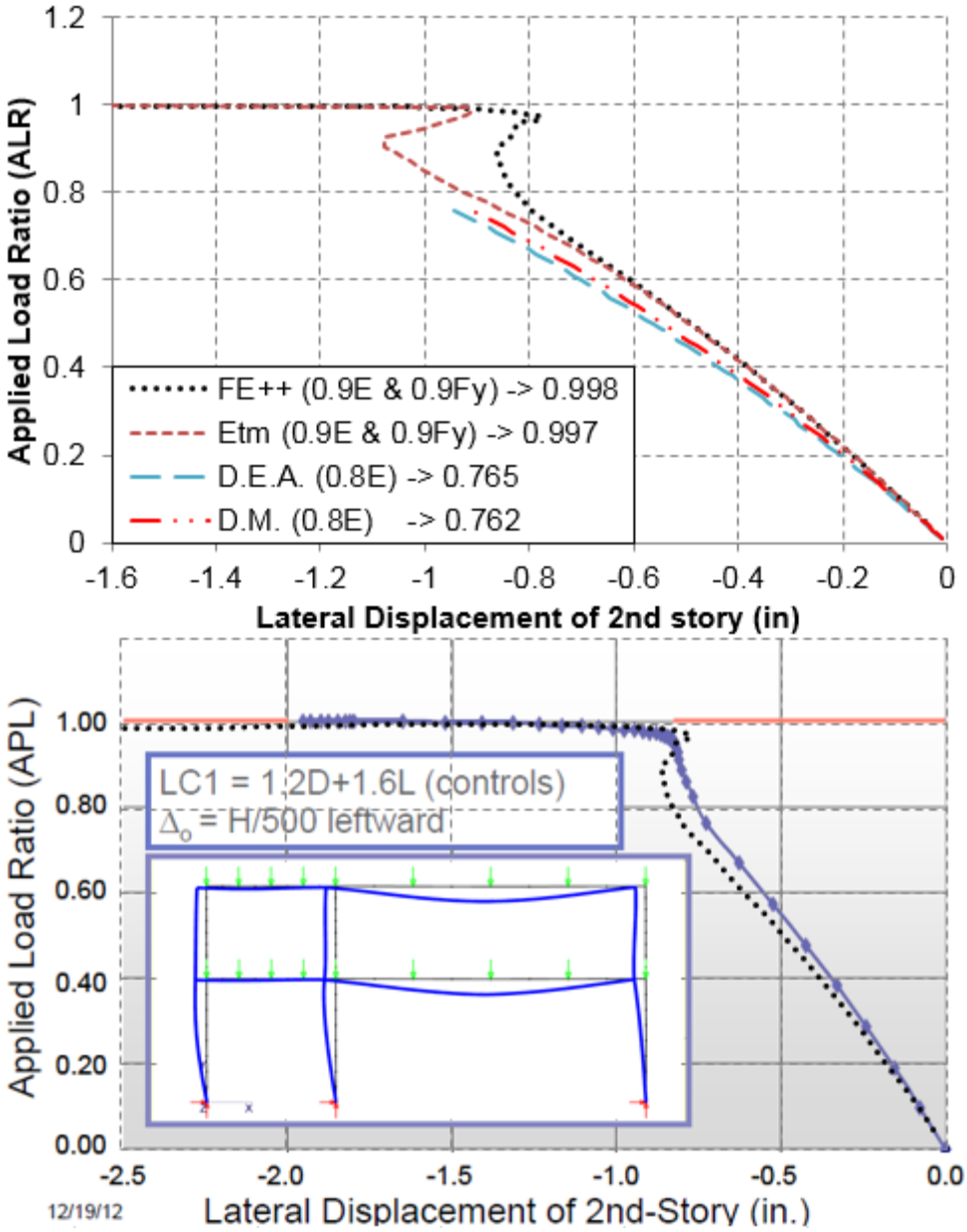

Figure C 2. System 1a Lateral Displacement Plots

C.2. System 1b – Ziemian (1990) Unsymmetrical Frame (Minor-axis)

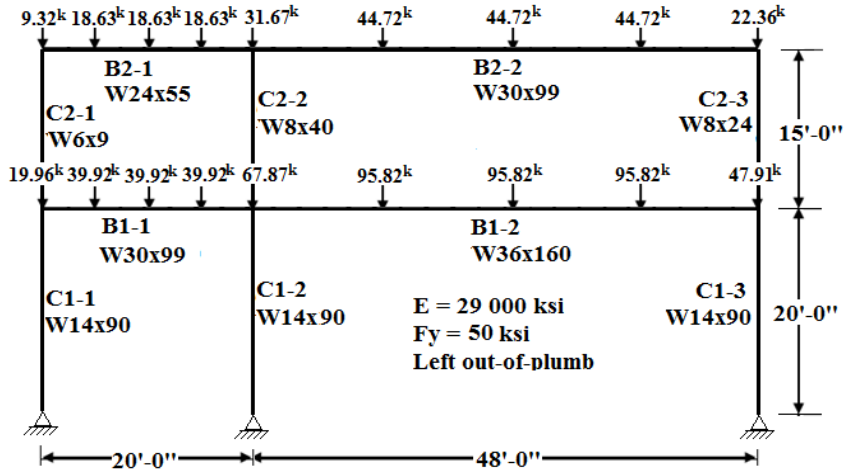

Figure C 3. System1b Factored Loads

Table C 2. System 1b H1-1 and λ values

1	H1-1 at Applied Load Ratio = 1.00								
	Direct Analysis Method			Elastic Analysis without member imperfections			Elastic Analysis with member imperfections		
Member	$P_u/\Phi P_n$	$M_u/\Phi M_n$	H1-1	$P_u/\Phi P_n$	$M_u/\Phi M_n$	H1-1	$P_u/\Phi P_n$	$M_u/\Phi M_n$	H1-1
C1-1	0.050	0.434	0.458	0.036	0.434	0.452	0.037	0.466	0.485
C1-2	0.580	0.605	1.118	0.426	0.605	0.964	0.426	0.632	0.988
C1-3	0.279	0.029	0.305	0.205	0.029	0.231	0.205	0.079	0.275
C2-1	0.764	0.100	0.853	0.097	0.100	0.148	0.097	0.087	0.136
C2-2	0.547	0.291	0.805	0.309	0.291	0.568	0.309	0.279	0.558
C2-3	0.617	0.674	1.216	0.247	0.674	0.846	0.248	0.647	0.823
B1-1	0.005	0.925	0.927	0.005	0.925	0.927	0.005	0.925	0.928
B1-2	0.001	0.710	0.710	0.001	0.710	0.710	0.000	0.713	0.714
B2-1	0.001	1.009	1.009	0.001	1.009	1.009	0.001	1.008	1.009
B2-2	0.002	0.682	0.683	0.002	0.682	0.683	0.002	0.683	0.684

* Note: Differences between secant τ_b and tangent τ_b are negligible

1	Applied Load Ratio when H1-1 = 1.00								
	Direct Analysis Method			Elastic Analysis without member imperfections			Elastic Analysis with member imperfections		
Member	$P_u/\Phi P_n$	$M_u/\Phi M_n$	Λ	$P_u/\Phi P_n$	$M_u/\Phi M_n$	Λ	$P_u/\Phi P_n$	$M_u/\Phi M_n$	Λ
C1-1	0.069	1.023	1.141	0.051	1.014	1.142	0.050	1.018	1.132
C1-2	0.552	0.523	0.940	0.432	0.632	1.017	0.428	0.642	1.005
C1-3	0.324	0.864	1.180	0.237	0.770	1.189	0.235	0.784	1.179
C2-1	0.878	0.128	1.149	0.320	0.814	1.522	0.310	0.756	1.506
C2-2	0.675	0.357	1.248	0.398	0.692	1.353	0.395	0.641	1.349
C2-3	0.508	0.550	0.826	0.285	0.793	1.160	0.295	0.801	1.182
B1-1	0.008	0.990	1.109	0.007	0.990	1.110	0.009	0.993	1.113
B1-2	0.002	0.980	1.259	0.002	0.980	1.259	0.003	1.004	1.254
B2-1	0.001	1.007	0.991	0.001	1.007	0.991	0.001	1.007	0.991
B2-2	0.005	0.992	1.367	0.004	0.992	1.367	0.004	1.002	1.364

* Note: Differences between secant τ_b and tangent τ_b are negligible

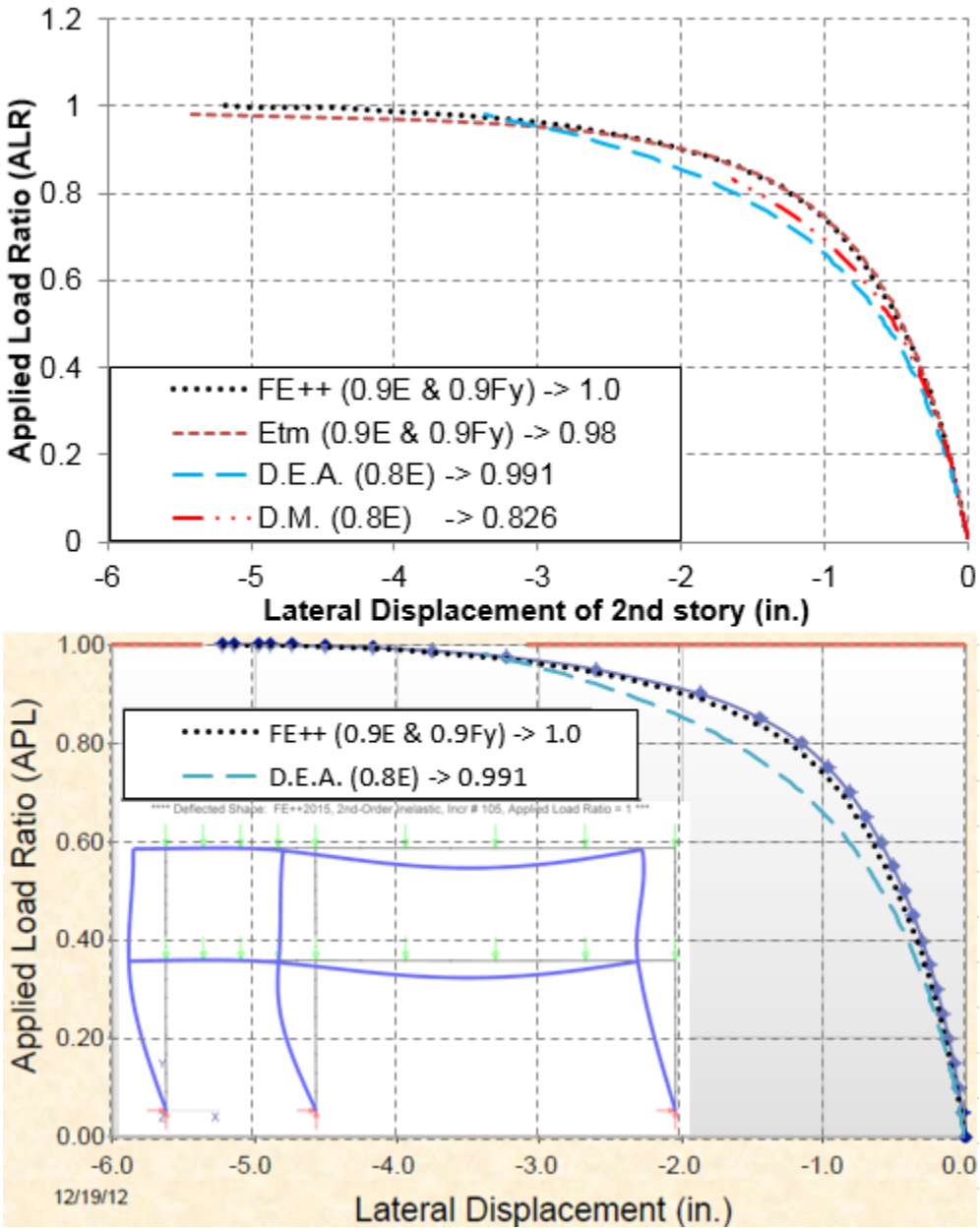

Figure C 4. System 1b Lateral Displacement Plots

C.3. System 2 Maleck (2001) Industrial Frame (Majox Axis)

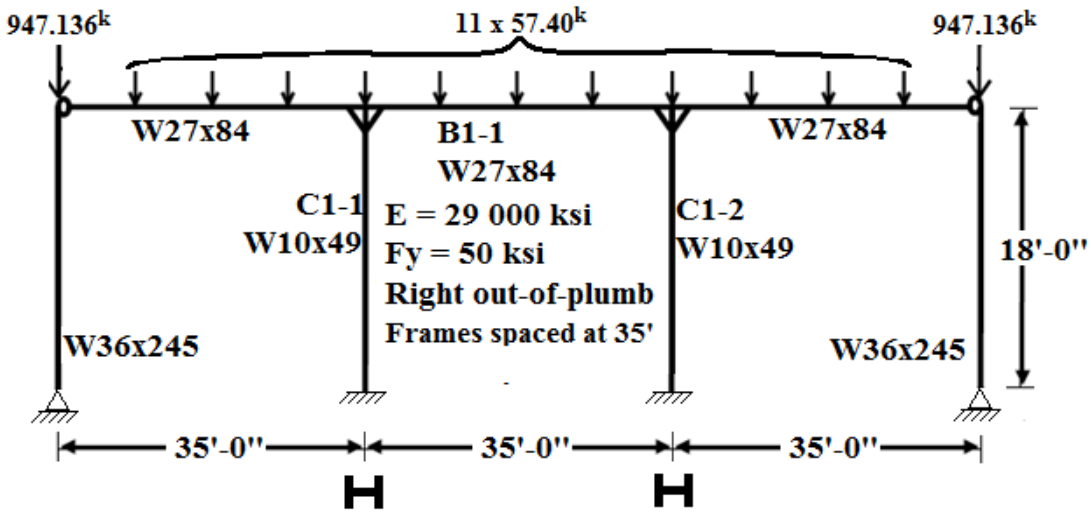

Figure C 5. System 2 Factored Loads

Table C 3. System 2 H1-1 and λ values

	H1-1 at Applied Load Ratio = 1.00								
	Direct Analysis Method			Elastic Analysis without member imperfections			Elastic Analysis with member imperfections		
Member	$P_u/\Phi P_n$	$M_u/\Phi M_n$	H1-1	$P_u/\Phi P_n$	$M_u/\Phi M_n$	H1-1	$P_u/\Phi P_n$	$M_u/\Phi M_n$	H1-1
C1-1	0.457	0.828	1.194	0.382	0.828	1.118	0.382	0.833	1.122
C1-2	0.473	0.591	0.998	0.395	0.591	0.920	0.395	0.597	0.926
B1-1	0.003	0.913	0.914	0.003	0.913	0.914	0.003	0.917	0.918

* Note: All $P_u/\Phi P_n < 0.5$, i.e. $\tau_b = 1$

	Applied Load Ratio when H1-1 = 1.00								
	Direct Analysis Method			Elastic Analysis without member imperfections			Elastic Analysis with member imperfections		
Member	$P_u/\Phi P_n$	$M_u/\Phi M_n$	Λ	$P_u/\Phi P_n$	$M_u/\Phi M_n$	Λ	$P_u/\Phi P_n$	$M_u/\Phi M_n$	Λ
C1-1	0.433	0.627	0.947	0.368	0.676	0.970	0.368	0.679	0.969
C1-2	0.478	0.637	1.000	0.401	0.661	1.016	0.402	0.676	1.015
B1-1	0.003	0.990	1.047	0.003	0.990	1.047	0.003	1.000	1.045

* Note: All $P_u/\Phi P_n < 0.5$, i.e. $\tau_b = 1$

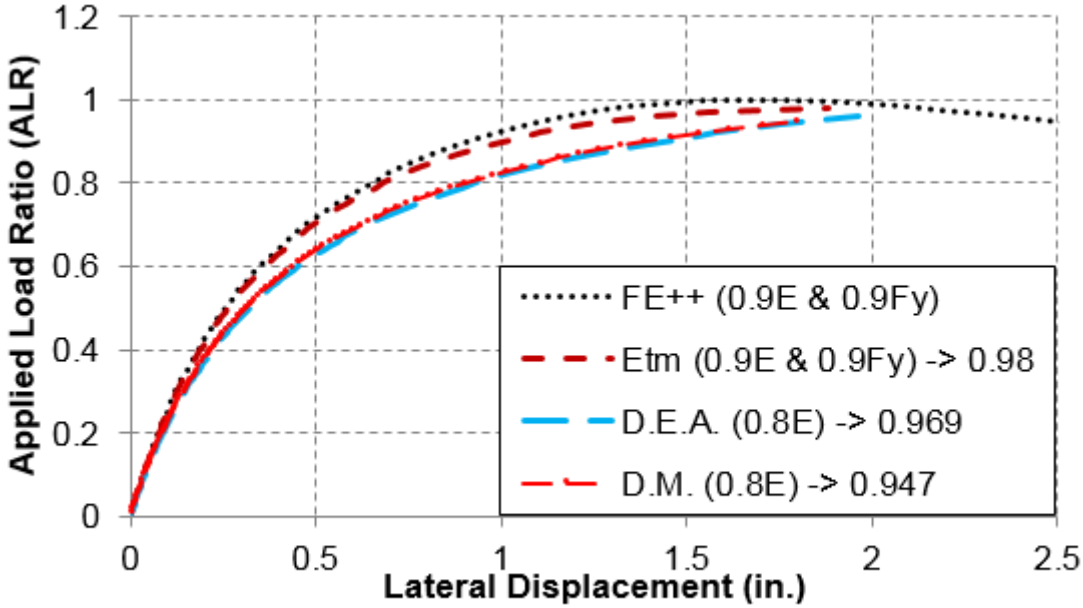

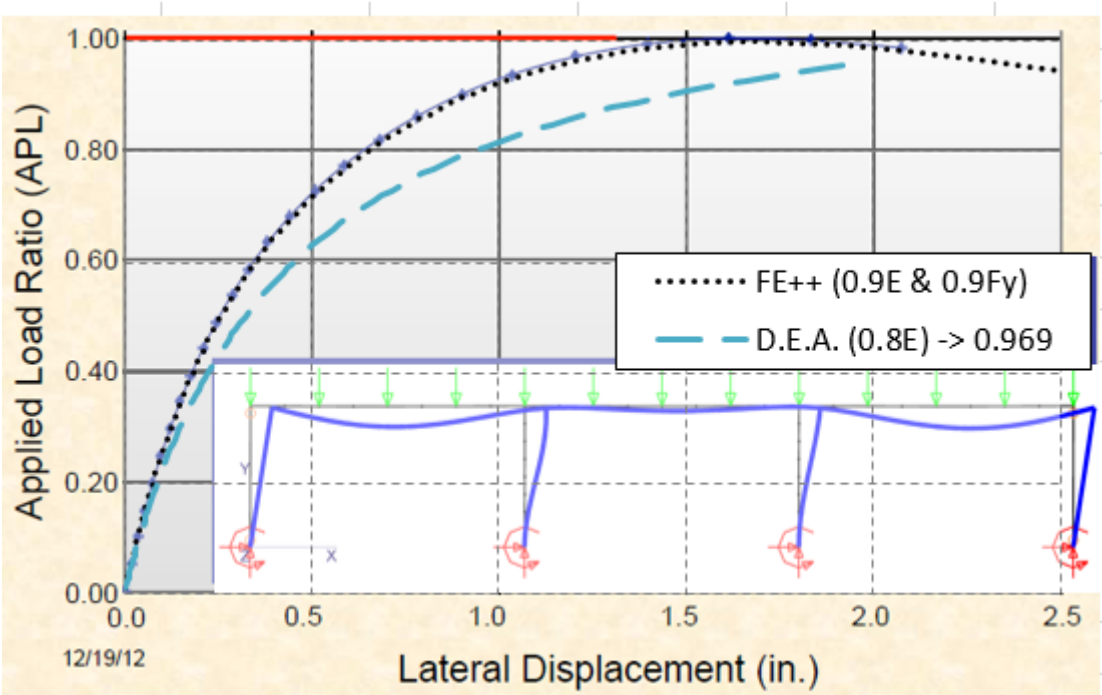

Figure C 6. System 2 Lateral Displacement Plots

C.4. System 3 Grain Storage Bin (major-axis)

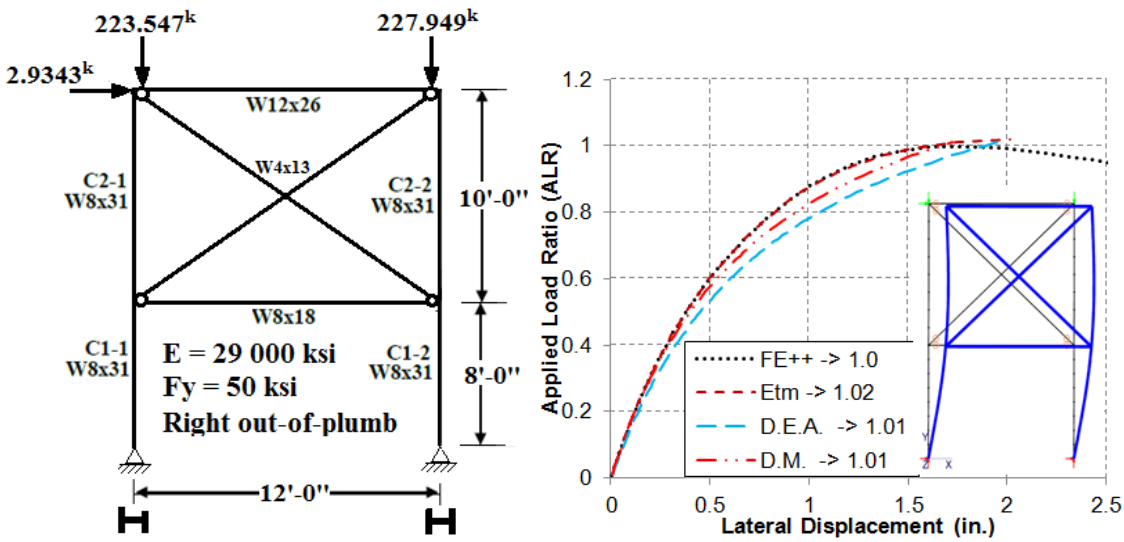

Figure C 7. System 3 Factored Loads and lateral displacement plot

Table C 4. System 3 H1-1 and λ values

	H1-1 at Applied Load Ratio = 1.00								
	Direct Analysis Method			Elastic Analysis without member imperfections			Elastic Analysis with member imperfections		
Member	$P_u/\Phi P_n$	$M_u/\Phi M_n$	H1-1	$P_u/\Phi P_n$	$M_u/\Phi M_n$	H1-1	$P_u/\Phi P_n$	$M_u/\Phi M_n$	H1-1
C1-1	0.548	0.403	0.906	0.518	0.403	0.876	0.516	0.440	0.907
C1-2	0.616	0.409	0.979	0.582	0.409	0.945	0.584	0.443	0.978
C2-1	0.532	0.403	0.890	0.487	0.403	0.845	0.486	0.440	0.877
C2-2	0.573	0.409	0.936	0.525	0.409	0.888	0.525	0.443	0.919

	Applied Load Ratio when H1-1 = 1.00								
	Direct Analysis Method			Elastic Analysis without member imperfections			Elastic Analysis with member imperfections		
Member	$P_u/\Phi P_n$	$M_u/\Phi M_n$	Λ	$P_u/\Phi P_n$	$M_u/\Phi M_n$	Λ	$P_u/\Phi P_n$	$M_u/\Phi M_n$	Λ
C1-1	0.576	0.487	1.053	0.546	0.494	1.069	0.535	0.504	1.049
C1-2	0.628	0.433	1.012	0.595	0.436	1.030	0.596	0.471	1.012
C2-1	0.566	0.508	1.061	0.527	0.541	1.083	0.516	0.552	1.064
C2-2	0.593	0.457	1.035	0.563	0.513	1.060	0.551	0.520	1.042

C.5. System 4 Vogel (1985) Multi-Story Frame (major-axis)

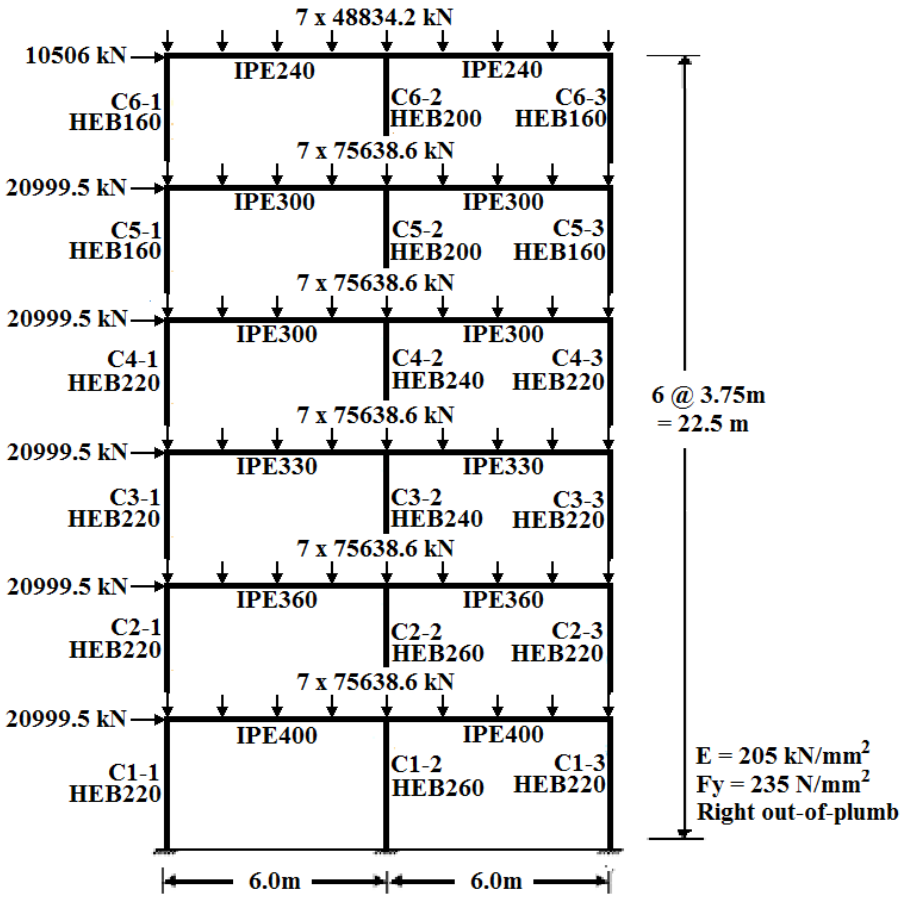

Figure C 8 System 4 Factored Loads

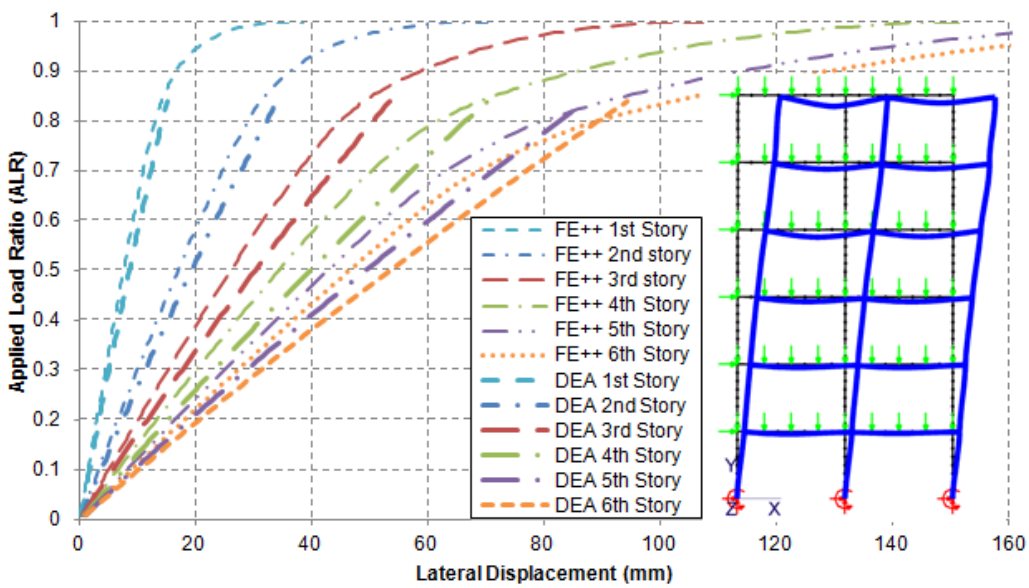

Figure C 9. System 4 Lateral Displacement Plot

Table C 5. System 4 H1-1 and λ values

	H1-1 at Applied Load Ratio = 1.00								
	Direct Analysis Method			Elastic Analysis without member imperfections			Elastic Analysis with member imperfections		
Member	$P_u/\Phi P_n$	$M_u/\Phi M_n$	H1-1	$P_u/\Phi P_n$	$M_u/\Phi M_n$	H1-1	$P_u/\Phi P_n$	$M_u/\Phi M_n$	H1-1
C1-1	0.383	0.340	0.686	0.355	0.340	0.657	0.354	0.337	0.654
C1-2	0.765	0.527	1.234	0.725	0.527	1.193	0.726	0.517	1.185
C1-3	0.518	0.545	1.002	0.479	0.545	0.963	0.479	0.543	0.962
C2-1	0.327	0.023	0.347	0.303	0.023	0.323	0.302	0.023	0.322
C2-2	0.627	0.423	1.002	0.594	0.423	0.969	0.594	0.420	0.967
C2-3	0.419	0.627	0.977	0.388	0.627	0.946	0.388	0.627	0.945
C3-1	0.264	0.058	0.315	0.244	0.058	0.296	0.244	0.053	0.292
C3-2	0.554	0.362	0.876	0.519	0.362	0.841	0.520	0.362	0.842
C3-3	0.320	0.579	0.835	0.297	0.579	0.811	0.297	0.578	0.810
C4-1	0.195	0.261	0.358	0.181	0.261	0.351	0.180	0.259	0.349
C4-2	0.406	0.261	0.638	0.381	0.261	0.613	0.381	0.262	0.613
C4-3	0.224	0.637	0.791	0.208	0.637	0.774	0.208	0.636	0.773
C5-1	0.221	0.276	0.466	0.190	0.276	0.371	0.190	0.271	0.366
C5-2	0.358	0.309	0.632	0.326	0.309	0.600	0.326	0.305	0.597
C5-3	0.242	0.783	0.938	0.208	0.783	0.904	0.208	0.779	0.901
C6-1	0.088	0.669	0.713	0.076	0.669	0.707	0.076	0.669	0.707
C6-2	0.141	0.098	0.169	0.128	0.098	0.162	0.128	0.097	0.161
C6-3	0.093	0.844	0.890	0.080	0.844	0.884	0.080	0.843	0.882

	Applied Load Ratio when H1-1 = 1.00								
	Direct Analysis Method			Elastic Analysis without member imperfections			Elastic Analysis with member imperfections		
Member	$P_u/\Phi P_n$	$M_u/\Phi M_n$	Λ	$P_u/\Phi P_n$	$M_u/\Phi M_n$	Λ	$P_u/\Phi P_n$	$M_u/\Phi M_n$	Λ
C1-1	0.522	0.534	1.377	0.498	0.565	1.415	0.496	0.560	1.418
C1-2	0.623	0.420	0.816	0.614	0.439	0.843	0.611	0.428	0.849
C1-3	0.513	0.539	0.998	0.497	0.567	1.035	0.496	0.565	1.036
C2-1			1.530			1.530			1.530
C2-2	0.622	0.419	0.998	0.606	0.433	1.029	0.617	0.439	1.031
C2-3	0.431	0.646	1.023	0.410	0.666	1.054	0.410	0.665	1.055
C3-1			1.530			1.530			1.530
C3-2	0.630	0.423	1.132	0.610	0.439	1.175	0.611	0.439	1.174
C3-3	0.381	0.698	1.184	0.361	0.717	1.216	0.361	0.715	1.217
C4-1			1.530			1.530			1.530
C4-2	0.610	0.432	1.519			1.530			1.530
C4-3	0.283	0.815	1.250	0.266	0.826	1.275	0.265	0.823	1.277
C5-1			1.530			1.530			1.530
C5-2			1.530			1.530			1.530
C5-3	0.258	0.837	1.064	0.231	0.872	1.102	0.230	0.865	1.105
C6-1	0.123	0.935	1.397	0.107	0.941	1.409	0.107	0.941	1.409
C6-2			1.530			1.530			1.530
C6-3	0.105	0.954	1.121	0.089	0.947	1.129	0.091	0.962	1.131

C.6. System 5 Martinez-García (2002) Gable Frame (major-axis)

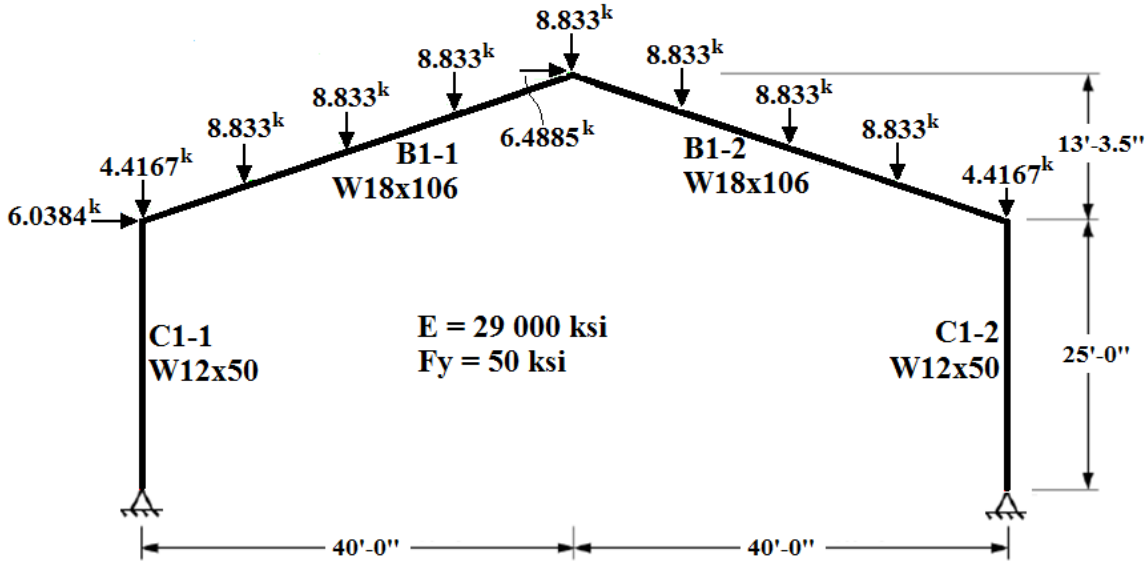

Figure C 10. System 5 Factored Loads

Table C 6. System 5 H1-1 and λ values

	H1-1 at Applied Load Ratio = 1.00								
	Direct Analysis Method			Elastic Analysis without member imperfections			Elastic Analysis with member imperfections		
Member	$P_u/\Phi P_n$	$M_u/\Phi M_n$	H1-1	$P_u/\Phi P_n$	$M_u/\Phi M_n$	H1-1	$P_u/\Phi P_n$	$M_u/\Phi M_n$	H1-1
C1-1	0.058	0.151	0.180	0.045	0.151	0.174	0.045	0.150	0.173
C1-2	0.080	1.562	1.602	0.063	1.562	1.593	0.063	1.562	1.593
B1-1	0.010	0.434	0.439	0.007	0.434	0.438	0.007	0.435	0.439
B1-2	0.025	0.488	0.501	0.018	0.488	0.497	0.018	0.488	0.497

* Note: All $P_u/\Phi P_n < 0.5$, i.e. $\tau_b = 1$

	Applied Load Ratio when H1-1 = 1.00								
	Direct Analysis Method			Elastic Analysis without member imperfections			Elastic Analysis with member imperfections		
Member	$P_u/\Phi P_n$	$M_u/\Phi M_n$	Λ	$P_u/\Phi P_n$	$M_u/\Phi M_n$	Λ	$P_u/\Phi P_n$	$M_u/\Phi M_n$	Λ
C1-1	0.151	0.918	2.957	0.119	0.932	2.968	0.119	0.939	2.966
C1-2	0.051	0.974	0.645	0.040	0.969	0.648	0.040	0.968	0.649
B1-1	0.019	0.987	2.108	0.014	0.995	2.113	0.014	0.988	2.109
B1-2	0.044	0.981	1.823	0.033	0.989	1.831	0.032	0.988	1.832

* Note: All $P_u/\Phi P_n < 0.5$, i.e. $\tau_b = 1$

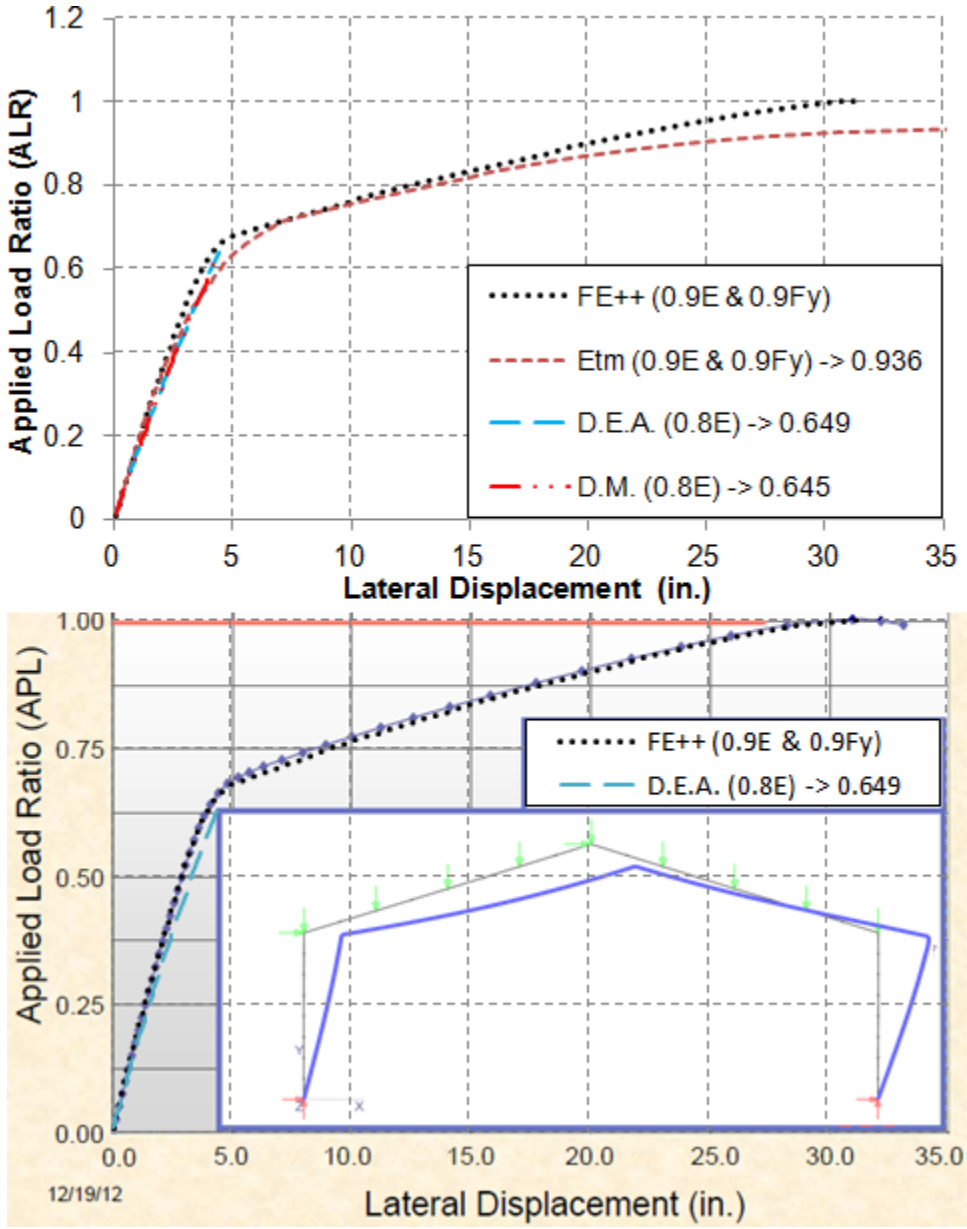

Figure C 11. System 5 Lateral Displacement Plots

C.7. System 6 Martinez-García (2002) Moment-Frame (major-axis)

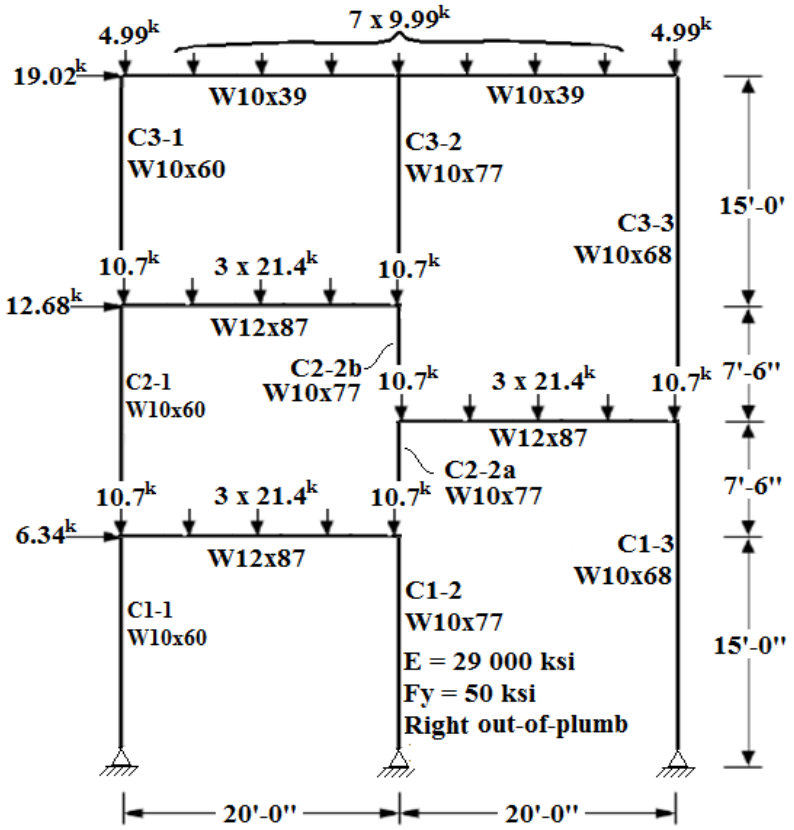

Figure C 12. System 6 Factored Loads

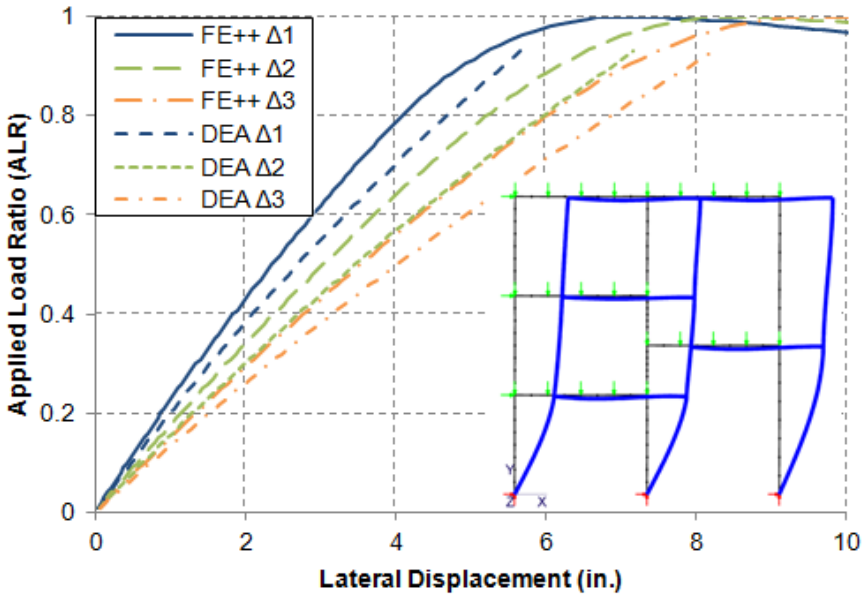

Figure C 13. System 6 Lateral Displacement Plots

Table C 7. System 6 H1-1 and λ values

	H1-1 at Applied Load Ratio = 1.00								
	Direct Analysis Method			Elastic Analysis without member imperfections			Elastic Analysis with member imperfections		
Member	$P_u/\Phi P_n$	$M_u/\Phi M_n$	H1-1	$P_u/\Phi P_n$	$M_u/\Phi M_n$	H1-1	$P_u/\Phi P_n$	$M_u/\Phi M_n$	H1-1
C1-1	0.072	0.884	0.920	0.064	0.884	0.916	0.064	0.888	0.920
C1-2	0.221	0.989	1.100	0.196	0.989	1.087	0.196	0.990	1.088
C1-3	0.125	0.628	0.691	0.096	0.628	0.676	0.096	0.626	0.674
C2-1	0.062	0.098	0.129	0.055	0.098	0.126	0.055	0.097	0.124
C2-2a	0.123	0.289	0.351	0.119	0.289	0.349	0.120	0.290	0.350
C2-2b	0.100	0.432	0.482	0.097	0.432	0.480	0.098	0.432	0.481
C3-1	0.021	0.019	0.029	0.019	0.019	0.028	0.019	0.019	0.028
C3-2	0.047	0.267	0.290	0.041	0.267	0.288	0.041	0.266	0.287
C3-3	0.033	0.278	0.294	0.026	0.278	0.290	0.026	0.278	0.291
B1-1	0.006	0.945	0.949	0.006	0.945	0.949	0.006	0.946	0.949
B2-1	0.012	0.517	0.522	0.010	0.517	0.522	0.010	0.516	0.521
B2-2	0.001	0.585	0.585	0.001	0.585	0.585	0.001	0.584	0.584
B3-1	0.047	0.629	0.652	0.037	0.629	0.648	0.037	0.630	0.649
B3-2	0.019	0.506	0.515	0.015	0.506	0.513	0.015	0.506	0.514

* Note: All $P_u/\Phi P_n < 0.5$, i.e. $\tau_b = 1$

	Applied Load Ratio when H1-1 = 1.00								
	Direct Analysis Method			Elastic Analysis without member imperfections			Elastic Analysis with member imperfections		
Member	$P_u/\Phi P_n$	$M_u/\Phi M_n$	Λ	$P_u/\Phi P_n$	$M_u/\Phi M_n$	Λ	$P_u/\Phi P_n$	$M_u/\Phi M_n$	Λ
C1-1	0.076	0.965	1.064	0.067	0.961	1.067	0.067	0.971	1.063
C1-2	0.204	0.898	0.924	0.183	0.910	0.934	0.183	0.911	0.934
C1-3	0.171	0.912	1.346	0.132	0.929	1.367	0.132	0.925	1.370
C2-1	0.188	0.903	3.326	0.167	0.922	3.333	0.167	0.908	3.328
C2-2a	0.254	0.844	2.152	0.248	0.853	2.161	0.246	0.843	2.158
C2-2b	0.200	0.906	1.960	0.193	0.903	1.965	0.194	0.904	1.964
C3-1			4.130			4.130			4.130
C3-2	0.149	0.928	3.341	0.133	0.938	3.360	0.133	0.931	3.358
C3-3	0.107	0.947	3.064	0.083	0.963	3.090	0.083	0.956	3.088
B1-1	0.007	0.996	1.045	0.007	0.996	1.045	0.007	0.998	1.044
B2-1	0.023	0.984	1.839	0.020	0.995	1.841	0.020	0.994	1.842
B2-2	0.003	0.992	1.569	0.003	0.992	1.569	0.003	1.006	1.571
B3-1	0.071	0.960	1.518	0.057	0.966	1.529	0.057	0.970	1.526
B3-2	0.034	0.986	1.902	0.027	0.983	1.909	0.027	0.984	1.907

* Note: All $P_u/\Phi P_n < 0.5$, i.e. $\tau_b = 1$

C.8. System 7a – Two Bay Moment Frames with Unequal Heights

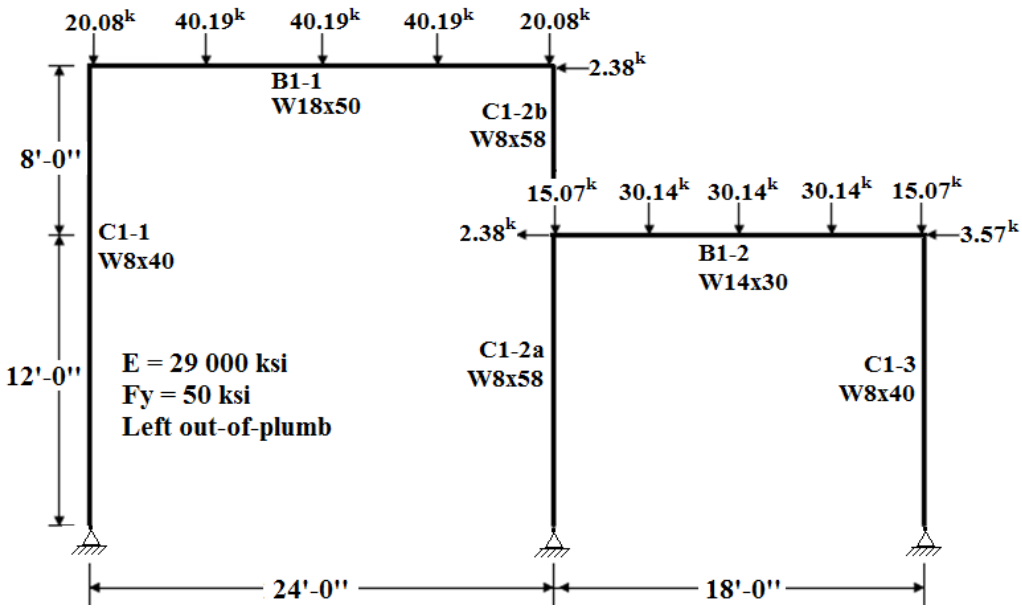

Figure C 14. System 7a Factored Loads

Table C 8. System 7a H1-1 and λ values

	H1-1 at Applied Load Ratio = 1.00								
	Direct Analysis Method			Elastic Analysis without member imperfections			Elastic Analysis with member imperfections		
Member	$P_u/\Phi P_n$	$M_u/\Phi M_n$	H1-1	$P_u/\Phi P_n$	$M_u/\Phi M_n$	H1-1	$P_u/\Phi P_n$	$M_u/\Phi M_n$	H1-1
C1-1	0.213	0.604	0.750	0.152	0.604	0.680	0.152	0.597	0.672
C1-2a	0.220	0.513	0.677	0.197	0.513	0.612	0.197	0.514	0.612
C1-2b	0.111	0.458	0.514	0.105	0.458	0.511	0.105	0.460	0.513
C1-3	0.108	0.202	0.255	0.095	0.202	0.249	0.095	0.194	0.241
B1-1	0.006	1.020	1.024	0.005	1.020	1.023	0.005	1.022	1.025
B1-2	0.018	1.205	1.214	0.016	1.205	1.213	0.015	1.208	1.215

	Applied Load Ratio when H1-1 = 1.00								
	Direct Analysis Method			Elastic Analysis without member imperfections			Elastic Analysis with member imperfections		
Member	$P_u/\Phi P_n$	$M_u/\Phi M_n$	Λ	$P_u/\Phi P_n$	$M_u/\Phi M_n$	Λ	$P_u/\Phi P_n$	$M_u/\Phi M_n$	Λ
C1-1	0.284	0.813	1.321	0.219	0.886	1.430	0.220	0.880	1.443
C1-2a	0.308	0.783	1.383	0.279	0.802	1.419	0.280	0.806	1.417
C1-2b	0.220	0.881	2.012	0.211	0.887	2.036	0.211	0.890	2.033
C1-3	0.210	0.874	2.448	0.186	0.913	2.454	0.185	0.897	2.437
B1-1	0.006	0.992	0.977	0.005	0.992	0.978	0.005	0.996	0.976
B1-2	0.016	0.984	0.838	0.014	0.983	0.839	0.013	0.986	0.838

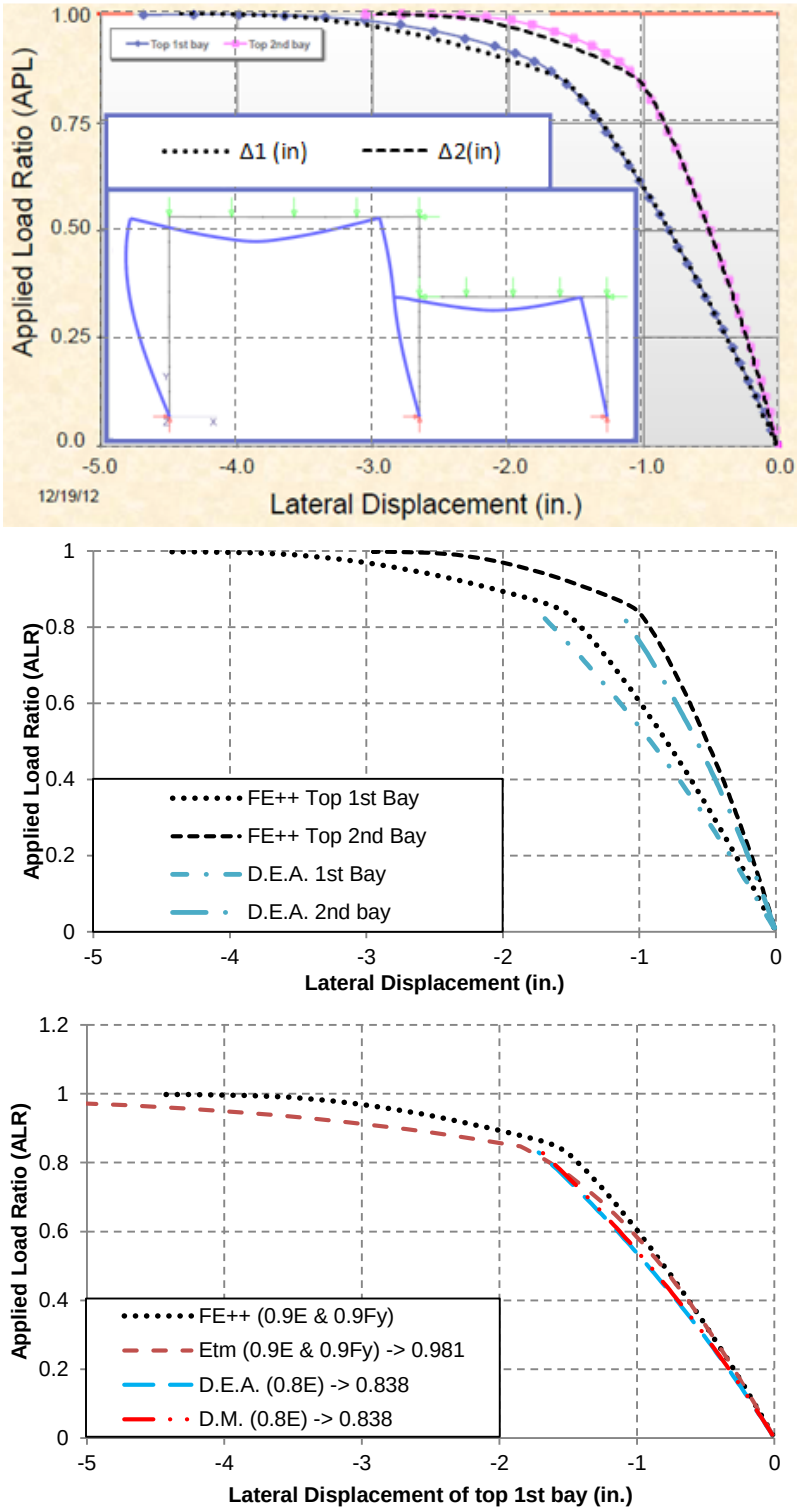

Figure C 15. System 7a Lateral Displacement Plots

C.9. System 7b – Two Bay Moment Frames, Unequal Heights

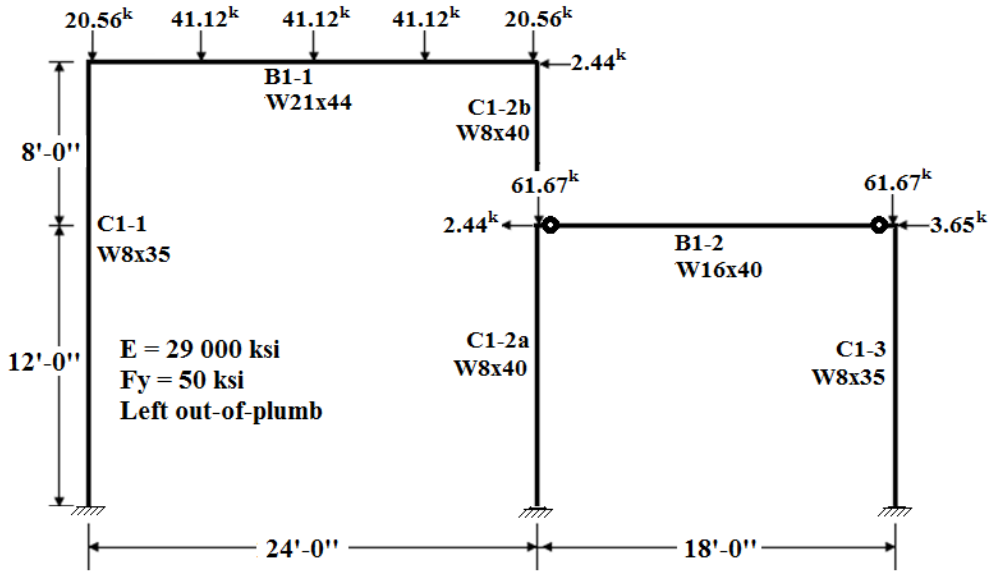

Figure C 16. System 7b Factored Loads

Table C 9. System 7b H1-1 and λ values

	H1-1 at Applied Load Ratio = 1.00								
	Direct Analysis Method			Elastic Analysis without member imperfections			Elastic Analysis with member imperfections		
Member	$P_u/\Phi P_n$	$M_u/\Phi M_n$	H1-1	$P_u/\Phi P_n$	$M_u/\Phi M_n$	H1-1	$P_u/\Phi P_n$	$M_u/\Phi M_n$	H1-1
C1-1	0.256	0.880	1.038	0.182	0.880	0.971	0.182	0.875	0.966
C1-2a	0.251	0.126	0.364	0.224	0.126	0.336	0.224	0.124	0.334
C1-2b	0.133	0.362	0.429	0.127	0.362	0.425	0.127	0.357	0.420
C1-3	0.150	0.135	0.210	0.133	0.135	0.202	0.133	0.134	0.200
B1-1	0.019	1.130	1.139	0.015	1.130	1.138	0.015	1.133	1.141
B1-2	0.005		0.003	0.005		0.002	0.005		0.002

	Applied Load Ratio when H1-1 = 1.00								
	Direct Analysis Method			Elastic Analysis without member imperfections			Elastic Analysis with member imperfections		
Member	$P_u/\Phi P_n$	$M_u/\Phi M_n$	Λ	$P_u/\Phi P_n$	$M_u/\Phi M_n$	Λ	$P_u/\Phi P_n$	$M_u/\Phi M_n$	Λ
C1-1	0.247	0.850	0.964	0.186	0.899	1.029	0.189	0.908	1.034
C1-2a	0.611	0.436	2.456	0.571	0.488	2.571	0.564	0.490	2.545
C1-2b	0.495	0.568	4.005	0.470	0.609	4.013	0.468	0.588	3.997
C1-3	0.401	0.671	2.667	0.366	0.720	2.740	0.364	0.715	2.735
B1-1	0.016	0.983	0.879	0.014	1.004	0.880	0.013	0.986	0.878
B1-2			4.370			4.370			4.370

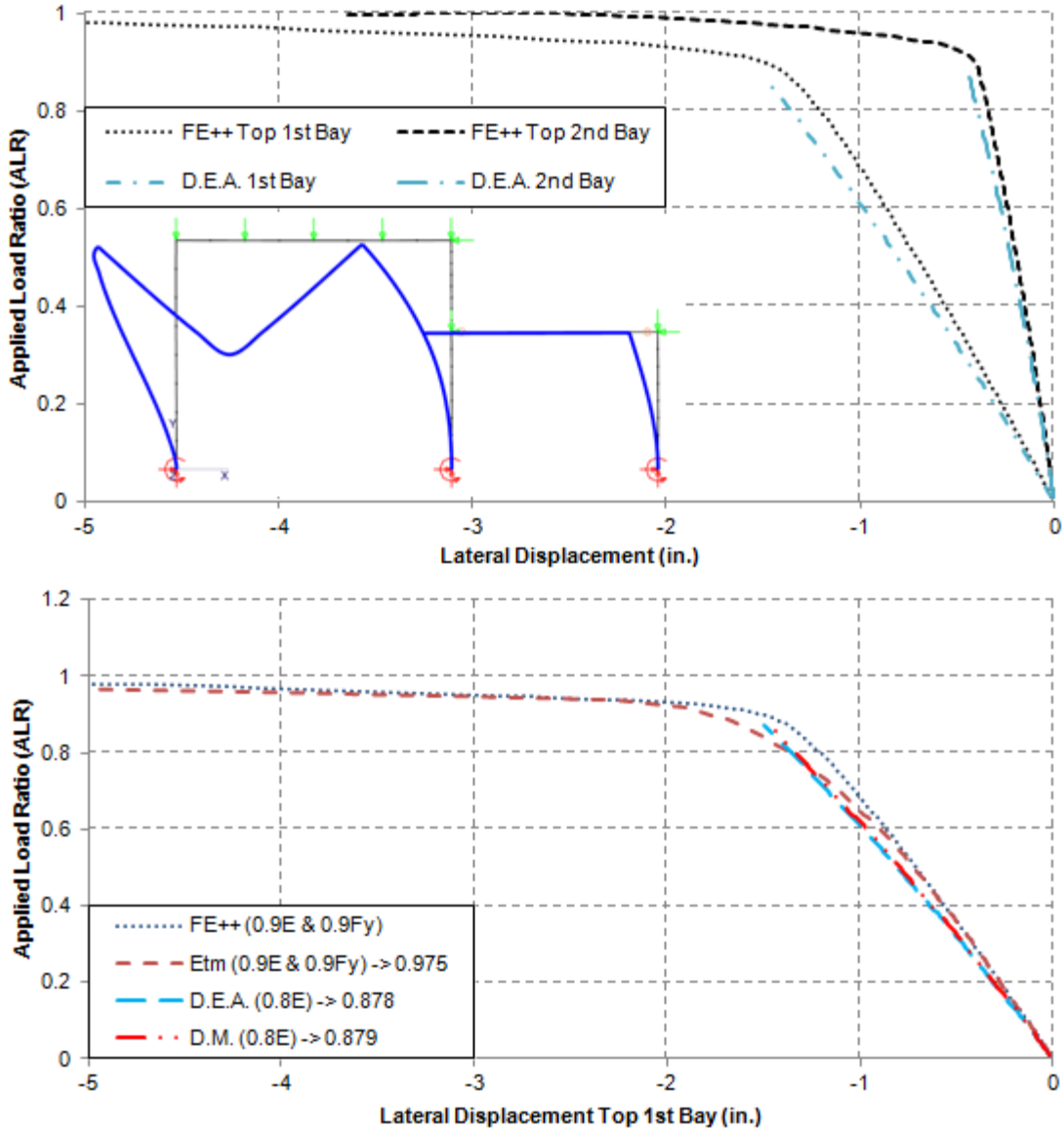

Figure C 17. System 7b Lateral Displacement Plots

C.10. System 7c – Two Bay Braced Frame with Unequal Heights

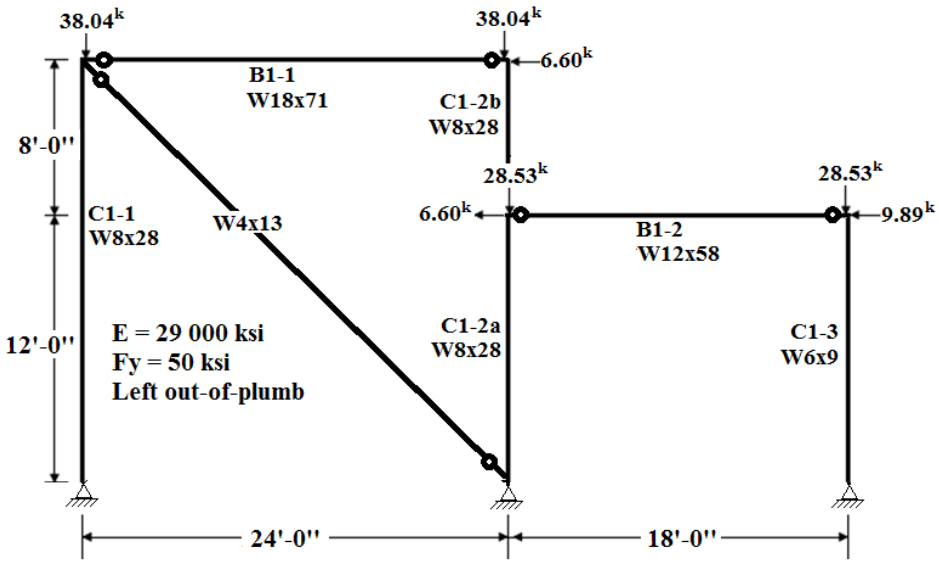

Figure C 18. System 7c Factored Loads

Table C 10. System 7c H1-1 and λ values

	H1-1 at Applied Load Ratio = 1.00								
	Direct Analysis Method			Elastic Analysis without member imperfections			Elastic Analysis with member imperfections		
Member	$P_u/\Phi P_n$	$M_u/\Phi M_n$	H1-1	$P_u/\Phi P_n$	$M_u/\Phi M_n$	H1-1	$P_u/\Phi P_n$	$M_u/\Phi M_n$	H1-1
C1-1	0.202		0.202	0.142		0.071	0.142	0.012	0.082
C1-2a	0.256	0.897	1.053	0.180	0.897	0.987	0.180	0.898	0.988
C1-2b	0.146	0.897	0.970	0.102	0.897	0.948	0.102	0.898	0.949
C1-3	0.303		0.303	0.237		0.237	0.237	0.014	0.249
B1-1	0.021		0.010	0.018		0.009	0.018		0.009
B1-2	0.015		0.008	0.014		0.007	0.014		0.007
BRACE	0.131		0.066	0.131		0.066	0.131		0.066

	Applied Load Ratio when H1-1 = 1.00								
	Direct Analysis Method			Elastic Analysis without member imperfections			Elastic Analysis with member imperfections		
Member	$P_u/\Phi P_n$	$M_u/\Phi M_n$	Λ	$P_u/\Phi P_n$	$M_u/\Phi M_n$	Λ	$P_u/\Phi P_n$	$M_u/\Phi M_n$	Λ
C1-1			3.800			3.800			3.800
C1-2a	0.244	0.852	0.954	0.183	0.916	1.012	0.183	0.918	1.011
C1-2b	0.149	0.921	1.027	0.107	0.942	1.047	0.107	0.944	1.046
C1-3	1.001	0.000	3.284			3.800	0.892	0.121	3.746
B1-1			3.800			3.800			3.800
B1-2			3.800			3.800			3.800
BRACE			3.800			3.800			3.800

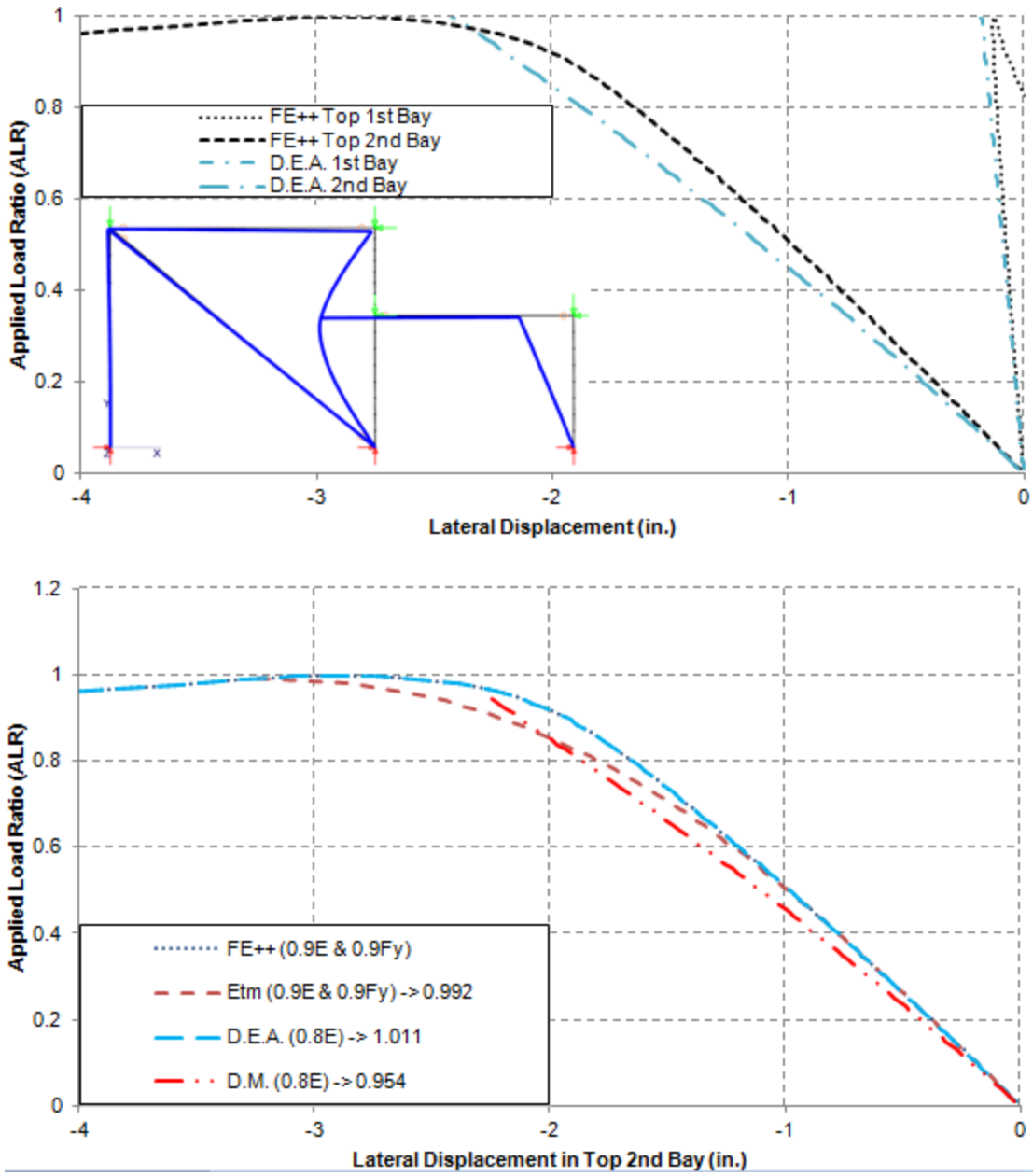

Figure C 19. System 7c Lateral Displacement Plots

C.11. System 8 – Vierendeel Truss

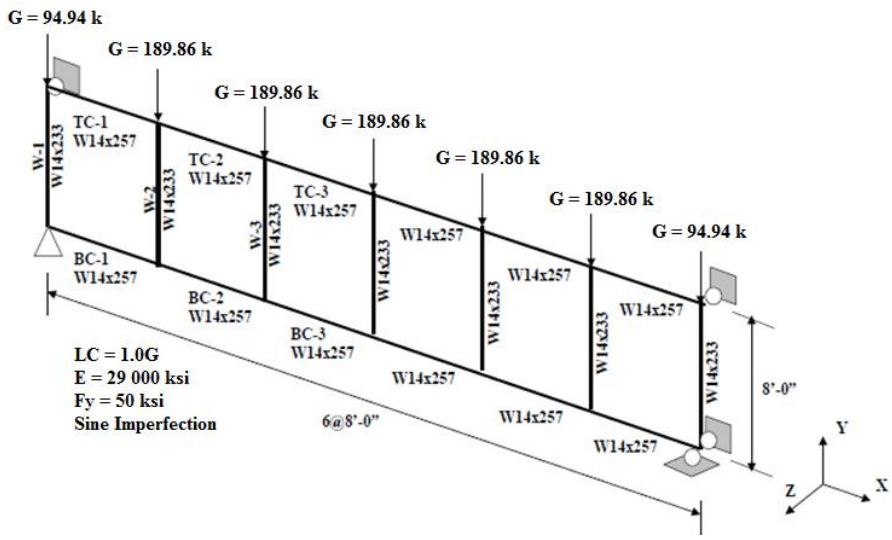

Figure C 20. System 8 Factored Loads

Table C 11. System 8 H1-1 and λ values

1	H1-1 at Applied Load Ratio = 1.00							
	Direct Analysis Method				Elastic Analysis with member imperfections			
Member	$P_u/\Phi P_n$	$M_{ux}/\Phi M_{nx}$	$M_{uy}/\Phi M_{ny}$	H1-1	$P_u/\Phi P_n$	$M_{ux}/\Phi M_{nx}$	$M_{uy}/\Phi M_{ny}$	H1-1
TC-1	0.279	0.414	0.363	0.969	0.072	0.413	0.364	0.813
TC-2	0.654	0.375	0.769	1.671	0.169	0.375	0.771	1.230
TC-3	0.858	0.205	0.930	1.867	0.221	0.205	0.932	1.232
BC-1	0.074	0.576	0.081	0.694	0.074	0.576	0.081	0.694
BC-2	0.169	0.408	0.027	0.520	0.169	0.408	0.027	0.520
BC-3	0.221	0.204	0.000	0.403	0.221	0.204		0.403
W-1	0.108	0.630	0.022	0.705	0.104	0.630	0.022	0.704
W-2	0.042	0.790	0.034	0.845	0.040	0.790	0.034	0.844
W-3	0.029	0.433	0.022	0.470	0.028	0.433	0.023	0.470
W-4	0.029		0.025	0.040	0.028		0.025	0.039

1	Applied Load Ratio when H1-1 = 1.00							
	Direct Analysis Method				Elastic Analysis with member imperfections			
Member	$P_u/\Phi P_n$	$M_{ux}/\Phi M_{nx}$	$M_{uy}/\Phi M_{ny}$	Λ	$P_u/\Phi P_n$	$M_{ux}/\Phi M_{nx}$	$M_{uy}/\Phi M_{ny}$	Λ
TC-1	0.282	0.393	0.431	1.012	0.076	0.278	0.683	1.085
TC-2	0.549	0.332	0.174	0.835	0.163	0.374	0.517	0.967
TC-3	0.697	0.170	0.179	0.803	0.217	0.203	0.750	0.971
BC-1	0.082	0.859	0.132	1.100	0.080	0.801	0.127	1.100
BC-2	0.213	0.648	0.223	1.318	0.213	0.647	0.223	1.318
BC-3	0.297	0.368	0.444	1.491	0.297	0.369	0.445	1.491
W-1	0.111	0.922	0.034	1.191	0.107	0.920	0.034	1.192
W-2	0.083	0.926	0.035	1.144	0.079	0.923	0.035	1.146
W-3				1.592				1.592
W-4				1.592				1.592

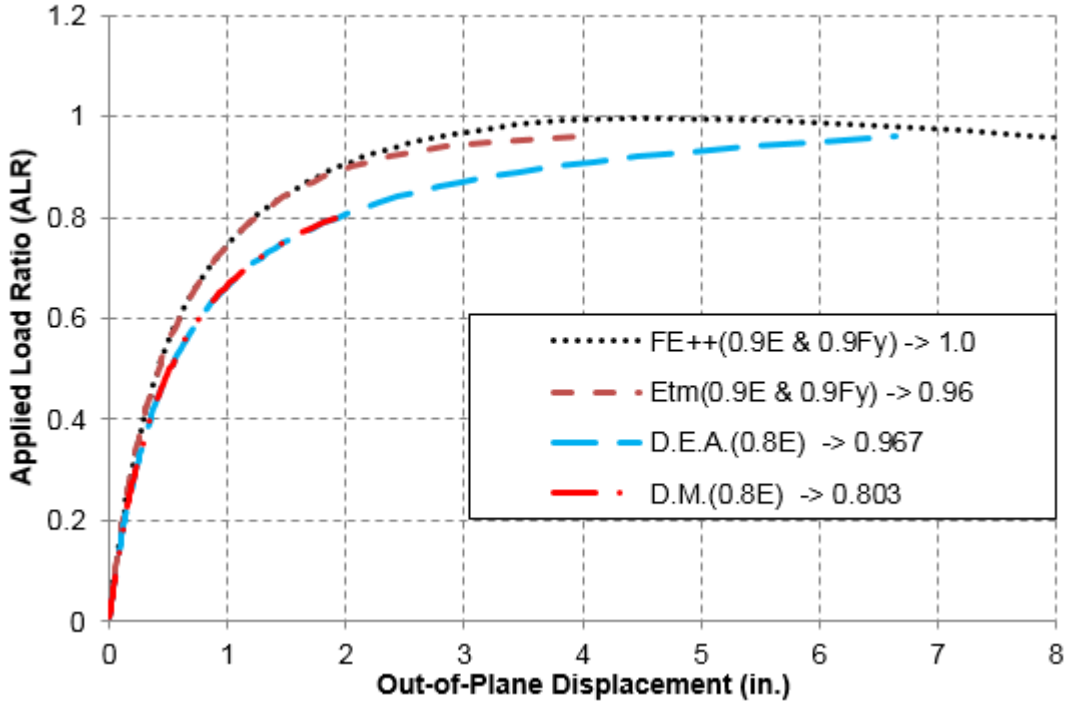

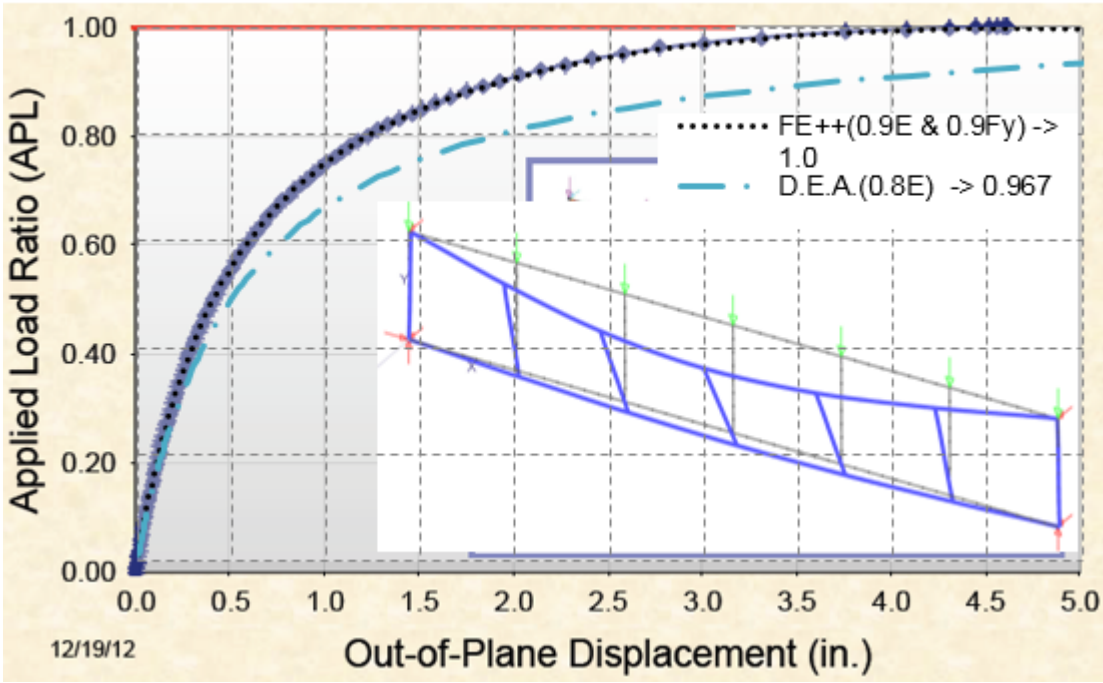

Figure C 21. System 8 Lateral Displacement Plots

C.12. System 9 – El Zanaty Frame

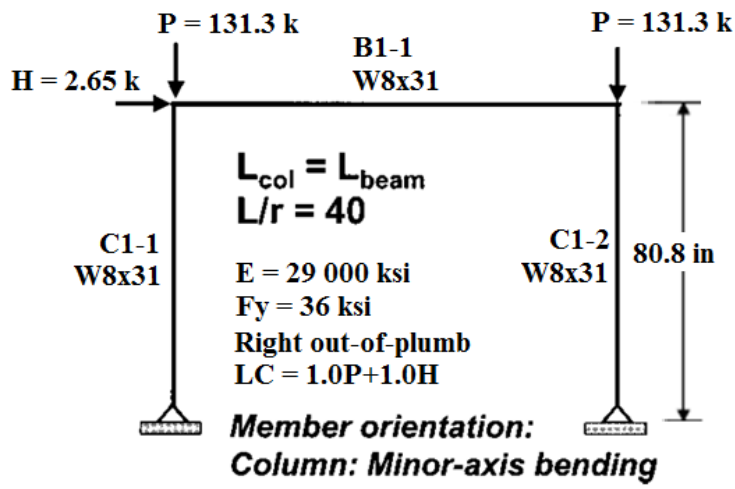

Figure C 22. System 9 Factored Loads

Table C 12. System 9 H1-1 and λ values

	H1-1 at Applied Load Ratio = 1.00								
	Direct Analysis Method			Elastic Analysis without member imperfections			Elastic Analysis with member imperfections		
Member	P_u/fP_n	M_u/fM_n	H1-1	P_u/fP_n	M_u/fM_n	H1-1	P_u/fP_n	M_u/fM_n	H1-1
C1-1	0.463	0.480	0.890	0.426	0.480	0.853	0.425	0.496	0.866
C1-2	0.503	0.478	0.928	0.463	0.478	0.888	0.463	0.492	0.901
B1-1	0.004	0.223	0.225	0.004	0.223	0.225	0.004	0.230	0.232

	Applied Load Ratio when H1-1 = 1.00								
	Direct Analysis Method			Elastic Analysis without member imperfections			Elastic Analysis with member imperfections		
Member	P_u/fP_n	M_u/fM_n	Λ	P_u/fP_n	M_u/fM_n	Λ	P_u/fP_n	M_u/fM_n	Λ
C1-1	0.500	0.555	1.088	0.471	0.583	1.119	0.468	0.598	1.105
C1-2	0.532	0.526	1.055	0.502	0.551	1.088	0.499	0.561	1.076
B1-1			1.395			1.395			1.376

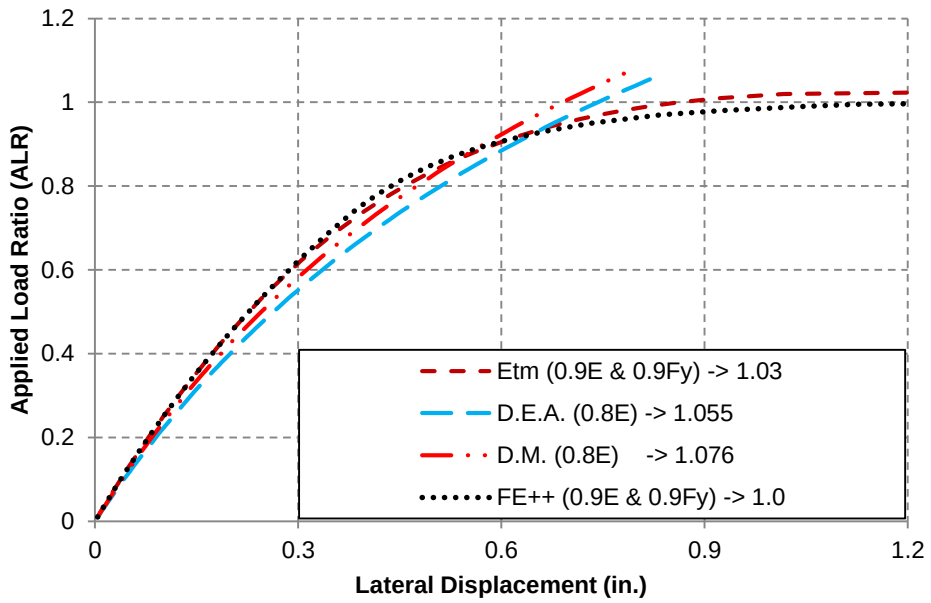

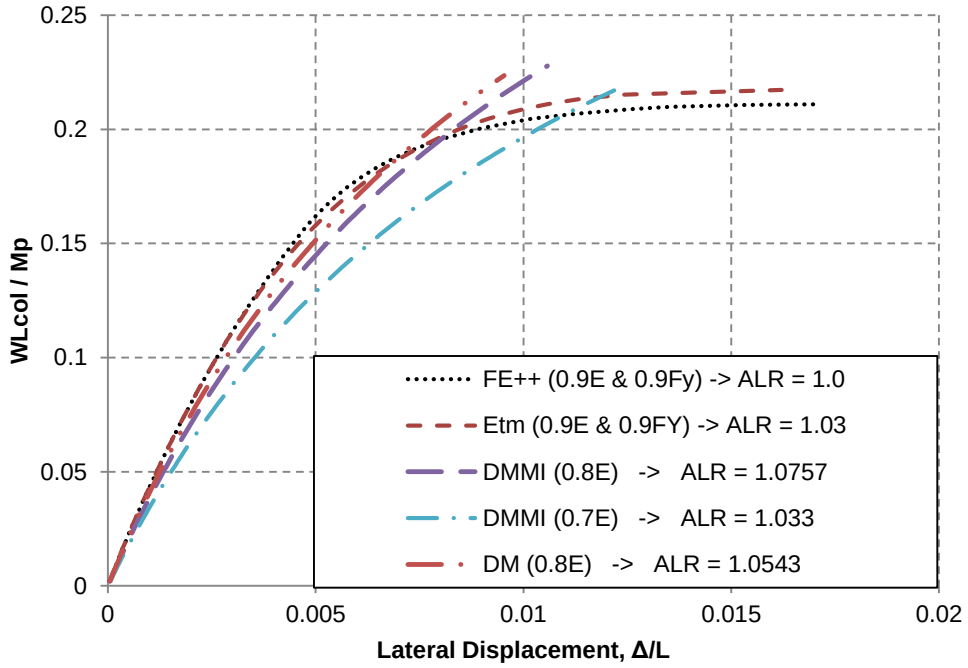

Figure C 23. System 9 Lateral Displacement Plots

Appendix D. Column Study Results

The results for a W8X58 column are representative of the other 10 square columns studied because of the small coefficients of variation present in the study.

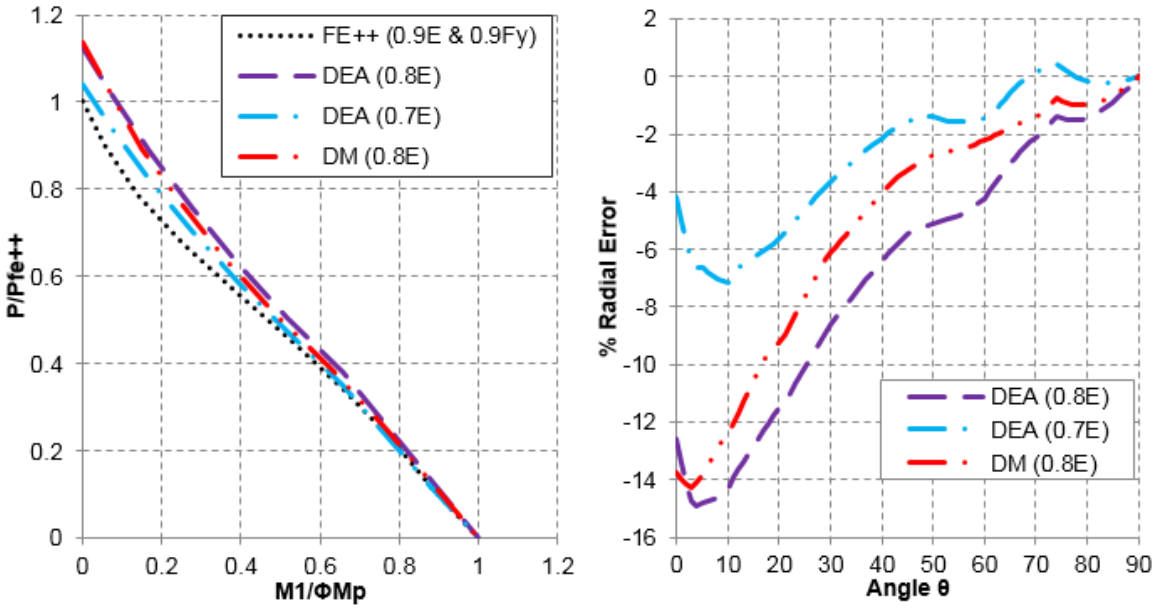

Figure D 1. W8X58, weak axis bending, L/r = 40, Fy = 50 ksi

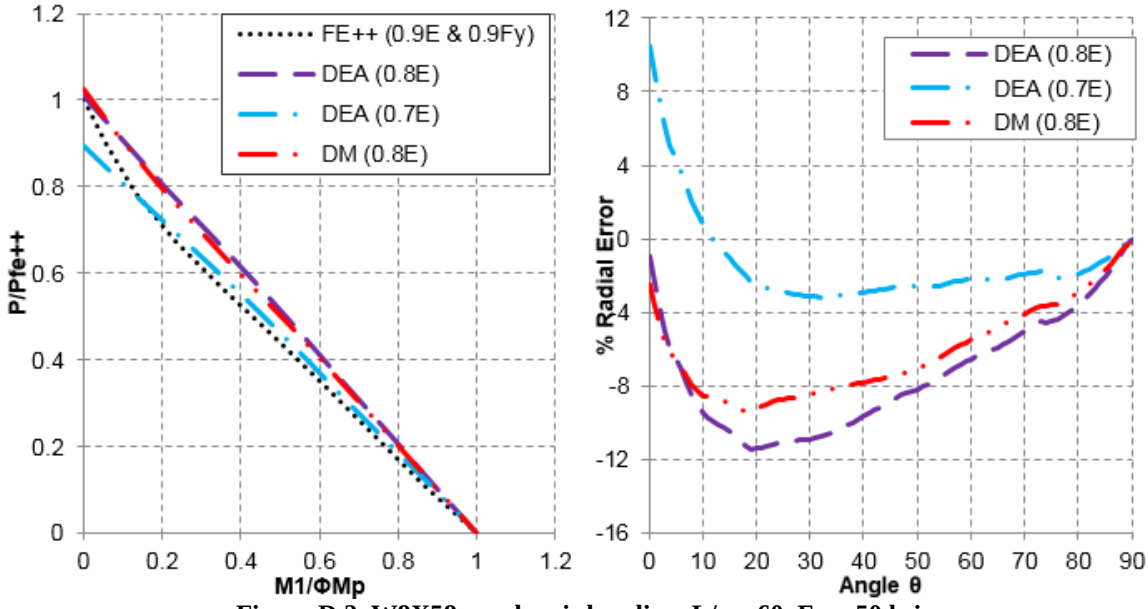

Figure D 2. W8X58, weak axis bending, L/r = 60, Fy = 50 ksi

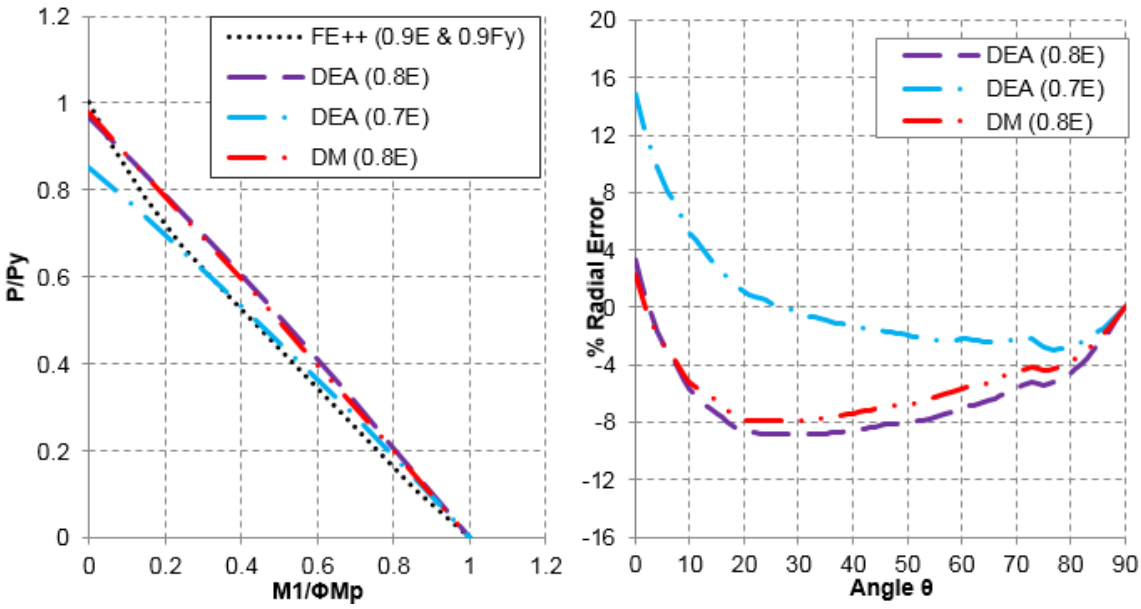

Figure D 3. W8X58, weak axis bending, L/r = 80, Fy = 50 ksi

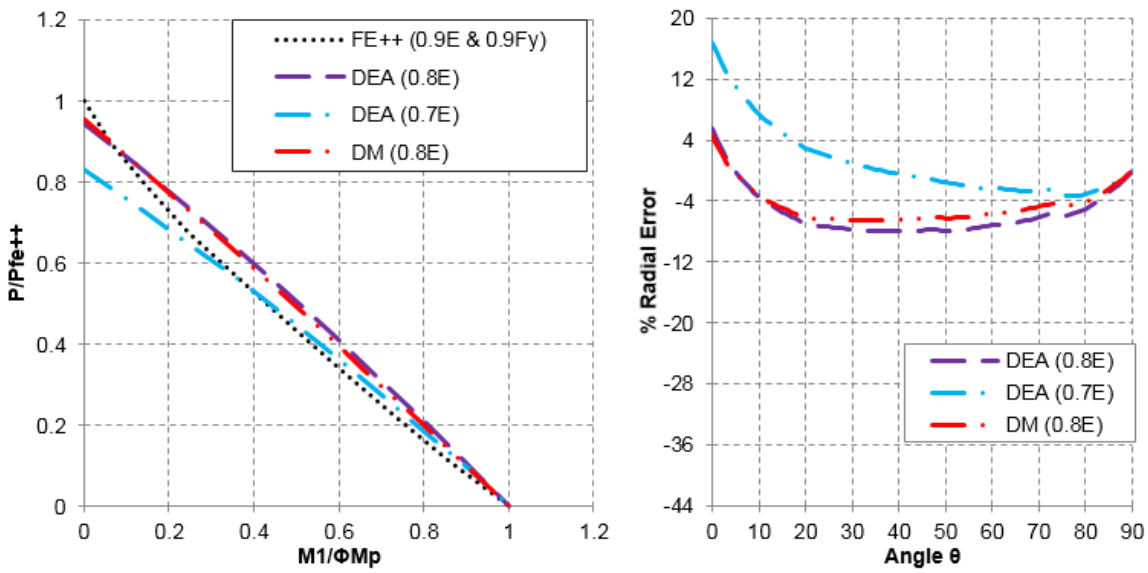

Figure D 4. W8X58, weak axis bending, L/r = 100, Fy = 50 ksi

The table below shows the maximum conservative and unconservative error present in each beam-column studied. The average and standard deviation values are shown in Table 7 in Section 4.3.

Table D 1. Conservative and Unconservative Errors in Minor-axis Column Study

Section Name	depth [in]	width [in]	Slenderness Ratio L/r	Max. Conservative% Error			Max. Unconservative% Error		
				DEA w/0.8E	DEA w/0.7E	DM w/0.8E	DEA w/0.8E	DEA w/0.7E	DM w/0.8E
W8X40	8.25	8.07	40	0.00	0.41	0.00	-15.03	-7.19	-14.37
			60	0.00	10.35	0.00	-11.36	-3.06	-9.32
			80	3.30	14.77	2.20	-8.70	-2.49	-7.70
			100	5.42	16.76	4.47	-7.83	-2.90	-6.42
W8X58	8.75	8.72	40	0.00	0.44	0.00	-14.91	-7.16	-14.29
			60	0.00	10.46	0.00	-11.51	-3.18	-9.50
			80	3.38	14.84	2.27	-8.86	-2.94	-7.87
			100	5.47	16.82	4.53	-7.97	-3.35	-6.60
W10X54	10.10	10.00	40	0.00	0.39	0.00	-14.87	-7.57	-14.51
			60	0.00	10.28	0.00	-11.69	-3.35	-9.68
			80	3.11	14.60	1.99	-9.03	-2.89	-8.09
			100	5.26	16.63	4.31	-8.18	-3.32	-6.77
W10X88	10.80	10.30	40	0.00	0.53	0.00	-14.48	-6.63	-13.85
			60	0.00	11.12	0.00	-10.75	-2.88	-8.76
			80	4.01	15.40	2.92	-8.03	-1.86	-7.04
			100	6.03	17.31	5.09	-7.21	-2.35	-5.78
W12X58	12.20	10.00	40	0.00	0.36	0.00	-15.18	-7.19	-14.66
			60	0.00	10.20	0.00	-11.48	-3.11	-9.48
			80	3.14	14.62	2.01	-8.78	-2.62	-7.91
			100	5.25	16.61	4.28	-7.96	-3.04	-6.57
W12X72	12.30	12.00	40	0.00	0.00	0.00	-15.67	-8.09	-15.01
			60	0.00	9.85	0.00	-12.11	-3.70	-10.08
			80	2.68	14.21	1.55	-9.40	-3.19	-8.50
			100	4.95	16.35	3.99	-8.57	-3.60	-7.18
W12X120	13.10	12.30	40	0.00	0.40	0.00	-15.14	-7.19	-14.51
			60	0.00	10.44	0.00	-11.48	-3.13	-9.47
			80	3.30	14.77	2.18	-8.78	-2.68	-7.84
			100	5.40	16.75	4.45	-8.09	-3.08	-6.58
W12X170	14.00	12.60	40	0.00	0.44	0.00	-14.75	-6.79	-14.11
			60	0.00	11.03	0.00	-10.94	-2.73	-8.94
			80	3.93	15.33	2.84	-8.32	-2.45	-7.31
			100	5.98	17.27	5.05	-7.52	-2.86	-6.06
W14X68	14.00	10.00	40	0.00	0.00	0.00	-15.35	-7.60	-15.21
			60	0.00	9.79	0.00	-12.03	-3.61	-10.02
			80	2.65	14.18	1.50	-9.40	-3.62	-8.50
			100	4.89	16.29	3.91	-8.60	-3.95	-7.19
W14X109	14.30	14.60	40	0.00	0.41	0.00	-15.12	-7.09	-17.06
			60	0.00	10.53	0.00	-11.36	-3.04	-11.57
			80	3.35	14.81	1.81	-8.63	-2.37	-9.19
			100	5.41	16.76	4.47	-7.76	-2.54	-6.37
W14X132	14.70	14.70	40	0.00	0.39	0.00	-15.25	-7.29	-14.60
			60	0.00	10.21	0.00	-11.67	-3.39	-9.65
			80	3.15	14.63	2.03	-8.94	-2.63	-8.00
			100	5.27	16.64	4.32	-8.07	-3.06	-6.68

References

Agüero, A., Pallarés, F.J., and Pallarés, L., (2015a). "Equivalent geometric imperfection definition in steel structures sensitive to lateral torsional buckling due to bending moment." *Engineering Structures* 96(2015)41-55 doi: 10.1016/j.engstruct.2015.03.066

Agüero, A., Pallarés, F.J., and Pallarés, L., (2015b). "Equivalent geometric imperfection definition in steel structures sensitive to flexural and/or torsional buckling due to compression." *Engineering Structures* 96(2015)160-177 doi: 10.1016/j.engstruct.2015.03.065

AISC (2000). *Code of standard practice for steel buildings and bridges. Manual of steel Construction–Load and resistance factor design* (2nd ed.). Chicago, Ill.: American Institute of Steel Construction.

AISC (2010). *ANSI/AISC 360-10 Specification for structural steel buildings.* (14th ed.). Chicago, Ill.: American Institute of Steel Construction.

AISC (2015), "Specification for structural steel buildings" *Draft. July 14th, Chicago, Ill.*

Alemdar, B. N. (2001). *Distributed plasticity analysis of steel building structural systems.* (Doctoral dissertation). Georgia Institute of Technology, Atlanta.

Alvarenga, A.R. and Silveria, R.A. (2009) "Second-order plastic-zone analysis of steel frames – part II: effects of initial geometric imperfection and residual stress." *Lat Am J Soilds Struct*, 120(5):1434-54

Galambos, T. V., and Ketter, R. L. (1959). "Columns under combined bending and thrust." *Journal of the Engineering Mechanics Division*, ASCE, 85(EM2)1-30

Kanchanalai, T. (1977). ''The design and behavior of beam columns in unbraced steel frames.'' *AISI Project No. 189, Rep. No. 2*, Civil Engineering/Structures Research Laboratory, University of Texas at Austin, Austin, TX.

Maleck, A. E. (2001). *Second-order inelastic and modified elastic analysis and design evaluation of planar steel frames.* (Doctoral dissertation). Georgia Institute of Technology, Atlanta.

Martinez-Garcia, J. (2002). *Benchmark studies to evaluate new provisions for frame stability using second-order analysis.* (Unpublished Master's Thesis) Bucknell University, Lewisburg, PA.

REFERENCES

Martinez-Garcia, J. M., and Ziemian, R. D. (2006, February). "Benchmark studies to compare frame stability provisions." *Proceedings – 2006 Annual Technical Session and Meeting, Structural Stability Research Council,* San Antonio, TX (8-11/2), pp. 425-442.

Nwe Nwe, M. T. (2014). *The modified direct analysis method: An extension of the direct analysis method* (honor's thesis). Bucknell University, Lewisburg, PA.(251)

Segui, W.T. (2013). *Steel Design* (5th Ed.) Stamford, CT.: Cengage Learning

Shaya. S, Rasmussen, K., and Zhang H. (2014). "On the modeling of initial geometric imperfections of steel frames in advanced analysis." *Journal of Constructional Steel Research, 98*(2014), 167-177. doi: 19.1061/j.jcsr.2014.02.016

Surovek, A. E. (2012). *Advanced Analysis in steel frame design*. Reston, VA: American Society of Civil Engineers.

Surovek-Maleck, A. E., and White, D. W. (2003). "Direct analysis approach for the assessment of frame stability: Verification studies." *Proceedings of the 2003 SSRC Annual Technical Sessions and Meeting,* Baltimore. 423.

Surovek-Maleck, A. E., and White, D. W. (2004a). "Alternative approached for elastic analysis and design of steel frames. I: Overview." *Journal of Structural Engineering, 130*(8), 1186. doi:10.1061/(ASCE)0733-9445(2004)130:8(1186)

Surovek-Maleck, A. E., and White, D. W. (2004b). "Alternative approached for elastic analysis and design of steel frames. II: Verification studies." *Journal of Structural Engineering, 130*(8), 1197-2005. doi:10.1061/(ASCE)0733-9445(2004)130:8(1197)

Vogel, U. (1984). "Calibrating Frames," Berlin: *Stahlbau*, 54, 295-301

Ziemian, R. D., and McGuire, W. (2002). "Modified tangent modulus approach, A contribution to plastic-hinge analysis." *Journal of Structural Engineering, 128*(10), 1301-1307.

Ziemian, R.D. and Miller, A. (1997), "Inelastic Analysis and Design: Frames with Members in Minor-Axis Bending." *Journal of Structural Engineering*, American Society of Civil Engineers, New York, New York.

Ziemian, R. D. (ed.) (2010). *Guide to stability design criteria for metal structures*. 6th Edition, Structural Stability Research Council, Hoboken, N.J.: John Wiley and Sons.

REFERENCES

Ziemian, R.D., and Mcguire, W. (2015) *MASTAN2* [Computer software]. Retrieved from: http://www.MASTAN2.com.